

UMTRI-91-32

**INVESTIGATION OF AIRBAG-INDUCED SKIN  
ABRASIONS USING DEPLOYMENTS INTO  
HUMAN VOLUNTEERS**

**Final Report**

Lawrence Schneider  
Gregory Johnson  
Mats Ostrom  
Matthew Reed  
Richard Burney  
Carol Flannagan

University of Michigan  
Transportation Research Institute  
2901 Baxter Road  
Ann Arbor, Michigan 48109-2150

Submitted to:  
Chrysler Motors Corporation  
Highland Park, Michigan

September 1991



1. Report No. UMTRI-91-32	2. Government Accession No.	3. Recipient's Catalog No.	
4. Title and Subtitle Investigation of Airbag-Induced Skin Abrasions Using Deployments Into Human Volunteers		5. Report Date September 1991	
		6. Performing Organization Code	
7. Authors Lawrence Schneider, Gregory Johnson, Mats Ostrom, Matthew Reed, Richard Burney, Carol Flannagan		8. Performing Organization Report No. UMTRI-91-32	
9. Performing Organization Name and Address University of Michigan Transportation Research Institute 2901 Baxter Road Ann Arbor, Michigan 48109-2150		10. Work Unit No.	
		11. Contract or Grant No.	
12. Sponsoring Agency Name and Address Chrysler Motors Corporation Highland Park, Michigan		13. Type of Report and Period Covered Final Report	
		14. Sponsoring Agency Code	
15. Supplementary Notes			
16. Abstract <p>The mechanisms and factors involved in skin abrasions to the face and neck due to airbag deployments were studied using deployments of airbags with different folding patterns, tethering, inflators, and airbag materials into the legs of volunteer subjects. A total of 48 tests were performed with two tests conducted on each subject in most cases. An integer injury scale from 1 to 6 was developed and used to score the injury results for each test. Data collected include pre- and post-test color photos of the targeted skin surface and high-speed films of most deployments.</p> <p>Skin abrasions were produced in subjects over a range of distances from 225 mm to 350 mm with untethered airbags, but only at distances of 225 to 250 mm with tethered airbags. Overall (i.e., for all distances), the test results indicate that airbag folding technique has the strongest and most consistent influence on reducing both the frequency and severity of abrasions. However, the effects of tethering are also very significant, especially for distances greater than 250 mm, for which no abrasions were observed. Changes in inflator pressure from 475 kPa to 350 kPa had little or no effect on skin abrasion for the distances used. The test results also suggest a possible U-shaped relationship of distance to abrasion whereby the likelihood and/or severity of abrasions are higher at distances less than 250 mm and between 325 and 350 mm. The coarseness or denier of the airbag material appeared to have little effect on abrasion-type injuries. Analysis of the high-speed films revealed two types of airbag kinematics corresponding to different injury mechanisms for the two types of airbag folding techniques used.</p>			
17. Key Words Airbag, Abrasion, Skin		18. Distribution Statement Restricted	
19. Security Classif. (of this report)	20. Security Classif. (of this page)	21. No. of Pages 182	22. Price





## ACKNOWLEDGEMENTS

The authors would like to acknowledge the valuable assistance and guidance offered throughout this project by Randy Edwards of Chrysler Motors Corporation. Mr. Edwards worked closely with project staff in designing the different matrices of test conditions and in analyzing and interpreting the test results. He also served as a test subject in the preliminary stage of testing, as did Turner Osborne of Morton Thiokol. The study also benefited from the advice and consultation of Dr. Donald Huelke, who provided expertise with regard to classification of abrasion injuries and who, along with Jamie Moore, provided valuable input to the research program from investigations of vehicle crashes involving airbag deployments where abrasion injuries occurred.

Special recognition is due to Eric Olson who worked with dedication and creativity to ensure the excellent quality of color photographs that document the pre- and post-test skin conditions, and to Brian Eby and Lloyd Dunlap who shared responsibility for the fabrication and assembly of the test facilities and technical details involved in coordinating and conducting the airbag deployments. Thanks also to Mary Freiman and Leda Ricci who helped in the preparation of this document.

Finally, the authors would like to express their appreciation to the subjects who volunteered to participate in this study, knowing that they might experience some abrasions and discomfort.



## CONTENTS

ACKNOWLEDGEMENTS .....	v
LIST OF TABLES .....	ix
LIST OF FIGURES .....	xi
SUMMARY .....	1
<b>I. BACKGROUND AND OBJECTIVES .....</b>	<b>3</b>
<b>II. TEST PROCEDURES, FACILITIES, AND MATRICES .....</b>	<b>5</b>
2.1 Overview .....	5
2.2 Test Conditions and Stages of Testing .....	7
2.2.1 Preliminary Tests.....	11
2.2.2 Taguchi Test Matrix .....	13
2.2.3 Deflection Plate Effects .....	18
2.2.4 Determination of Abrasion Distances.....	18
2.2.5 Full-Factorial Test Matrix.....	20
2.3 Skin Preparation and Data Collection .....	20
2.4 Abrasion Ratings .....	24
2.5 Airbag Velocities.....	26
<b>III. RESULTS .....</b>	<b>27</b>
3.1 Preliminary Tests.....	27
3.1.1 Measurement of Airbag Contact Force .....	27
3.1.2 Tests With Volunteer Subjects.....	27
3.1.3 Measurement of Reaction Forces .....	29
3.2 Taguchi Test Matrix .....	39
3.3 Deflection Plate Effects .....	43
3.4 Determination of Abrasion Distances.....	44
3.5 Full-Factorial Matrix .....	46
3.6 Compilation of Results from All Tests.....	50
3.6.1 Contingency-Table Analysis.....	52
3.6.2 Effect of Distance on Abrasion Injuries .....	55
3.6.3 Effect of Tether by Distance.....	57

3.7 Mechanisms of Abrasions .....	59
3.8 Estimations of Airbag Velocities .....	63
<b>IV. DISCUSSION, CONCLUSIONS, AND RECOMMENDATIONS FOR FUTURE WORK .....</b>	<b>81</b>
<b>APPENDIX A: Photographs of subjects' legs taken before and five minutes after airbag deployments in the Taguchi test matrix .....</b>	<b>87</b>
<b>APPENDIX B: Photographs of subjects' legs taken before and five minutes after airbag deployments in the deflection-plate effects and determination-of-abrasion-distances test matrix .....</b>	<b>105</b>
<b>APPENDIX C: Photographs of subjects' legs taken before and five minutes after airbag deployments in the full-factorial test matrix .....</b>	<b>151</b>

## LIST OF TABLES

1. Summary of Test Stages .....	5
2. Airbag Conditions Used .....	7
3. Tests Conditions in Preliminary Tests.....	12
4. Test Conditions in the Taguchi Matrix.....	17
5. Test Conditions for Further Evaluation of the Chest Deflection Plate .....	19
6. Test Conditions used in Determining Abrasion Distances .....	19
7. Test Conditions in the Full-Factorial Matrix .....	21
8. Preliminary Abrasion Classification Scheme Based on Width of the Abrasion.....	25
9. Abrasion Injury Scores .....	25
10. Abrasion Injury Scores from Preliminary Tests .....	35
11. Abrasion Injury Scores for the Tests in the Taguchi Matrix .....	41
12. Sums of Abrasion Injury Scores from the Taguchi Matrix .....	42
13. Results of Analysis of Variance on Abrasion Scores from tests in the Taguchi Matrix.....	43
14. Abrasion Injury Scores from Tests to Evaluate the Chest Deflection Plate.....	44
15. Abrasion Injury Scores from Tests to Determine Abrasion Distances .....	45
16. Abrasion Injury Scores from Tests in the Full-Factorial Matrix .....	47
17. Mean Injury Scores for Combinations of Tether and Airbag-Fold Conditions from Tests in the Full-Factorial Matrix.....	48
18. Results of Analysis of Variance on Abrasion Scores from Tests in the Full-Factorial Matrix.....	50
19a. Contingency Tabulation and Chi-Square Statistic for Effects of <i>AIRBAG FOLD TECHNIQUE</i> on Skin Abrasion from the Combined Data Base .....	53

19b.	Contingency Tabulation and Chi-Square Statistic for Effects of <i>TETHER</i> on Skin Abrasion from the Combined Data Base .....	53
19c.	Contingency Tabulation and Chi-Square Statistic for Effects of <i>INFLATOR PRESSURE</i> on Skin Abrasion from the Combined Data Base .....	53
20.	Three-Way Contingency Table for Fold, Tether, and Abrasion from the Combined Data Base.....	54
21.	Mean Injury Scores for Combinations of Tether and Airbag-Fold Conditions for the Combined Data Base.....	56
22.	Contingency Tabulation and Chi-Square Statistic for Effects of <i>DISTANCE</i> on Skin Abrasion from the Combined Data Base.....	57
23.	Three-Way Contingency Table for Tether, Distance, and Abrasion from the Combined Data Base.....	60
24.	Velocities Estimated from Tests in the Full-Factorial Matrix .....	75

## LIST OF FIGURES

1.	Test setup in UMTRI sled lab for Preliminary Test Series .....	6
2a.	UMTRI airbag laboratory for abrasion testing .....	8
2b.	UMTRI airbag laboratory (continued) .....	9
3.	Leg positioning relative to steering wheel and airbag module .....	10
4.	Test setup for deployments into load cells .....	12
5a.	Graphical representation of steering wheel and test dummies from Chrysler/Morton Thiokol deployment tests .....	14
5b.	Reorientation of steering wheel and test dummy for vertical wheel positioning.....	15
5c.	Orientations of steering wheel, leg, and deflection plate derived from static deployment tests with crash dummies .....	16
6.	Positioning of subject's leg and deflection plate just prior to airbag deployment.....	16
7.	Modified orientation of subject's leg relative to the deflection plate.....	17
8a.	Side one of abrasion injury documentation form.....	22
8b.	Side two of abrasion injury documentation form .....	23
9.	Force-time traces from deployments into load cell with 6-in-diameter face plate .....	28
10a.	Abrasions and erythema resulting from deployment of untethered airbag into the tibia region of first subject positioned at a distance of 350 mm (14 in) .....	31
10b.	Abrasions and erythema resulting from deployment of untethered airbag into the calf region of first subject positioned at a distance of 350 mm (14 in) .....	33
11.	Pre- and post-test photographs of subject's leg showing abrasions on front of tibia possibly due to upward motion of the airbag caused by the deflection plate .....	37

12.	Force-time traces from load cell mounted between steering wheel and rigid support structure .....	40
13.	Plot of mean abrasion injury scores at two levels of different airbag and deployment factors and their interactions from the Taguchi matrix of tests .....	42
14.	Bar graph of mean injury scores for different test conditions used in the full-factorial test matrix .....	46
15.	Plot of mean injury score for different combinations of tether and fold in the full-factorial test matrix .....	48
16.	Plot of percentages of <i>abrasion</i> and <i>no abrasion</i> from contingency tables derived from the full-factorial test matrix.....	49
17a.	Bar graph showing numbers of tests conducted with different airbag and deployment test conditions .....	51
17b.	Percentages of tests involving the different levels of deployment and airbag conditions .....	51
18.	Plot of percentages of <i>abrasions</i> and <i>no abrasions</i> from contingency tables derived from the combined data base .....	54
19.	Plot of mean injury scores for different combinations of tether and fold in the combined data base .....	56
20a.	Plot of percentage of tests producing <i>abrasions</i> and <i>no abrasions</i> at different distances for the combined data base.....	58
20b.	Plot of mean injury scores at different distances for combined data base.....	58
21.	Effect of tether on abrasion frequency at different distances for the combined data base .....	60
22.	Side-view, stop-action photographs from high-speed films of untethered (top) and tethered (bottom) airbags with <i>accordion-type folding</i> .....	61
23.	Abrasions and erythema resulting from deployments of airbags installed in module with <i>accordion-type folding</i> .....	65
24.	Surfaces of airbags with <i>accordion-type folding</i> showing smeared colors along the centerline of the airbag that were picked up from subject's leg.....	67



25.	Side-view, stop-action photograph from high-speed films of untethered (top) and tethered (bottom) airbags with <i>reverse-type folding</i> .....	69
26.	Pre- and post-test photographs of subjects' legs after tests using airbags with <i>reverse-type folding</i> .....	71
27.	Surfaces of airbags with <i>reverse-type folding</i> showing colors picked up at the center of the airbag without smearing .....	73
28.	Side-view, stop-action photograph from high-speed films of tethered airbag with <i>reverse-type folding</i> and <i>350-kPa inflator</i> .....	77
29.	Pre- and post-test photographs of subjects' leg after test with tethered airbag with <i>reverse-type folding</i> , and <i>350-kPa inflator</i> at a distance of <i>225 mm</i> (9 in) .....	79
30.	Chin-to-steering-wheel distance for 100 subjects seated in test buck configured to sport (G-body), sedan (H-body), and minivan (S-body) seating packages .....	84
31.	Photos of subjects seated in sedan- and sport-type vehicle-package configurations with close chin-to-steering-wheel distances .....	85



## SUMMARY

This study was undertaken to investigate the mechanisms and factors involved in skin abrasions to the driver's face and neck due to airbag deployments in motor-vehicle crashes. Testing involved deployment of airbags with different folding patterns, tethering, inflators, and airbag materials into the legs of volunteer subjects with the modules positioned at various distances from the skin surface.

A total of 48 tests were performed, with two tests conducted on each subject in most cases. For 38 of the tests, a physician examined the skin injuries immediately after the test and, in most cases where an abrasion occurred, a follow-up contact was made two to three days later. An integer injury scale from 1 to 6 was developed and used to score the injury results for each test based on the width of the abrasion. Scores of 1 and 2 indicate *no abrasions* while scores of 3 through 6 indicate *abrasions* of increasing severity. Data collected include pre- and post-test color photos of the targeted skin surface, overlay sketches of the abrasions and areas of hyperemia, and high-speed films of most deployments taken at nominal film speeds of 1000 or 3000 frames per second (fps). Also, in a few tests airbag contact forces and steering-wheel reaction forces were measured for different module-to-subject distances.

The tests can be grouped into several categories or stages according to the different goals and issues of concern over the course of the study. A set of preliminary tests was conducted to measure contact forces, become familiar with the airbag deployment experience, and establish test procedures and conditions. These tests were followed by a set of eight tests in which the Taguchi method was used to vary two levels of five variables, including distance, airbag material, airbag fold, inflator pressure, and airbag tether. Subsequently, an additional series of tests was conducted to search for a distance or range of distances at which skin abrasions would be consistently produced by an untethered airbag with accordion-type fold and 475-kPa inflator. Finally, a set of eight tests was conducted using a full-factorial design to investigate the effects of tether, fold, and inflator pressure at a distance of 225 mm.

Skin abrasions were produced in subjects over a range of distances from 225 mm to 350 mm with untethered airbags, but only at distances of 225 to 250 mm with tethered airbags. At a distance of 225 mm, the results of the full-factorial test series suggest that airbag fold technique has the greatest effect on reducing abrasions, with reverse-type folding offering a substantial reduction to the likelihood and severity of abrasions. At this distance, tethering of the airbag also significantly reduces abrasions, but changing the inflator pressure from 475 kPa to 350 kPa has little effect.

For distances greater than 250 mm, no abrasions occurred for tests involving airbags with either reverse-type folding or tethers, or both. However, there were not enough tests with these conditions to determine which of these factors has the greatest effect on reducing abrasions for distances greater than 250 mm.

Overall (i.e., for all distances), the test results indicate that the reverse-type fold has the strongest and most consistent influence on reducing both the frequency and severity of abrasions. However, the effects of tethering are also very significant, especially for distances greater than 250 mm as previously noted.

With regard to inflator pressure, the overall results support the findings at 225 mm that changing the inflator pressure from 475 kPa to 350 kPa has little influence on skin abrasions. With regard to distance, the overall test results suggest a U-shaped relationship to abrasion whereby the likelihood and/or severity of abrasions is higher at distances less than 250 mm and between 325 and 350 mm. The coarseness or denier of the airbag material also appears to have little influence on the abrasion results.

Analysis of the high-speed films has revealed two types of airbag kinematics corresponding to the two types of airbag folding techniques used in this study. With accordion-type folding, the airbag deploys with two wings or flaps at the leading edge. These flaps make initial contact with the skin about three inches from the center of the targeted area which correspond to the areas receiving abrasions for these types of airbags. The mechanism of abrasion therefore appears to be the high-velocity impact and wiping action of these uninflated flaps of airbag material, particularly the material near the region of the airbag seams.

For airbags installed with the reverse-type folding, the center of the airbag deploys first and impacts into the center region of the targeted area with more of a stamping motion than the wiping or shearing motion seen with the accordion-type folding. While the potential for abrasion is greatly reduced for these airbags, the fact that abrasions were obtained with these kinematics suggests that the wiping action by the airbag material may not be required to produce skin abrasions at these levels of airbag material velocity.

## I. BACKGROUND AND OBJECTIVES

Investigations of motor-vehicle accidents involving airbag deployments are providing clear and convincing evidence of the added protection offered by airbags to drivers involved in severe frontal impacts. However, they have also demonstrated the occurrence of facial and neck abrasions that appear to be directly attributable to the deploying airbag. While these skin abrasions are not life-threatening, they have often occurred in accidents where the impact severity is just above the airbag deployment threshold, where damage to the vehicle is minor, and where resulting injuries to the driver without the airbag would have been minimal or nonexistent.

In an attempt to understand the factors contributing to skin abrasions during airbag deployment, a large number of static (i.e., nonimpact) deployment tests have been conducted by Chrysler and Morton Thiokol using instrumented Hybrid III anthropomorphic test dummies positioned at various distances from the pre-deployed airbag. In different tests, the dummy's face and neck were coated with various materials such as colored chalk, wax, and clay. In addition to forces measured by the neck load cells of the test dummy, contact of the airbag with the dummy was indicated by markings in the material on the dummy and by the presence of material on the airbag after the test.

While some measure of the severity of airbag contact can be obtained from these tests, it is not known which of these contacts, if any, correspond to actual skin abrasion. In order to make knowledgeable decisions about changes in future airbag-system designs that will reduce the likelihood and severity of skin abrasions, more definitive information about the factors contributing to skin abrasion is needed.

In a previous study conducted by UMTRI, airbags were deployed into young, shaved, anesthetized pigs to determine if skin abrasion would occur, and under what conditions. From this limited series of tests it was determined that serious skin abrasions resulted with an initial skin-to-airbag distance of 240 mm with either a tethered or untethered airbag. At a distance of 260 mm, only reddening (erythema or hyperemia) of the skin occurred with both tethered and untethered airbags.

The results of these pig tests demonstrated that airbag-induced abrasions, similar to those seen in the field, could be induced in pig skin under certain test conditions. Thus, the anesthetized pig appeared to offer a viable model for studying the effects of changing airbag/deployment conditions such as airbag folding technique, initial distance, airbag material, deployment velocity, etc. relative to the occurrence and severity of skin abrasions. However, in order to have confidence in these test results with regard to making decisions on airbag design factors, it was considered important to determine and compare the abrasion tolerance of pig skin to that of human skin.

With this background and purpose, the present study,<sup>1</sup> involving deployments of airbags into the skin of human volunteers, was undertaken with the objectives of:

1. determining the airbag design and deployment factors under which human skin experiences abrasion, as well as the relative contributions of these factors to the likelihood and severity of skin abrasions;
2. comparing abrasion results obtained with human skin to those obtained with anesthetized pigs; and
3. exploring and understanding the mechanisms of airbag-induced skin abrasions.

---

<sup>1</sup> The rights, welfare, and informed consent of the volunteer subjects who participated in this study were observed under guidelines established by the U.S. Department of Health, Education, and Welfare Policy (now Health and Human Services) on Protection of Human Subjects and accomplished under medical research design protocol standards approved by the Committee to Review Grants for Clinical Research and Investigation Involving Human Beings, Medical School, The University of Michigan.

## II. TEST PROCEDURES, FACILITIES, MATRICES

### 2.1. OVERVIEW

Because this was an exploratory study with wide-ranging objectives, and because there were no recently published studies of airbag-induced skin abrasions using human volunteers for reference, the testing was conducted in several stages. These are listed in Table 1 in order of performance along with a summary of the general goals or purposes of each.

Table 1  
Summary of Test Stages

Test Series	Purpose
Preliminary Human Testing and Force Measurements	Conducted using project staff as subjects to evaluate initial test conditions, determine suitable and acceptable tissue sites, determine the magnitude of contact forces and pressures associated with deployments of untethered airbags at different distances, assess the overall experience of airbag deployments, and determine the effects of using a deflection plate to simulate the chest.
Taguchi Matrix	An orthogonally designed array of eight tests with varying test conditions to evaluate relative effects of tethering, distance, airbag fold, airbag material, and deployment pressure.
Deflection Plate Effects	Four tests conducted with and without the <i>chest deflection</i> plate to determine whether the plate should continue to be used.
Determination of Abrasion Distances	A series of tests to explore the role of module-to-skin distance on the occurrence and severity of abrasions and determine the distance or range of distances that produce consistent abrasions with untethered, high-pressure airbags.
Full-Factorial Matrix	A final set of controlled tests designed to evaluate and quantify the effects of tethering, fold technique, and deployment pressure on abrasion.

Testing took place in two different laboratories over the course of the study. Preliminary testing was conducted in the UMTRI Impact Sled Facility using the sled platform as a base and the steering wheel mounting fixture used in the pig tests to secure the airbag module in position. Figure 1 illustrates the setup for these tests. It was

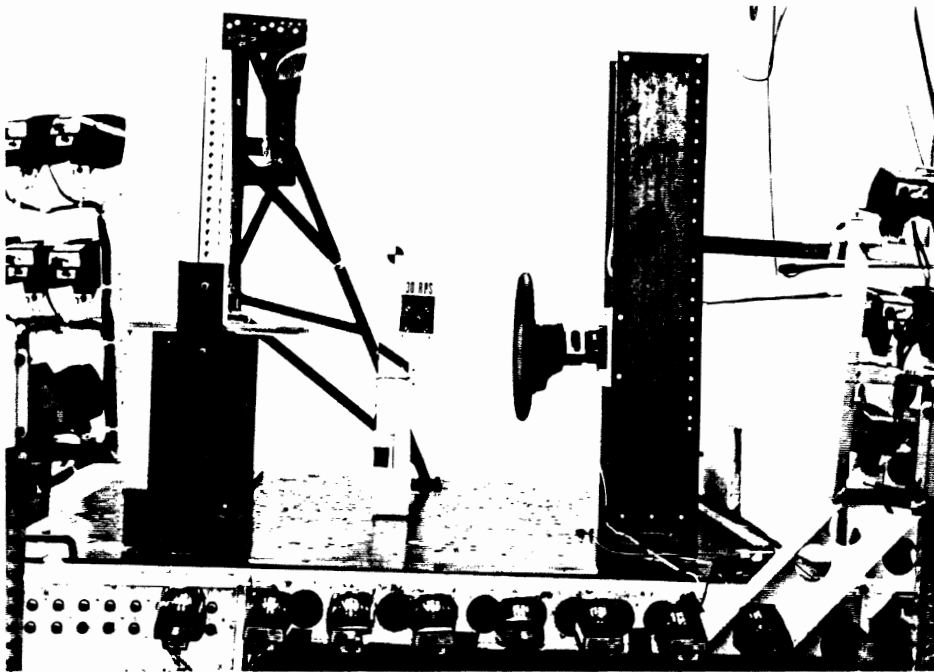


Figure 1. Test setup in UMTRI sled lab for Preliminary Test Series.



subsequently decided that testing could be more conveniently and effectively conducted if a separate laboratory were dedicated to these tests. Figures 2a and 2b show the test platform and fixtures in a new airbag-deployment laboratory which includes lighting and facilities for high-speed filming and color photo documentation of the subjects' skin before and after airbag deployments. The laboratory includes a special venting system which effectively exhausts the airbag gases outside of the building.

Prior to each test, the subject was positioned in front of the airbag module as shown in Figure 3 and provided with foam earplugs to reduce noise exposure. The front of the tibia of one leg was positioned at the specified distance from the face of the airbag module so that the center of the tibia was in line with the center of the module, both vertically and horizontally.

## 2.2 TEST CONDITIONS AND STAGES OF TESTING

Airbag conditions that were varied in the study include airbag tethering, airbag-inflation pressure, airbag material, and airbag-fold technique. Table 2 lists these variables and the two conditions of each used in testing. For the remainder of this report the terms "accordion" and "reverse" will be used to refer to the two types of fold techniques involved in these tests. In addition to the two levels of the four variables listed, the distance from the center of the airbag module to the surface of the skin was varied from 350 mm to 225 mm over the course of testing. Tables 3 through 7 on the following pages summarize conditions of the tests conducted in the different stages of testing defined in Table 1.

Table 2  
Airbag Conditions Used

Variable	Condition 1	Condition 2
Material	840 denier	420 denier
Tethering	No tether	With tether
Inflator Pressure	475 kPa	350 kPa
Fold Technique	Accordion or Standard	Reverse or E Fold

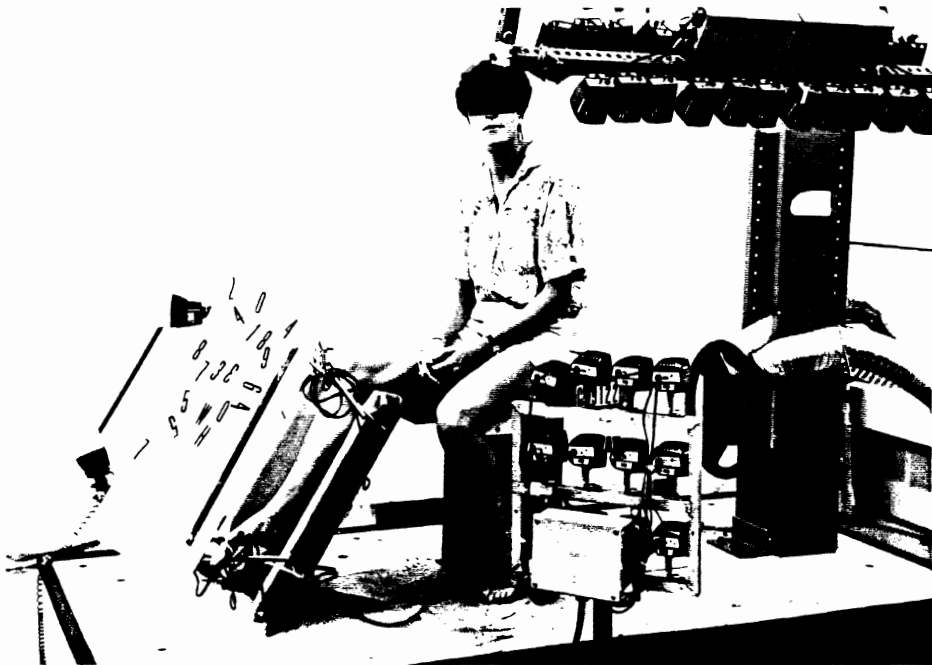
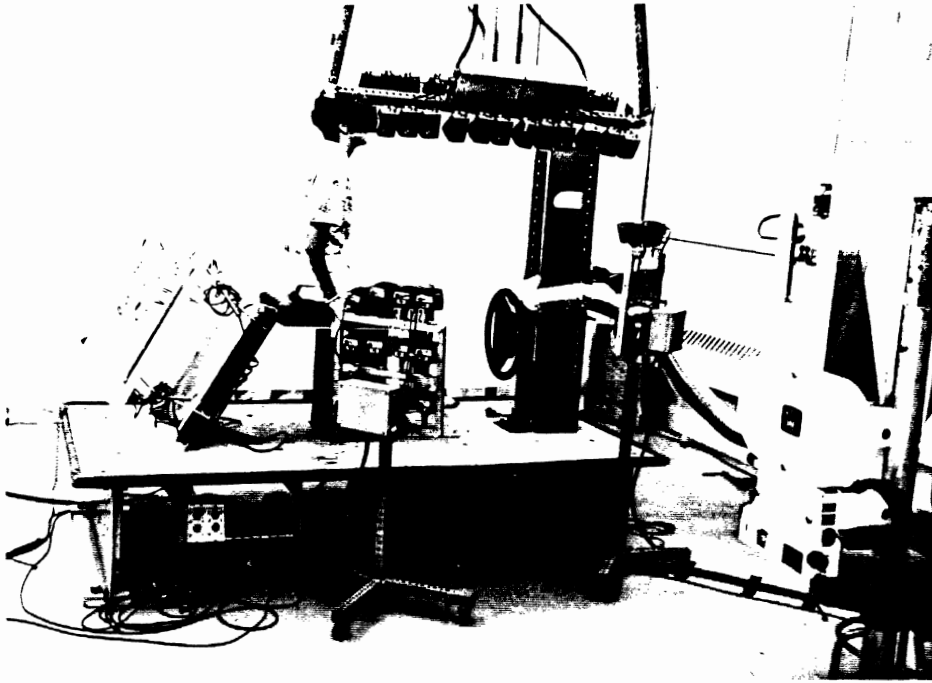


Figure 2a. UMTRI airbag deployment laboratory for abrasion testing.

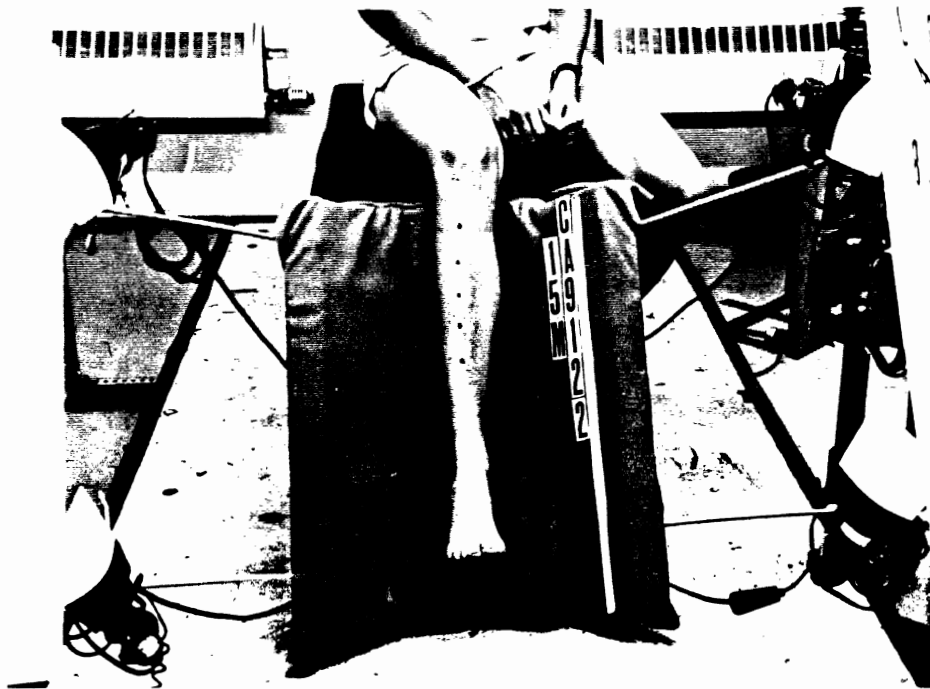
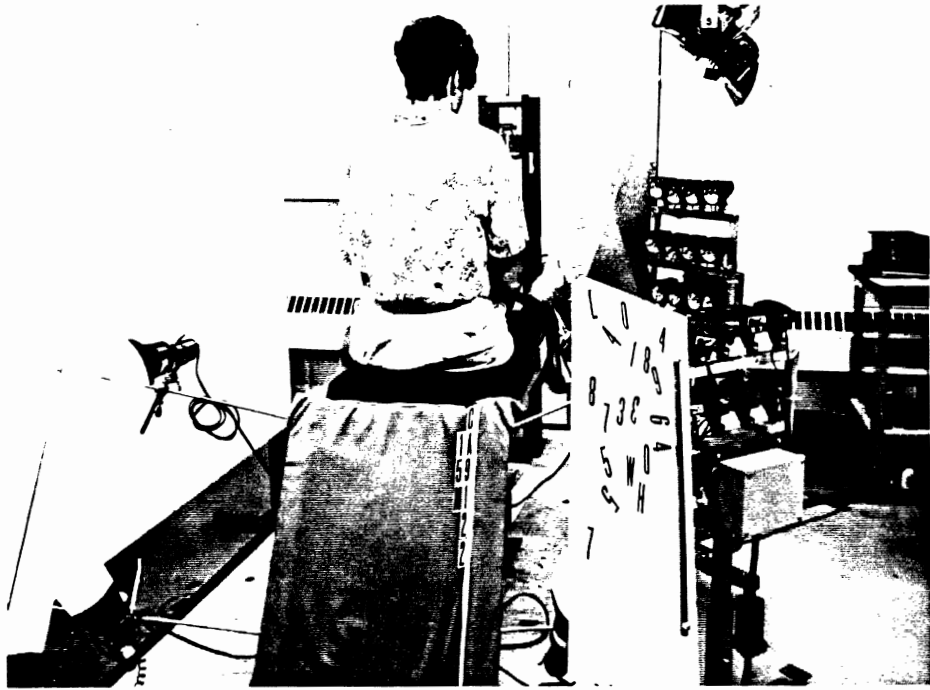


Figure 2b. UMTRI airbag deployment laboratory.

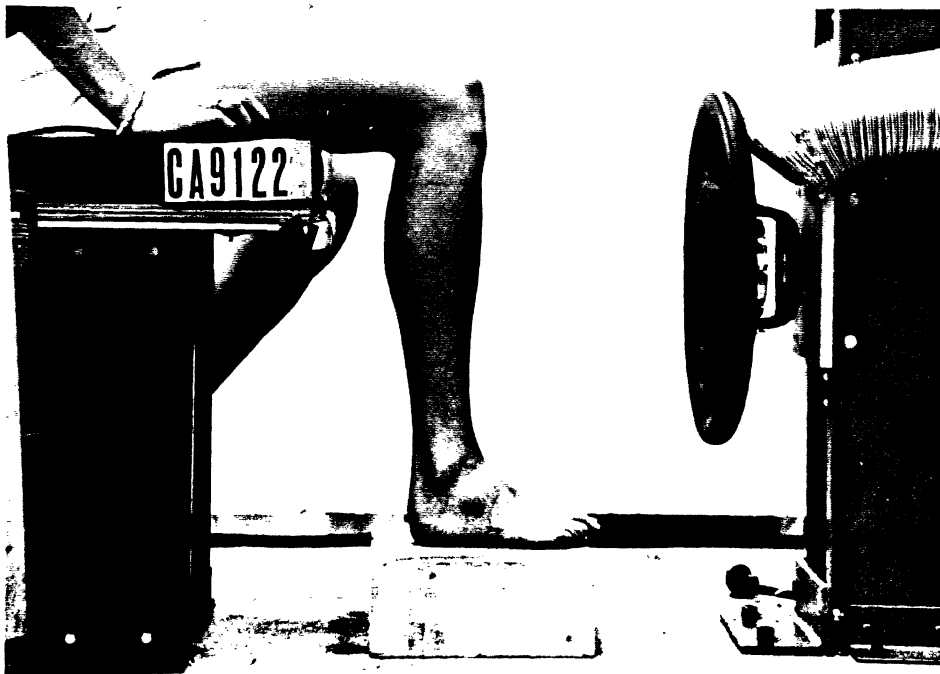


Figure 3. Leg positioning relative to steering wheel and airbag module.

## 2.2.1 Preliminary Tests

2.2.1.1 Force Measurements. Prior to conducting deployments into human skin, it was desired to examine the contact forces produced by a deploying airbag for different initial distances from the airbag module cover to the contact surface. As illustrated in Figure 4, these tests were conducted with the plane of the steering wheel and airbag module mounted in a vertical orientation and with a strain gage load cell (Denton model 2089) mounted to a vertical post that was bolted to the 1/4"-steel plate on the UMTRI sled. As shown in Table 3, tests were conducted using untethered airbags made of 840-denier material and installed with the accordion-type fold and the 475-kPa inflator. Three tests were performed for distances of 250 mm, 300 mm, and 350 mm. Forces on the load cell were recorded on analog tape and played back on Brush recorder paper for measurement purposes. High-speed films of these deployments were taken using a nominal film speed of 1000 fps.

In addition to airbag contact forces, reaction forces at the steering wheel mounting plate were measured during four of the preliminary deployments into human tissue (Tests CA9101 through CA9104 in Table 3). The Denton load cell was also used in these tests and the output signals were processed and recorded on the sled lab data-acquisition system.

2.2.1.2 Initial Subject Testing. Subsequent to the measurement of airbag contact forces, a series of preliminary tests using project staff for subjects was conducted. Table 3 lists the initial conditions for these tests. All tests were performed with the plane of the steering wheel positioned vertically and all deployments were into the subject's leg with the longitudinal axis of the tibia also positioned vertically as shown in Figure 3. The targeted area for all but one test was the front of the tibia approximately halfway between the ankle and the knee. The subject was seated facing the steering wheel with the knee flexed at 90 degrees and the foot resting on a loose piece of balsa wood so that the foot and leg could move freely upon airbag contact. For one test, the targeted area was the surface of the calf behind the leg. In this case, the subject stood upright on one leg with the targeted leg positioned in front of the steering wheel with the foot suspended just above the platform.

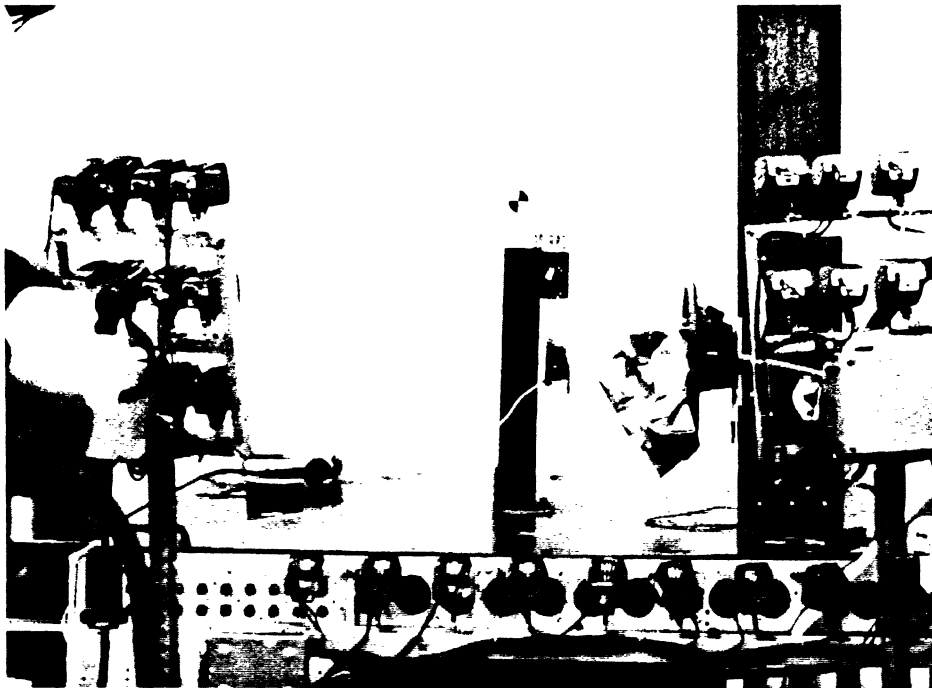


Figure 4. Test setup for deployments into load cells.

Table 3  
Tests Conditions in Preliminary Tests

Test No.	Subject Gender	Deflect. Plate	Distance (mm)	Wheel Rotation	Inflator kPa	Bag Matl (denier)	Tether	Bag Fold
CA91xx	M	No	350	0°	475	840	No	Acc
CA91xx	M	No	350	0°	475	840	No	Acc
CA9101 *	M	No	300	0°	475	420	Yes	Acc
CA9102 *	M	No	300	0°	475	840	No	Acc
CA9103 *	M	No	250	0°	475	420	Yes	Acc
CA9104 *	M	No	350	0°	475	840	No	Acc
CA9105 *	M	Yes	325	0°	475	840	No	Acc
CA9106	M	Yes	325	0°	475	840	No	Acc

\*Tests in which load cell was placed between steering wheel and support structure.

2.2.1.3 Testing with a Deflection Plate. During the investigative phase of preliminary testing, high-speed films of tests conducted by Morton Thiokol using test dummies with chalk painted on the face and neck were carefully reviewed. An analysis of airbag motion suggested that two phases were involved in many tests. In the first phase, the airbag projects outward from the module contacting and loading the dummy chest, neck, and chin. In the second phase, the inflated airbag deflects upward due to the angle of the chest and constraints imposed by the pelvis and legs of the dummy. This latter motion results in an upward wiping along the neck and chin and it was hypothesized that this motion could make an important contribution to skin abrasion.

As a result of these observations, the idea of adding a deflection plate just in front of the subject's leg was considered and implemented for several of the deployment tests. Figures 5a through 5c illustrate the process of translating the vehicle steering wheel and dummy geometry to that of the abrasion test setup where the steering wheel and skin surface are oriented vertically. In this analysis, the initial positions of the small and mid-size test dummies seated at full-forward and mid-track positions, respectively, were used and a line between the chin and the bottom of the neck was considered the target surface corresponding to the front of the tibia in the human abrasion tests. Figure 6 shows the test setup with the deflection plate positioned in front of a subject's tibia.

## 2.2.2 Taguchi Test Matrix

As indicated in Table 3 and reported in the results, the deflection plate was implemented in two preliminary tests (CA9105 and CA9106), one of which produced an abrasion to the front of the tibia which appeared to be directly attributable to the secondary upward airbag motion caused by the deflection plate (see Section 3.1.2 and Figure 10). As a result of this finding, the deflection plate was used in all eight of the tests comprising the Taguchi test matrix although the orientation of the leg relative to the plate was modified based upon the experience of the preliminary tests. Figure 7 illustrates the new leg orientation in which the tibia was angled forward slightly so as to have greater exposure to the upward-deflecting airbag. Other conditions for tests in the Taguchi matrix are listed in Table 4 and involve variations in five conditions including distance, inflation pressure, airbag material, airbag tethering, and airbag fold as previously noted in Table 2.

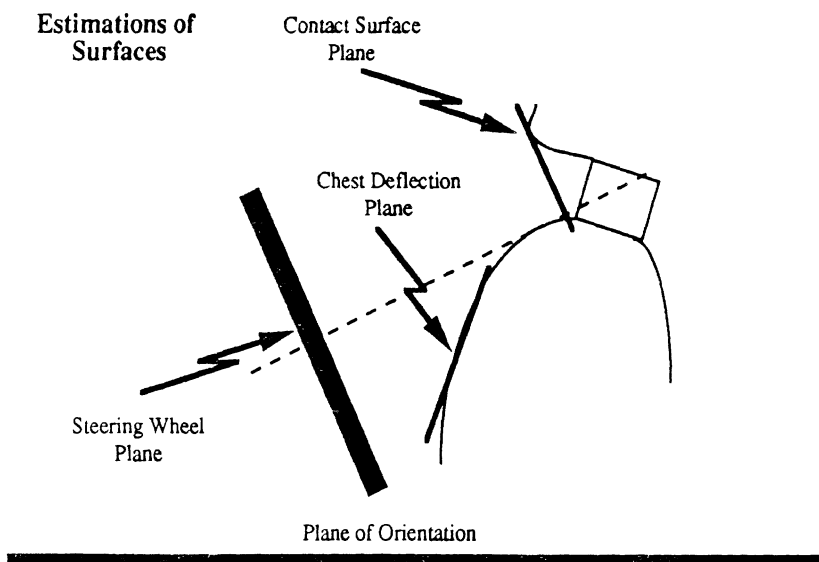
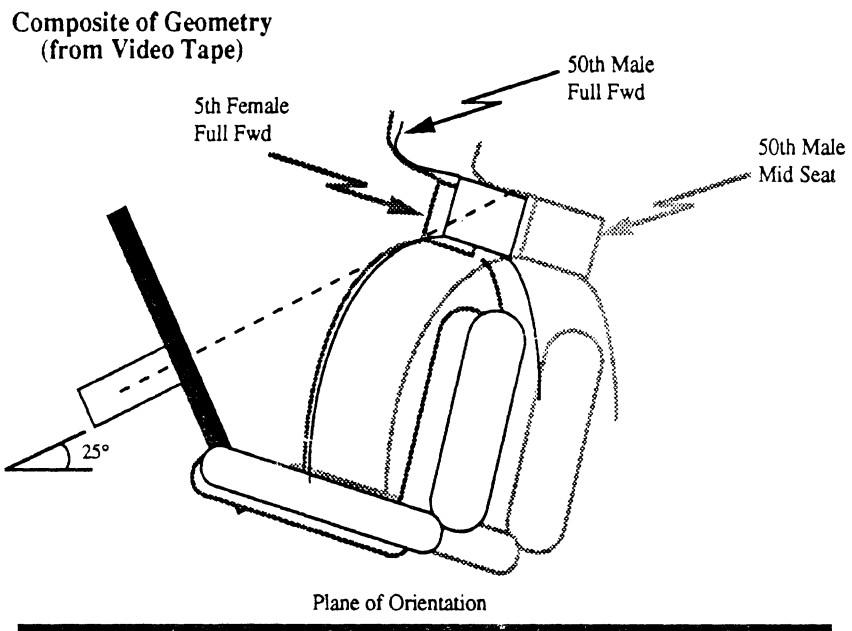


Figure 5a. Graphical representation of steering wheel and test dummies from Chrysler/Morton Thiokol deployment tests.



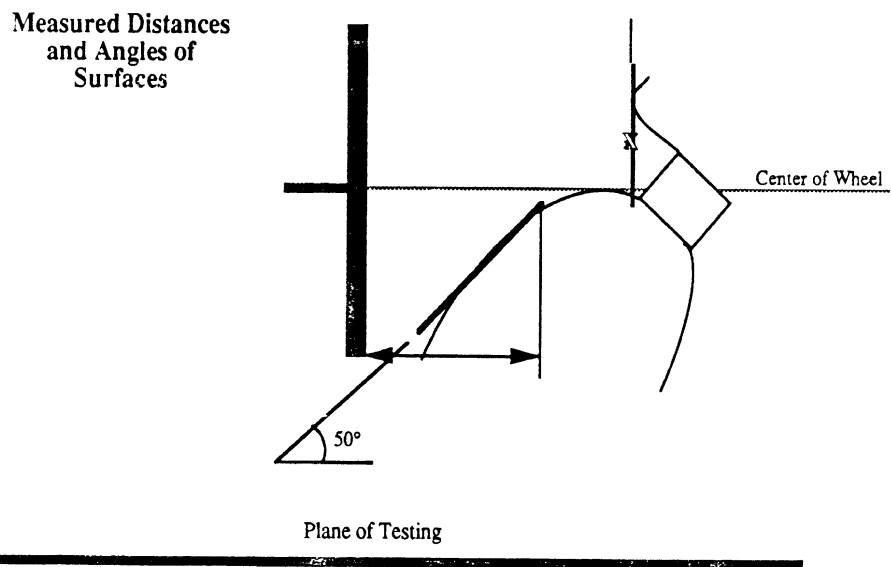
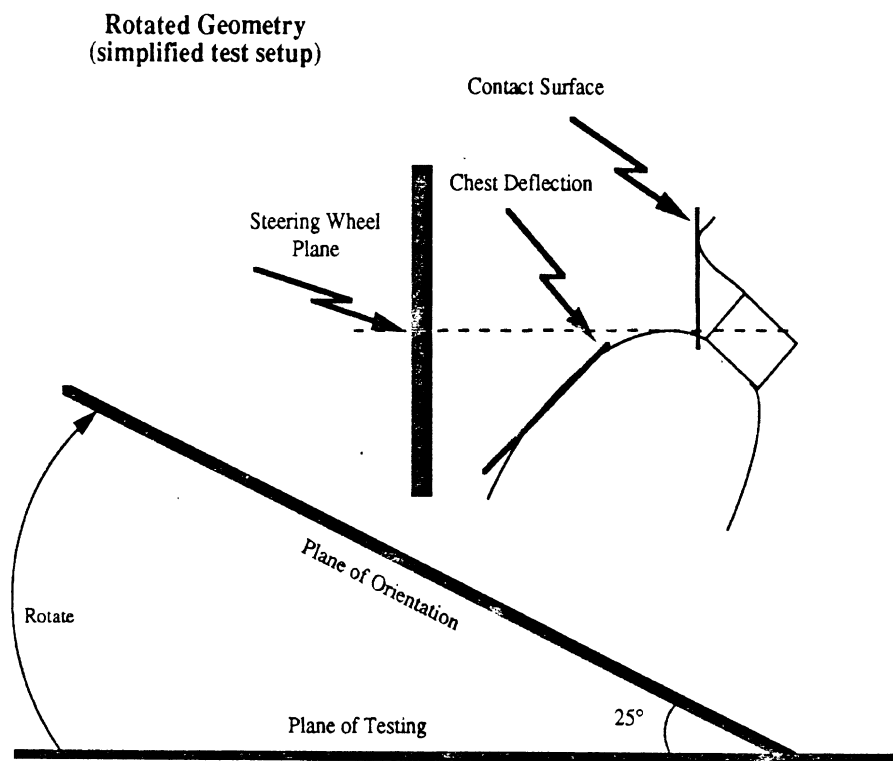


Figure 5b. Reorientation of steering wheel and test dummy for vertical wheel positioning.

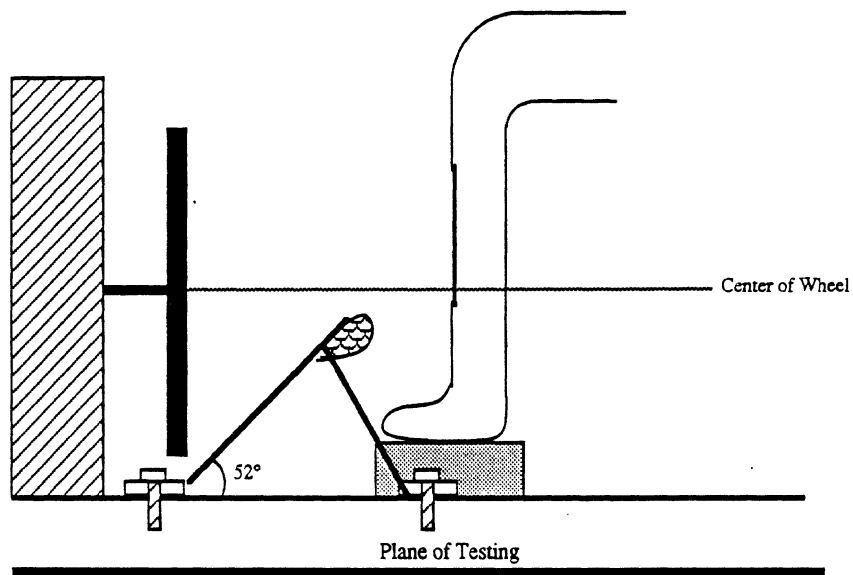


Figure 5c. Orientations of steering, leg, and deflection plate derived from static deployment tests with crash dummies.



Figure 6. Positioning of subject's leg and deflection plate just prior to airbag deployment.

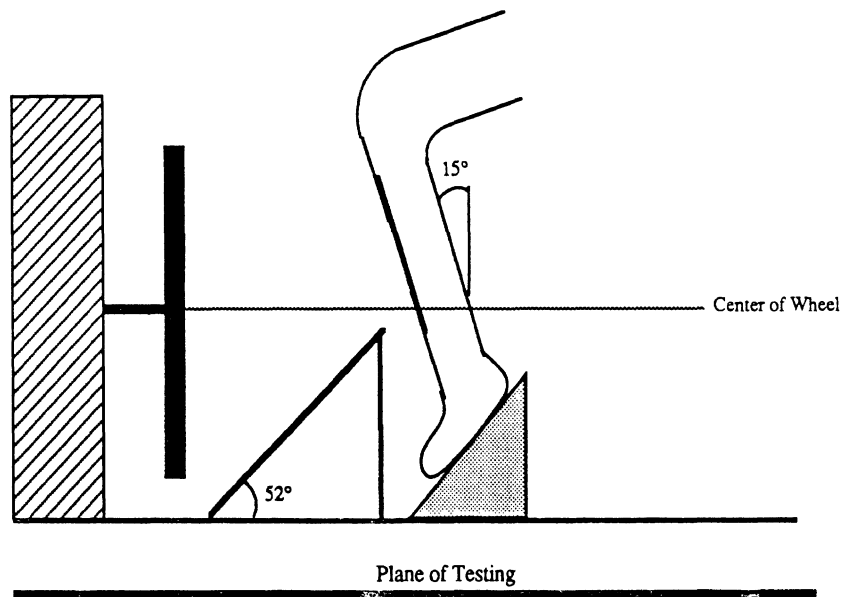


Figure 7. Modified orientation of subject's leg relative to the deflection plate.

Table 4  
Test Conditions in the Taguchi Matrix

Test No.	Subject Gender	Deflect. Plate	Distance (mm)	Wheel Rotation	Inflator kPa	Bag Matl (denier)	Tether	Bag Fold
CA9107	F	Yes	300	0°	350	420	Yes	Rev
CA9108	F	Yes	300	0°	475	420	No	Rev
CA9109	F	Yes	250	0°	475	420	Yes	Acc
CA9110	F	Yes	250	0°	350	420	No	Acc
CA9111	F	Yes	300	0°	475	840	Yes	Acc
CA9112	F	Yes	300	0°	350	840	No	Acc
CA9113	F	Yes	250	0°	350	840	Yes	Rev
CA9114	F	Yes	250	0°	475	840	No	Rev

It will also be noted that all subjects used in the Taguchi test matrix were female. This was done primarily to eliminate concerns about the effects of leg hair on skin abrasion and to obtain a better view of the skin surface without shaving the legs. In addition, since most abrasions in vehicle crashes have been reported for female drivers, it was thought that female skin might be more sensitive to abrasion and would be more representative of the conditions in the real-world.

### 2.2.3 Deflection Plate Effects

As will be described in Section III, only minor abrasions and hyperemia were obtained in the Taguchi tests. While a number of factors may have been involved in these results, it was suspected that the deflection plate may have taken up much of the energy of the deploying airbag and that the effects of this plate at different distances and for different airbag conditions were likely to vary in an unknown manner. In an attempt to evaluate the plate effect further, four tests were conducted using untethered, 840-denier, accordion-type-fold airbags with 475-kPa inflators (see Table 5). These tests were conducted at distances of 300 and 350 mm with one test conducted with the deflection plate and one without at each distance. The abrasion results were inconclusive with regard to the plate effects and there was some evidence that the effect of the plate was strongly dependent on the distance between the module and the skin. While the plate did appear to produce airbag kinematics similar to those seen in static deployment tests with crash dummies, it was decided to eliminate the plate from future tests since it was not fully understood how it affects the energy delivered to the skin under the different test conditions.

### 2.2.4 Determination of Abrasion Distances

Since the conditions used in the Taguchi test matrix resulted in very few and minor abrasions (see Section 3.2), additional exploratory testing was considered important to determine a distance or range of distances at which consistent and significant skin abrasions occur. Tests CA9119 through CA9136 listed in Table 6 were conducted with this goal in mind and primarily used the untethered, 840-denier airbags with 475-kPa inflator and accordion-type folding. In addition, all but the last four tests in this series were conducted with female subjects for reasons previously noted.

Table 5  
Test Conditions for Further Evaluation  
of Chest Deflection Plate

Test No.	Subject Gender	Deflect. Plate	Distance (mm)	Wheel Rotation	Inflator kPa	Bag Matl (denier)	Tether	Bag Fold
CA9115	F	Yes	300	0°	475	840	No	Acc
CA9116	F	No	300	0°	475	840	No	Acc
CA9117	F	Yes	350	0°	475	840	No	Acc
CA9118	F	No	350	0°	475	840	No	Acc

Table 6  
Test Conditions used in Determining Abrasion Distances

Test No.	Subject Gender	Deflect. Plate	Distance (mm)	Wheel Rotation	Inflator kPa	Bag Matl (denier)	Tether	Bag Fold
CA9119	F	No	350	0°	475	840	No	Acc
CA9120	F	No	300	0°	475	840	No	Acc
CA9121	F	No	300	0°	475	840	No	Acc
CA9122	F	No	250	0°	475	840	No	Acc
CA9123	F	No	300	90°	475	840	No	Acc
CA9124	F	No	250	90°	475	840	No	Acc
CA9125	F	No	250	90°	475	840	No	Acc
CA9126	F	No	225	90°	475	840	No	Acc
CA9127	F	No	250	90°	475	840	No	Acc
CA9128	F	No	225	90°	475	840	No	Acc
CA9129	F	No	350	90°	475	840	No	Acc
CA9130	F	No	325	90°	475	840	No	Acc
CA9131	F	No	250	90°	475	420	Yes	Acc
CA9132	F	No	225	90°	475	420	Yes	Acc
CA9133	M	No	350	90°	475	840	No	Acc
CA9134	M	No	300	90°	475	840	No	Acc
CA9135	M	No	250	90°	475	840	No	Acc
CA9136	M	No	225	90°	475	840	No	Acc

The steering wheel was rotated ninety degrees from the normal straight-ahead position after the first four tests in this series. This condition was implemented after review of high-speed films indicated that the airbag with the accordion-type fold deploys with two flaps extending to the left and right of a steering wheel oriented in the straight-ahead driving position, and the observation that regions of the skin experiencing significant hyperemia and abrasion correlated with the areas of contact by these flaps. By rotating the steering wheel and module ninety degrees to the straight-ahead orientation, these flaps deploy upward and downward along the length of the tibia, thereby increasing the likelihood of skin contact by these deploying flaps of airbag material and improving the view of the injury mechanism from a side-view camera. With the steering wheel and module in the standard position and the leg positioned at the center of the airbag module, there was a high probability that the flaps would miss the leg (i.e., would be to the left or right of the leg) at times in the deployment when abrasion might be produced.

#### 2.2.5 Full-Factorial Test Matrix

While the results of tests for abrasion distance showed that abrasions could occur over a wide range of distances up to 350 mm for untethered airbags, a distance of 225 mm was determined to be a distance at which one could expect to consistently achieve an abrasion for untethered, accordion-type-fold airbags with 475-kPa inflators. As a result, this distance was selected for use in a final set of eight tests in which the effects of tethering, airbag fold, and inflator pressure would be more closely studied. Using these three variables, the full-factorial matrix of tests shown in Table 7 was designed in which only one condition is different for each pair of tests. The first four tests used the 475-kPa inflator while the last four tests used the 350-kPa inflator. For each subject, one test was conducted with an untethered airbag and one with a tethered airbag. Also, one subject at each inflator level was tested with the accordion-type-fold airbag and one with the reverse-type-fold airbag. Because airbag material had not been demonstrated to be a major factor influencing abrasion in previous tests, all airbags used the 420-denier material. Also, the steering wheel was rotated to the ninety-degree position previously described and all subjects were males whose legs were shaved with an electric razor immediately prior to the tests.

Table 7  
Test Conditions in the Full-Factorial Matrix

Test No.	Subject Gender	Deflect. Plate	Distance (mm)	Wheel Rotation	Inflator kPa	Bag Matl (denier)	Tether	Bag Fold
CA9137	M	No	225	90°	475	420	No	Acc
CA9138	M	No	225	90°	475	420	Yes	Acc
CA9139	M	No	225	90°	475	420	No	Rev
CA9140	M	No	225	90°	475	420	Yes	Rev
CA9141	M	No	225	90°	350	420	No	Acc
CA9142	M	No	225	90°	350	420	Yes	Acc
CA9143	M	No	225	90°	350	420	No	Rev
CA9144	M	No	225	90°	350	420	Yes	Rev

### 2.3 SKIN PREPARATION AND DATA COLLECTION

For tests conducted after the Preliminary Test Series, the legs of the subject were targeted along the midline of the tibia with colored, water-base paint or marking pen, and were photographed to record the pre-test condition of the skin and locations of these targets. During airbag contact with the skin, the colored markings transferred to the airbag material, thereby indicating the portions of the airbag making contact with the different regions of the leg and also indicating the nature of the contact (e.g., wiping or stamping) by the degree of smudging of the colors.

In order to control lighting and achieve consistent colors and quality in the photographs, a special photo frame was designed and fabricated as shown in Figure 2b. This was positioned behind the platform used for subject seating so that it was easy for the subject to turn around for photographic documentation of the targeted area before and after each deployment.

Post-deployment photos were taken immediately after the test and at 5-, 10-, 15-, and 30-minute intervals thereafter. If a noticeable abrasion occurred, an effort was made to have the subject return for a final photograph two to four days later. In addition to photographic documentation, the skin was examined by a physician immediately after each test and the areas of discoloration (i.e., erythema/hyperemia) and abrasion were measured and traced onto transparent film. The data form shown in Figures 8a and 8b was also used to record and document the injuries.

SUBJECT NO. \_\_\_\_\_  
PHONE: \_\_\_\_\_

TEST NO. \_\_\_\_\_  
TEST TIME \_\_\_\_\_

**HUMAN SKIN INJURIES DUE TO AIRBAG DEPLOYMENT**

- |   |  |   |
|---|--|---|
| 1. Sex<br>[1] Male<br>[2] Female                    | 2. Age<br>____ Yrs.  | 3. Deployment Location<br>[1] Left Tibia<br>[2] Right Tibia |
| 4. Distance from Module<br>____ mm                  | 5. Inflator Type<br>[1] 475 kPa (85g)<br>[2] 350 kPa (78g) | 6. Tethers<br>[1] Yes<br>[2] No                             |
| 7. Fold Pattern<br>[1] Accordion<br>[2] "E" Pattern | 8. Airbag Fabric<br>[1] 840 Denier<br>[2] 420 Denier       | 9. Tenderness/Contusion<br>[1] Yes<br>[2] No                |

**INJURY NO. 1:**  
**Location** \_\_\_\_\_

- |   |   |  |
|---|---|--|
| 10. Type of Injury<br>[0] None<br>[1] Hyperemia<br>[2] Petechial Bleedings<br>[3] Abrasion Without<br>[4] Burn<br>[5] Abrasion With<br>[6] Severe Abrasion/Lac. | 11. Injury First Visible<br>[0] Immediately<br>____ Minutes<br>12. Duration of Injury<br>____ Minutes<br>____ Hours | 13. Max. Area of Injury<br>a. ____ x ____ mm<br>b. ____ x ____ mm<br>c. ____ x ____ mm<br>d. ____ x ____ mm<br>e. ____ x ____ mm |
|---|---|--|

COMMENTS: \_\_\_\_\_

**INJURY NO. 2:**  
**Location** \_\_\_\_\_

- |   |   |  |
|---|---|--|
| 10. Type of Injury<br>[0] None<br>[1] Hyperemia<br>[2] Petechial Bleedings<br>[3] Abrasion Without<br>[4] Burn<br>[5] Abrasion With<br>[6] Severe Abrasion/Lac. | 11. Injury First Visible<br>[0] Immediately<br>____ Minutes<br>12. Duration of Injury<br>____ Minutes<br>____ Hours | 13. Max. Area of Injury<br>a. ____ x ____ mm<br>b. ____ x ____ mm<br>c. ____ x ____ mm<br>d. ____ x ____ mm<br>e. ____ x ____ mm |
|---|---|--|

COMMENTS: \_\_\_\_\_

Figure 8a. Side one of abrasion injury documentation sheet.



**INJURY NO. 3:**

**Location** \_\_\_\_\_

- |                          |                          |                         |
|--------------------------|--------------------------|-------------------------|
| 10. Type of Injury       | 11. Injury First Visible | 13. Max. Area of Injury |
| [0] None                 | [0] Immediately          | a. _____ x _____ mm     |
| [1] Hyperemia            | ____ Minutes             | b. _____ x _____ mm     |
| [2] Petechial Bleedings  |                          | c. _____ x _____ mm     |
| [3] Abrasion Without     | 12. Duration of Injury   | d. _____ x _____ mm     |
| [4] Burn                 | ____ Minutes             | e. _____ x _____ mm     |
| [5] Abrasion With        | ____ Hours               |                         |
| [6] Severe Abrasion/Lac. |                          |                         |

**COMMENTS:** \_\_\_\_\_

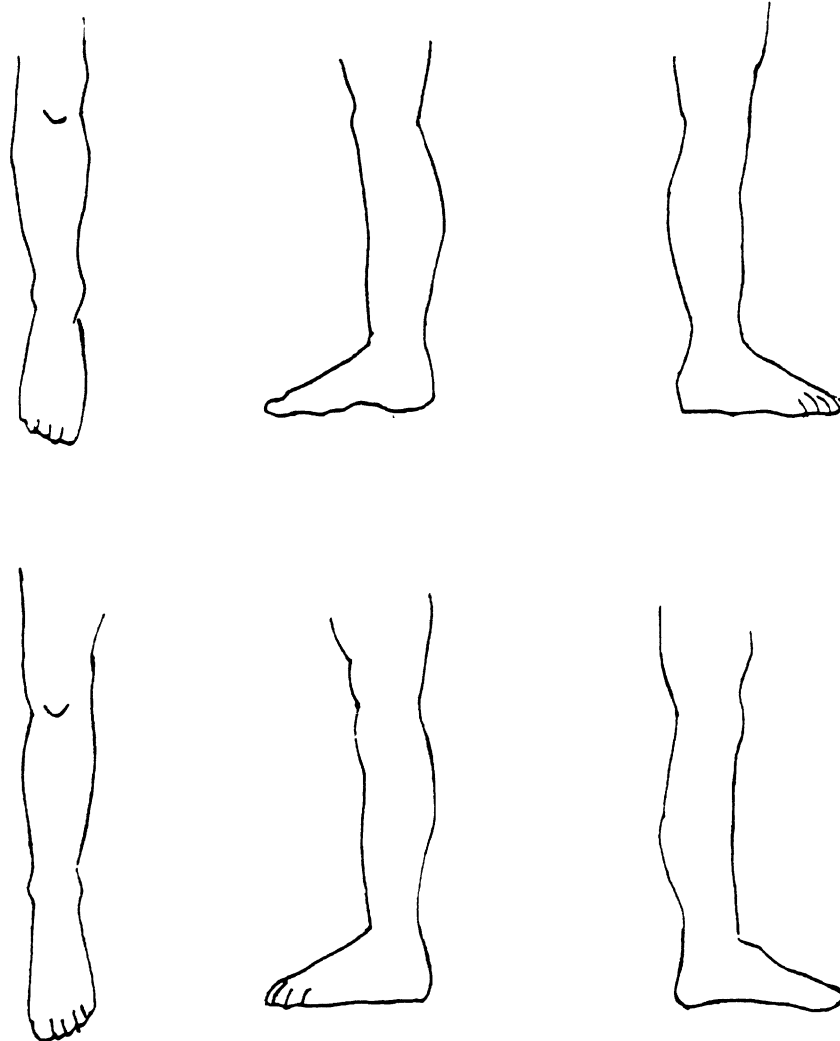


Figure 8b. Side two of abrasion injury documentation sheet.

In most tests, high-speed films were taken at 1000 or 3000 fps using a NAC 16-mm camera positioned to obtain a side view of the airbag module and subject's leg. Those films taken at 3000 fps were subsequently analyzed to obtain estimates of airbag deployment velocities as discussed below. In all tests, the airbag deployments and high-speed filming were controlled and sequenced automatically with an UMTRI-designed and fabricated timing system.

Because of concerns about effects of skin conditioning on abrasion results, female subjects were instructed not to shave or lotion their legs for at least 24 hours prior to the tests. For the male subjects tested in the full-factorial test series, the fronts of the legs were shaved just prior to testing to provide a better view of the skin surface and eliminate any effects of hair on abrasion results.

## 2.4 ABRASION RATINGS

Since one of the primary goals of the study was to determine the relative importance of the different airbag and deployment factors with regard to the likelihood and severity of skin abrasion, it was important to be able to assign a numerical value to linearly quantify the severity of abrasion injuries in each test so that statistical analyses and comparisons could be made. For these purposes, skin abrasion was considered to be the occurrence of a disruption in the epidermal tissue and capillary blood vessels so as to effect a long-term (i.e., more than two hours) change in the appearance of the skin, characterized by subsequent crusting or scab (eschar) formation.

In addition to the occurrence of skin abrasions in some deployments, all tests involving contact of the deploying airbag with the skin resulted in brief periods of red or purple discoloration of the skin surface. These discolorations would appear and deepen in the first two to three minutes after a test, but would then slowly fade within one to two hours. In a number of tests beginning with the Taguchi matrix of tests, these areas of discoloration were traced onto the transparent paper and subsequently quantified in size. This was done in an effort to obtain a quantitative measure and comparison of the severity of skin contact for statistical analysis when actual abrasions were minimal or nonexistent. In later tests, and for the final analysis, these areas of skin discoloration were not considered important and were not recorded or considered in the severity rating.

The first attempt to quantify and rank abrasion injuries took place subsequent to the Taguchi test series and resulted in the abrasion class ranking shown in Table 8. With this scheme, abrasions were classified according to the width of the abrasion and, within each class, the abrasions were assigned a value based on the length of the abrasion.

Table 8  
Preliminary Abrasion-Classification Scheme  
Based on Width of the Abrasion

Class	Condition
0	No Abrasions
I	Abrasion 1-2 mm wide
II	Abrasion 3-4 mm wide
III	Abrasion >5 mm wide

After working through several other rating systems and subsequent to completion of all but the last series of full-factorial tests, the integer abrasion-severity rating scheme shown in Table 9 was developed and a numerical injury score was assigned to each test result. The score was assigned by a physician who was on site for each test and who utilized first-hand observations of the injuries as well as measurements, notes, and photographs taken at the time of the tests. In addition, a follow-up phone call was made to all subjects two to four days after the tests to confirm any abrasions and ensure that no complications had occurred. If a subject received abrasions and was available, he/she was rescheduled for a second photo and follow-up examination by the attending physician.

Table 9  
Abrasion Injury Scores

Rating	Condition
1	Hyperemia
2	Hyperemia and/or petechial bleeding
3	Abrasion: pinpoint
4	Abrasion: light
5	Abrasion: medium
6	Abrasion: severe

According to this final rating system, the injuries received from a test are classified into three basic categories: hyperemia or erythema, petechial bleeding, and abrasion. Hyperemia is a reversible discoloration beneath the skin surface caused by engorgement of the capillaries (redness) or the veins (blueness). Petechial bleeding is evident as small red spots beneath the skin surface caused by breakage of the dermal capillaries or venules but does not include any kind of damage at the skin surface, the effects being only beneath the surface. The abrasion category includes any injury which resulted in disruption of the epidermal (skin) surface where the classifications of "light," "medium," and "severe" correspond to abrasion levels of I, II, and III shown in Table 8 and are based primarily on the width of abrasion. In some cases bleeding was apparent, and in others, the abrasion was not deep enough to cause noticeable bleeding. Also, in some instances, small bruises in the subcutaneous tissue were apparent but these contusions were considered to be the result of subcutaneous injury and therefore of lesser cosmetic significance, rather than abrasion, and were not considered in the final abrasion injury score.

## 2.5 AIRBAG VELOCITIES

For the last set of tests conducted using the full-factorial matrix of test conditions, high-speed, lateral-view films were taken of the airbag deployments using a nominal frame rate of 3000 fps. These films were subsequently analyzed using a NAC film analyzer to estimate velocities at the leading edge of airbag material.

Two sets of velocities were computed. One velocity is the average velocity of the leading edge of the airbag material during the first half of the deployment, with the first half defined as half the distance from the airbag module face to the front of the subject's leg. (Note that this distance was set at 225 mm for all tests in the full-factorial matrix.) The second velocity is for the second half of the deployment, from the midpoint to the point of first contact with the subject's leg. Because the material at the leading edge of the airbag seen by the camera may change during the deployment of the airbag and the estimates are obtained from a two-dimensional analysis of a three-dimensional event, these measurements are not considered to be precise measures of airbag-material velocity, but rather provide rough estimates of deployment velocities for comparison between the different deployment and airbag conditions tested.

## III. RESULTS

### 3.1 PRELIMINARY TESTS

#### 3.1.1 Measurement of Airbag Contact Force

Prior to conducting tests with human subjects, several airbags were deployed in the test fixture to check the firing and timing mechanisms and adjust lighting conditions for high-speed filming. In addition, three tests were conducted with a Denton load cell positioned in front of the airbag module at distances of 200, 250, and 300 mm. With a 6-in-diameter aluminum plate on the front of the load cell, the force traces in Figure 9 were recorded for the three deployments with untethered airbags and 475-kPa inflators.

These curves are characterized by two spikes in force within the first 10 ms after contact with the load cell, followed by a longer duration rise to a force that peaks at about 18 to 20 ms. The magnitude of the second force spike is in excess of 500 lb in all cases and is greatest at about 700 lb for the largest distance of 300 mm. The force at 20 ms is highest for the 200-mm distance at about 1000 lb and is smallest for the 300-mm distance at about 550 lb. This later force would appear to be due to trapping of the inflated airbag between the steering wheel and the load cell whereas the earlier force spikes are due to the deployment of the airbag and could involve mechanical noise or ringing in the measurement system. Since the surface area of the plate on the front of the load cell has an area of about 31 in<sup>2</sup>, a force of 500 lb corresponds to an average pressure of about 16 psi while a force of 1000 lb corresponds to a pressure of about 32 psi.

#### 3.1.2 Tests With Volunteer Subjects

The purpose of the preliminary tests was to gain first-hand experience in the deployment of airbags into human volunteers and thereby establish basic parameters for conducting the tests. The first two tests were conducted on legs of the principal investigator using the untethered, 840-denier airbag with accordion-type fold and 475-kPa inflator at a distance of 350 mm. The first test was conducted into the front of the tibia and resulted in significant hyperemia and a narrow abrasion accompanied by minor

**Air Bag Tests: Load Cell Measurements of Impact Forces in Space**

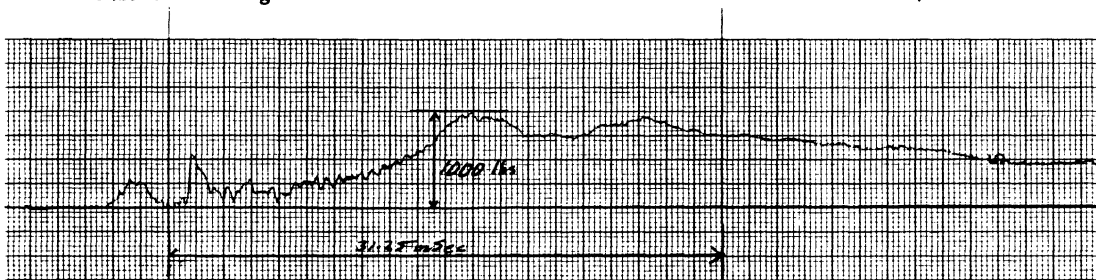
**Recorder Settings**  
Vertical 50 mV/div  
Paper Speed 200 div/sec  
Playback Speed 1/16 recorded

**Load Cell Output**  
1mVolt / lb

**Graph Scale Values**  
Force 50 lbs / div  
Time 0.3125 msec / div

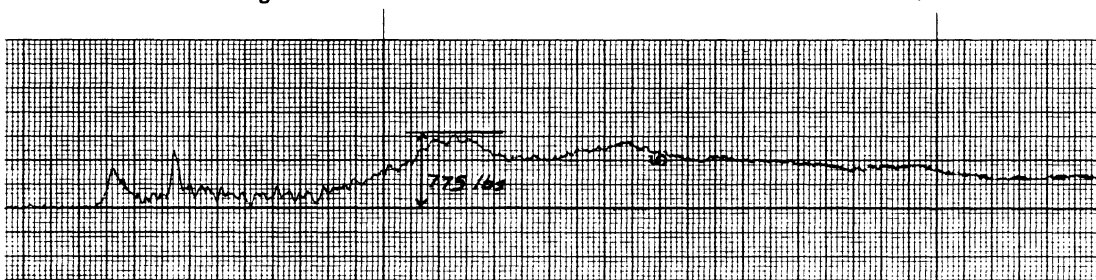
**Test #1 Bag to Load Cell Distance = 200 mm**

**November 16, 1990**



**Test #2 Bag to Load Cell Distance = 250 mm**

**November 16, 1990**



**Test #3 Bag to Load Cell Distance = 300 mm**

**November 16, 1990**

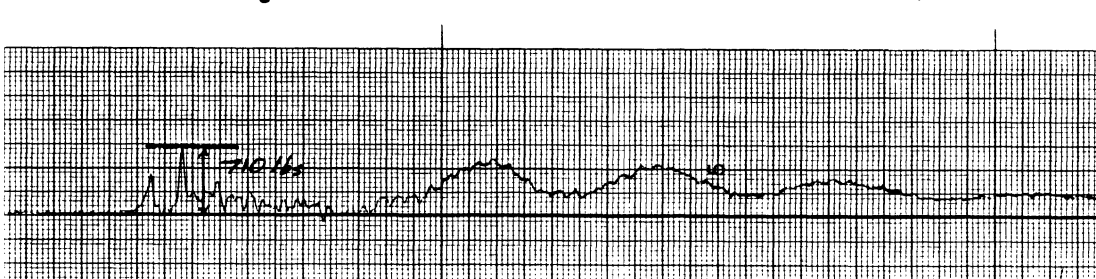


Figure 9. Force-time traces from deployments into load cell with 6-in-diameter face plate.

bleeding along the front of the tibia as indicated in Figure 10a. The second test was conducted into the back of the leg in the region of the calf muscle and resulted in a more severe abrasion with substantial bleeding as indicated in Figure 10b. Additionally, this latter test caused bruising and soreness in the soft tissues which lasted several days. While it had originally been thought that the likelihood and severity of abrasions might be increased by the presence of bony structures under the skin (e.g., the jaw), the results of these two tests suggested that skin supported by muscle tissue may be more susceptible to both superficial and deep injury than is skin supported closely by bone. As a result of this observation and concerns about causing unwanted injury to muscle and fascia, all remaining tests in the study were conducted into the tibia region of the subjects' legs.

Subsequent to these initial tests, several additional tests were conducted on project staff using shorter distances. While procedures for classifying the levels of abrasion had not been established for these tests and therefore no injury score has been assigned to the results, Table 10 summarizes the findings in terms of the occurrence of skin abrasion evidenced by subsequent eschar formation. Only two tests in the preliminary series were conducted with tethered airbags, one at distance of 250 mm and the other at 300 mm. Also, the last two tests in this series were conducted with the deflection plate in position as previously described. In addition to providing information necessary to establish the conditions and procedures for conducting the tests and document the injuries, these results suggested that:

- Skin abrasions can result from deployment of untethered airbags for initial distances up to 350 mm (14 in).
- Airbag tethering virtually eliminates substantial airbag contact and skin abrasions for distances greater than 300 mm.
- The deflection plate produced a secondary movement of the inflated airbag in the upward direction similar to the motion seen in static tests into crash dummies and this movement appeared to correspond to the occurrence of skin abrasion in one subject as shown in Figure 11.

### 3.1.3 Measurement of Reaction Forces

In four of the preliminary tests with human subjects (identified by an asterisk in Tables 3 and 10), a load cell was positioned between the steering wheel and its support





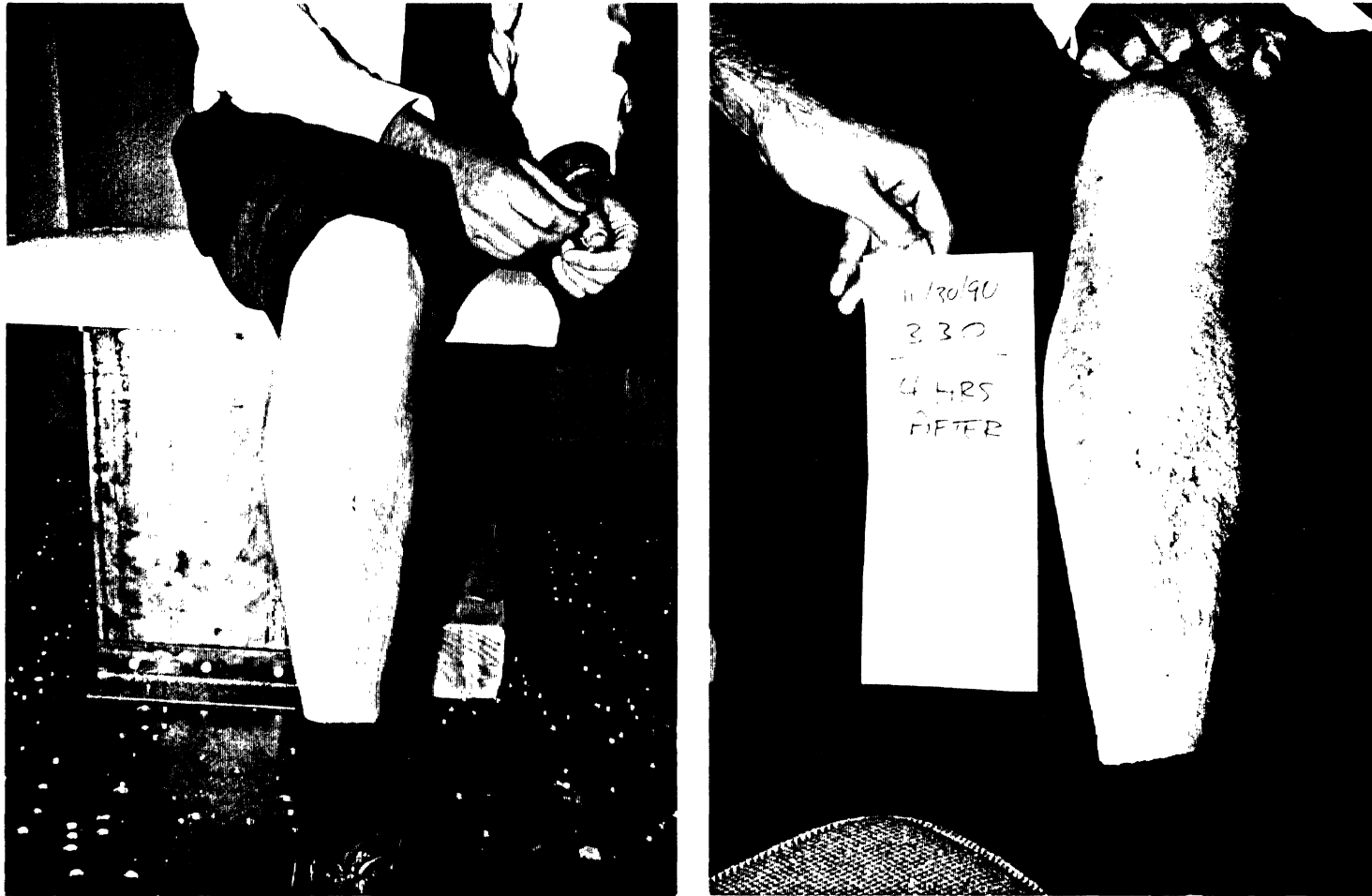


Figure 10a. Abrasions and erythema resulting from deployment of an untethered airbag into the tibia region of first subject positioned at a distance of 350 mm (14 in).



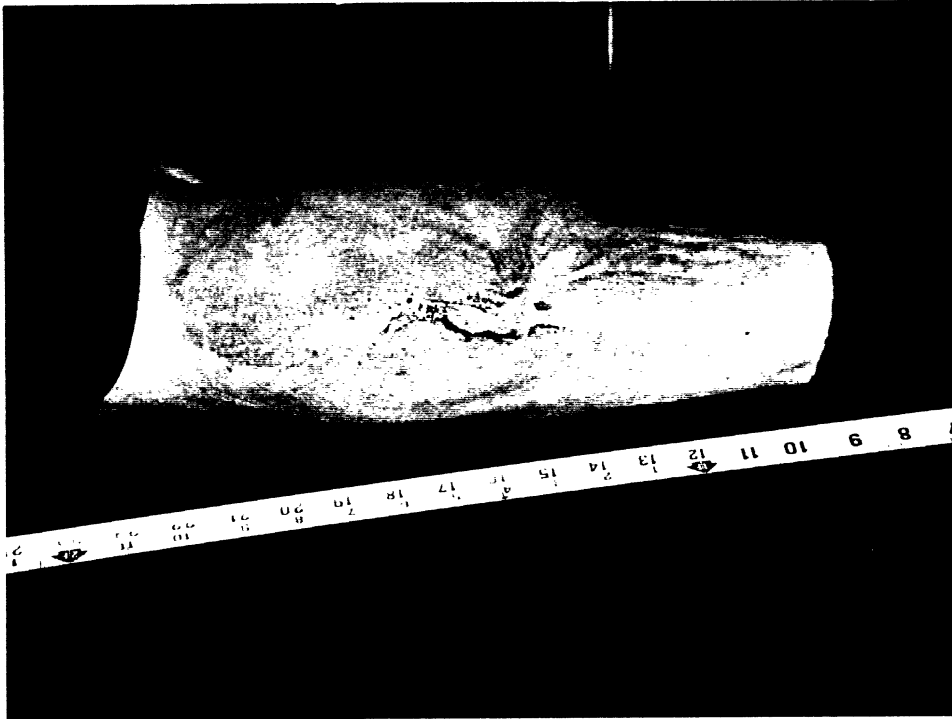


Figure 10b. Abrasions and erythema resulting from deployment of an untethered airbag into the calf region of first subject positioned at a distance of 350 mm (14 in).



Table 10  
Abrasion Injury Scores from Preliminary Tests

Test No.	Subject Gender	Deflect. Plate	Distance (mm)	Wheel Rotation	Inflator kPa	Bag Matl (denier)	Tether	Bag Fold	Abrasion Score
CA91xx	M	No	350	0°	475	840	No	Acc	Y
CA91xx	M	No	350	0°	475	840	No	Acc	Y
CA9101 *	M	No	300	0°	475	420	Yes	Acc	N
CA9102 *	M	No	300	0°	475	840	No	Acc	N
CA9103 *	M	No	250	0°	475	420	Yes	Acc	Y
CA9104 *	M	No	350	0°	475	840	No	Acc	Y
CA9105	M	Yes	325	0°	475	840	No	Acc	Y
CA9106	M	Yes	325	0°	475	840	No	Acc	Y

\* Tests in which load cell was placed between steering wheel and support structure.



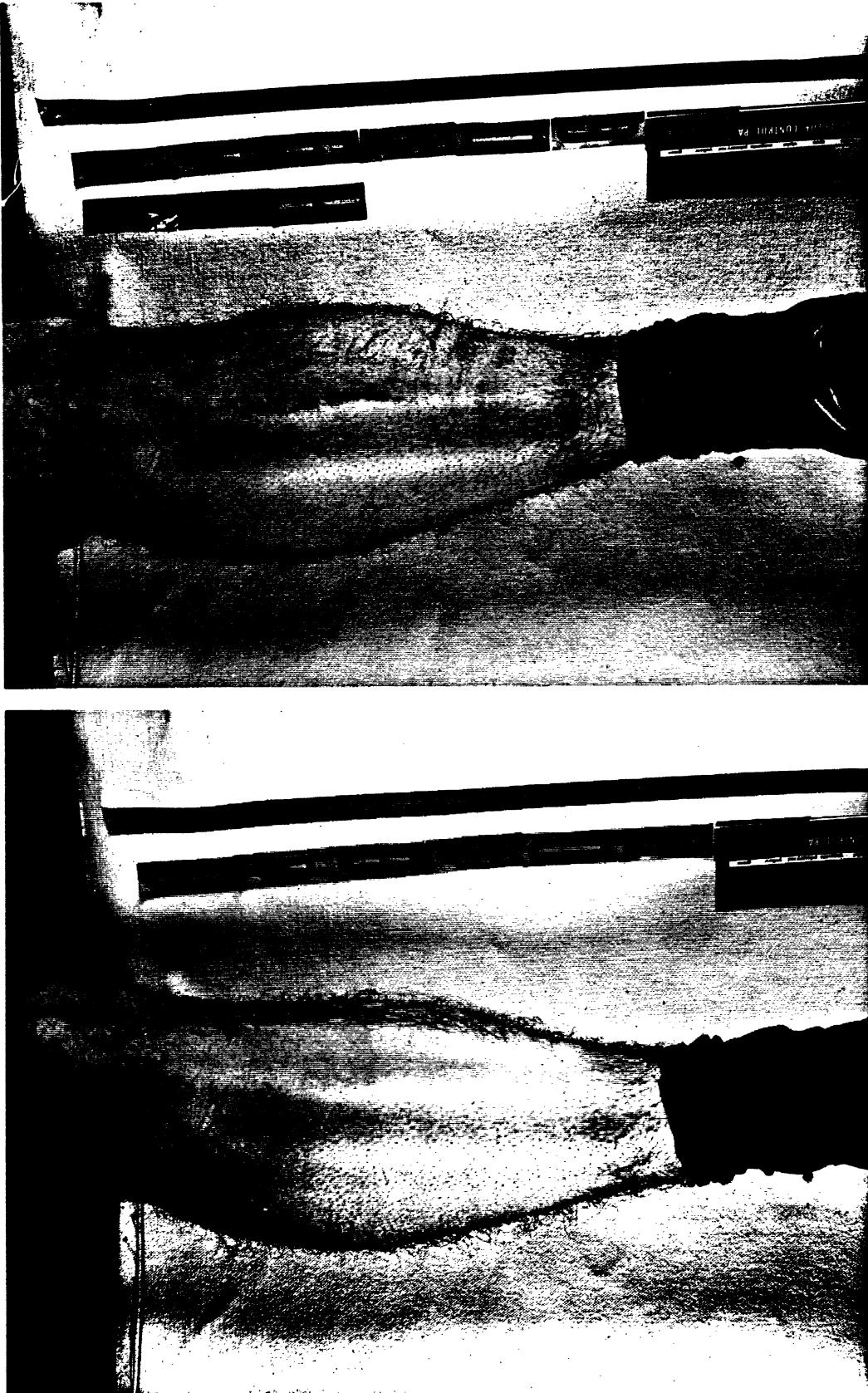


Figure 11. Pre- and post-test photos of subject's leg showing abrasion on the front of tibia possibly due to upward motion of the airbag due to deflection plate.





structure to measure the reaction forces experienced at the steering column. These tests included both tethered and untethered airbags with 475-kPa inflators and were conducted at distances ranging from 250 to 350 mm from the face of the module cover to the subject.

The results are shown in Figure 12. In each case, the force curve begins with a period of sinusoidal oscillation that lasts for approximately 12 ms or less. This is in the time period prior to contact of the airbag material with the subject's leg and these oscillations are undoubtedly initiated by the deploying airbag. There is, however, some question as to whether the magnitudes of these oscillations, which range from 1000 to 1650 lb, are meaningful, since the oscillations are likely to be the result of ringing and vibration in the transducer/support system.

At approximately 12 ms, the force signals tend to flatten out for a period of about 12 ms prior to showing an increase in compressive force which peaks at about 24 to 30 ms. This secondary force is likely due to squeezing of the inflated airbag against the subject's leg which has not yet moved out of the way. The magnitudes of these secondary forces range from about 600 to 1100 lb.

### 3.2 TAGUCHI TEST MATRIX

Table 11 summarizes the injury scores assigned to the test results obtained in the eight deployments of the Taguchi matrix, while Appendix A shows the pre- and post-test photos of the targeted skin taken immediately before and approximately five minutes after each test, respectively. (It should be noted that, because of the short-term hyperemia that was independent of abrasion injury, the five-minute photos are not always the best indication of the severity of *abrasion* but are used to present a pictorial representation of the skin condition immediately after the test.) As previously indicated, the abrasion results for these tests were not very dramatic, perhaps as a result of the deflection plate but perhaps also because distances of 250 and 300 mm are distances at which consistent and significant abrasions do not occur with the airbag systems used. Other factors that potentially reduced the occurrence and severity of abrasions in these tests are the orientation of the module relative to the orientation of the leg and precondition of the legs of female subjects with lotions and creams which was not controlled in these tests.

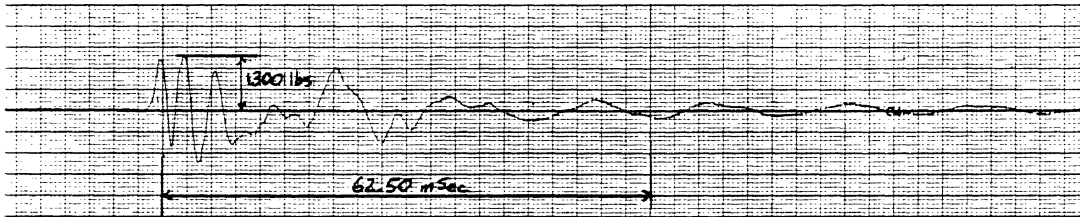
Air Bag Tests: Load Cell Measurements of Compression/Expansion Forces Behind Wheel

Recorder Settings  
Vertical 100 mV/div  
Paper Speed 100 div/sec  
Playback Speed 1/16 recorded

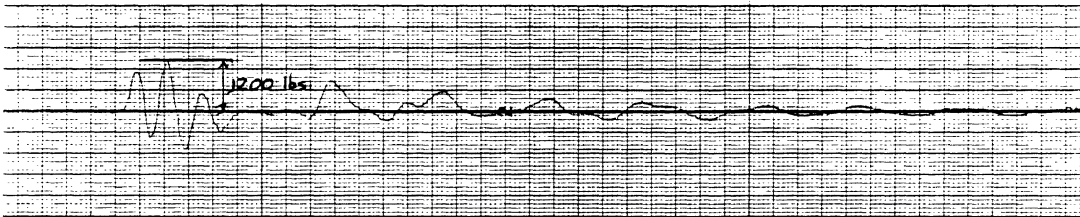
Load Cell Output  
1mVolt/lb

Graph Scale Values  
Force 100 lbs / div  
Time 0.6250 msec / div

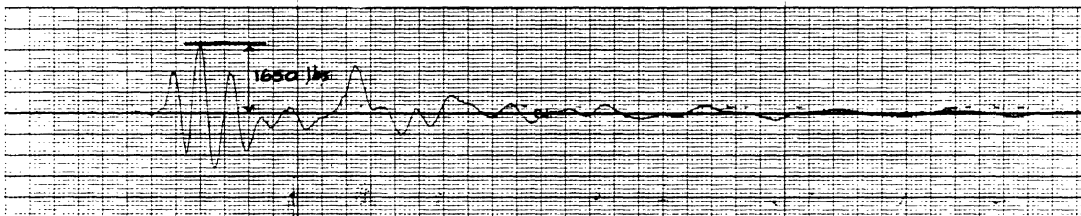
Test CB001T Bag to Subject Distance = 300 mm Bag Type L-28-3-T-85-420 December 14, 1990



Test CB002U Bag to Subject Distance = 300 mm Bag Type S-28-2-U-85-840 December 14, 1990



Test CB003T Bag to Subject Distance = 250 mm Bag Type L-28-3-T-85-420 December 14, 1990



Test CB004U Bag to Subject Distance = 350 mm Bag Type S-28-2-U-85-840 December 14, 1990

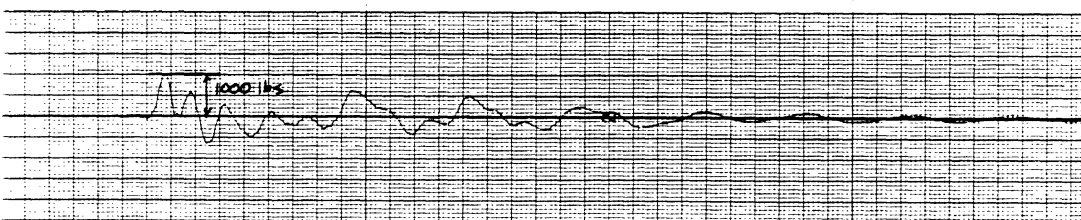


Figure 12. Force-time traces from load cell mounted between steering wheel and rigid support structure.

Table 11  
Abrasion Injury Scores for tests in the Taguchi Matrix

Test No.	Subject Gender	Deflect. Plate	Distance (mm)	Wheel Rotation	Inflator kPa	Bag Matl (denier)	Tether	Bag Fold	Abrasion Score
CA9107	F	Yes	300	0°	350	420	Yes	Rev	1
CA9108	F	Yes	300	0°	475	420	No	Rev	1
CA9109	F	Yes	250	0°	475	420	Yes	Acc	1
CA9110	F	Yes	250	0°	350	420	No	Acc	3
CA9111	F	Yes	300	0°	475	840	Yes	Acc	1
CA9112	F	Yes	300	0°	350	840	No	Acc	4
CA9113	F	Yes	250	0°	350	840	Yes	Rev	1
CA9114	F	Yes	250	0°	475	840	No	Rev	2

In spite of these minimal injury results, an injury score from 1 to 6 was assigned to each test based upon the first-hand observations and measurements of the team physician. These scores were used to conduct an analysis of the factors contributing to skin abrasion. As indicated by the scores in the last column of Table 11, all but three tests received an injury rating of 1, indicating that, in five tests, only hyperemia resulted from the contact of the airbag with the skin. For the last test in the series (CA9114) conducted at a distance of 250 mm using an untethered airbag with reverse-type fold and a 475-kPa inflator, petechial bleeding resulted. The two tests that produced abrasions of levels 3 and 4 were both for untethered airbags with 350-kPa inflators and accordion-type folds. The more serious abrasion occurred at a distance of 250 mm, while the less-severe abrasion occurred at 300 mm.

Table 12 contains the sum of the injury scores for each of the variable levels while Figure 13 shows a plot of the average injury score for each level of each factor. An inspection of these results indicates that the tether had the greatest influence on injury followed by airbag fold and inflator pressure. According to these test results, the addition of a tether and use of reverse-type folding reduce the potential for abrasion injuries and the 350-kPa inflator results in a greater potential for injury than does the 475-kPa inflator. This latter finding is contrary to expectations since the 475-kPa inflator should produce more energy and higher airbag material velocities. It should be kept in mind, however, that these results are based on only two abrasions with injury scores of 3 and 4, both of which occurred for the 350-kPa inflators. With only four subjects and eight tests in the total sample, the influence of subject skin variability or susceptibility to abrasion could be a confounding factor that is not accounted for. These results also suggest that there is no effect of distance between 250 and 300 mm, and that airbag

Table 12  
Sums of Abrasion Injury Scores from the  
Taguchi Matrix

Level*	Inflator Pressure	Distance	Pressure x Distance	Tether	Bag Fold	Distance x Tether	Bag Material
1	5	7	6	4	9	7	8
2	9	7	8	10	5	7	6
Sums	14	14	14	14	14	14	14

\*Level 1 = 475 kPa, 300 mm, tethered, accordion-type fold, and 840 denier.  
Level 2 = 350 kPa, 250 mm, untethered, reverse-type fold, and 420 denier.

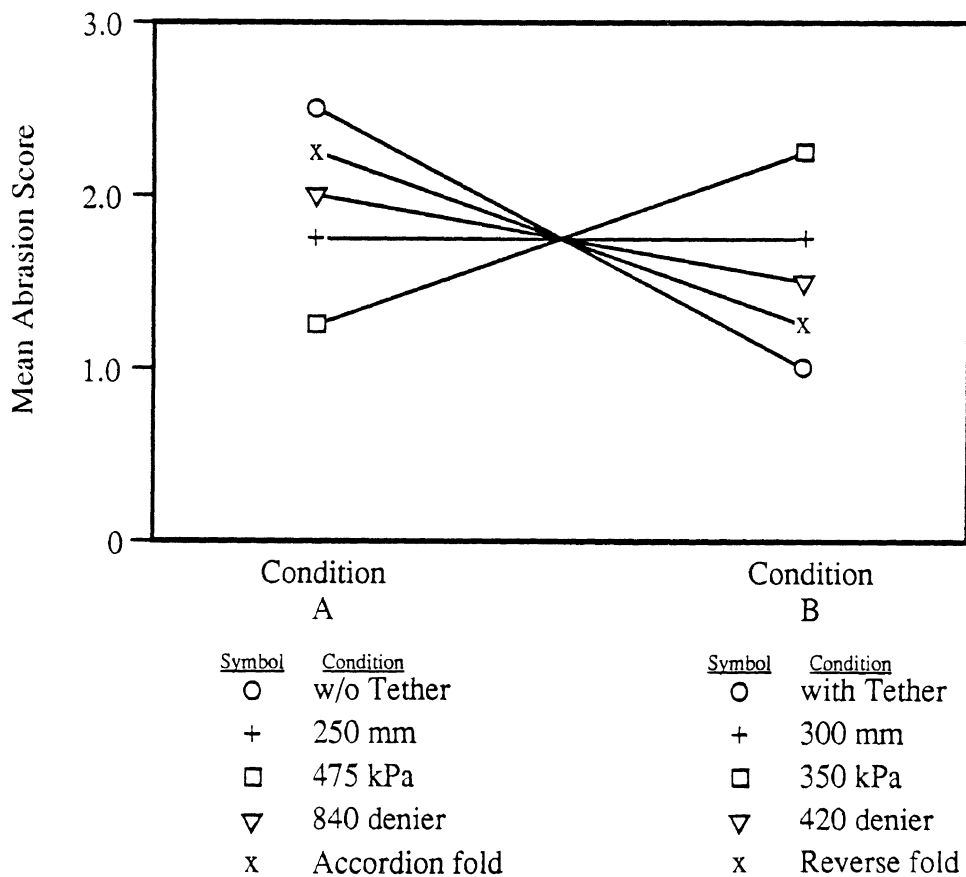


Figure 13. Plot of mean abrasion injury scores at two levels for different airbag and deployment factors and their interactions from Taguchi matrix of tests.

material has very little influence on abrasion for these test conditions. Also, the interactive effects of inflator pressure and distance, or distance and tether, appear to have little or no influence on abrasion.

Table 13 summarizes the results of analysis of variance on these data which supports the observations made above based on the sums and averages of injury scores. The tether has the strongest effect on abrasion at these distances with the presence of a tether reducing the injury potential. Inflator pressure and airbag fold play lesser roles as noted above.

Table 13  
Results of Analysis of Variance on  
Abrasion Scores from Tests in the Taguchi Matrix

Condition	DF	SS	MS	F Statistic
Inflator	1	2	2	8
Distance	1	0	0	-
Inf. x Dist.	1	.5	.5	-
Tether	1	4.5	4.5	18
Airbag Fold	1	2	2	8
Dist. x Tether	1	0	0	-
Airbag Material	1	.5	.5	-
Totals	7	9.5	9.5	

### 3.3 DEFLECTION PLATE EFFECTS

Subsequent to obtaining rather minimal abrasion results from the eight tests in the Taguchi Matrix, further evaluation of the effects of the chest deflection plate seemed warranted before proceeding. The test conditions used in four tests are repeated in Table 14 along with the abrasion injury scores obtained. Photographs of the subjects' legs before and after each of these tests are contained in Appendix B. For each distance of 300 mm and 350 mm used, two tests were conducted on one subject using an untethered airbag with 475-kPa inflator and accordion-type folding. One test was conducted with the chest deflection plate and the other without the plate.

Table 14  
Abrasion Results from Tests to Evaluate  
Chest Deflection Plate Effects

Test No.	Subject Gender	Deflect. Plate	Distance (mm)	Wheel Rotation	Inflator kPa	Bag Matl (denier)	Tether	Bag Fold	Abrasion Score
CA9115	F	Yes	300	0°	475	840	No	Acc	2
CA9116	F	No	300	0°	475	840	No	Acc	4
CA9117	F	Yes	350	0°	475	840	No	Acc	4
CA9118	F	No	350	0°	475	840	No	Acc	4

As indicated, at a distance of 300 mm an abrasion score of 2 (i.e., no abrasion) was obtained when the deflection plate was used while an abrasion score of 4 was obtained without the deflection plate. At a distance of 350 mm, both tests resulted in an abrasion score of 4. While these findings did not clarify the value of the chest deflection plate with regard to producing appropriate airbag kinematics relative to the occurrence of abrasions, they did raise concerns about differences in the effects of the deflection plate on abrasion for different distances and variability in the energy taken up by the deflection plate which was not easily controlled. Because of these concerns and the desire to more cleanly study the effects of airbag fold and deployment kinematics on airbag abrasion, it was decided to not use the chest deflection plate in further testing.

### 3.4 DETERMINATION OF ABRASION DISTANCES

The injury scores assigned to tests conducted in the stage of testing aimed at determining the distances for which abrasions are consistently produced are summarized in Table 15, while the five-minute post-test photos of the targeted skin areas for these tests are provided in Appendix B. A separate analysis of these injury results was not conducted but a review of the injury scores indicates that a substantial number of abrasions at Level 5 were produced when the steering wheel and module were rotated 90 degrees to the normal position. Except for two instances, these tests used 840-denier untethered airbags with accordion-type folds and 475-kPa inflators. Two tests were conducted with tethered airbags with 475-kPa inflators and accordion-type folding. Distances ranged from 225 mm to 350 mm.

All tests at 225 mm, including one with a tethered airbag, produced abrasion scores of 5. Also, the two tests at 350 mm with untethered airbags produced abrasions at

Table 15  
Abrasion Injury Scores from Tests to Determine Abrasion Distances

Test No.	Subject Gender	Deflect. Plate	Distance (mm)	Wheel Rotation	Inflator kPa	Bag Matl (denier)	Tether	Bag Fold	Abrasion Score
CA9119	F	No	350	0°	475	840	No	Acc	3
CA9120	F	No	300	0°	475	840	No	Acc	4
CA9121	F	No	300	0°	475	840	No	Acc	1
CA9122	F	No	250	0°	475	840	No	Acc	4
CA9123	F	No	300	90°	475	840	No	Acc	1
CA9124	F	No	250	90°	475	840	No	Acc	5
CA9125	F	No	250	90°	475	840	No	Acc	1
CA9126	F	No	225	90°	475	840	No	Acc	5
CA9127	F	No	250	90°	475	840	No	Acc	5
CA9128	F	No	225	90°	475	840	No	Acc	5
CA9129	F	No	350	90°	475	840	No	Acc	4
CA9130	F	No	325	90°	475	840	No	Acc	3
CA9131	F	No	250	90°	475	420	Yes	Acc	1
CA9132	F	No	225	90°	475	420	Yes	Acc	5
CA9133	M	No	350	90°	475	840	No	Acc	5
CA9134	M	No	300	90°	475	840	No	Acc	5
CA9135	M	No	250	90°	475	840	No	Acc	5
CA9136	M	No	225	90°	475	840	No	Acc	5

Levels 4 and 5. Two of the tests in which no abrasions resulted (i.e., an injury rating of 1) were for untethered airbags at distances of 250 and 300 mm, while one test with no abrasions was for a tethered airbag at a distance of 250 mm. As a result of these findings, a decision was made to use a distance of 225 mm and a steering wheel rotated 90 degrees from the normal position in a Full-Factorial Matrix of tests designed to evaluate the influence of inflator pressure, tethering, and airbag fold on skin abrasion.

### 3.5 FULL-FACTORIAL MATRIX

Table 16 summarizes the test conditions and resulting injury scores for the final eight tests in this study comprising the Full-Factorial Matrix on the variables of inflator pressure, airbag fold, and tether. Figure 14 provides a graphical summary of these results by showing the abrasion injury scores for each of the different test conditions. It can first be noted that there is little difference in total injury scores (i.e., areas under the two sets of bar graphs) for the tests with the two different inflators, although the higher inflator pressure did produce a slightly greater total injury score (15 vs. 12). Also, except for the conditions of accordion-type folding and 475-kPa inflator, the presence of a tether resulted in a reduction of the severity of abrasion injuries. The most dramatic effect is seen to occur between the accordion- and reverse-type folding, whereby the reverse-type folding resulted in a significantly lower injury level for both tethered and untethered conditions. This effect is observed at both inflator pressures although the effect is most dramatic for the 350-kPa inflator. The sums of the injury scores with the 475-kPa inflator are 10 and 5 with the accordion- and reverse-type folds, respectively. With the 350-kPa inflator, these sums are 9 and 3.

Figure 15 plots the mean injury scores for the different combinations of tether and airbag-fold conditions where the results at the two inflator pressures have been combined. These mean scores are summarized in Table 17 and further demonstrate the dramatic effect of airbag folding technique on reducing injury levels with both tethered and untethered conditions. They also show the effect of tethering for both fold conditions, with the injury-reducing effects of a tether appearing to be much greater for reverse-type folding than for accordion-type folding.

The relative effects of these factors are further compared in Figure 16 which was compiled by grouping the injury results into *no abrasion* (injury scores of 1 and 2) and *abrasion* (injury scores of 3 through 6). As indicated, all tests with the accordion-type



Table 16  
Abrasion Injury Scores from tests in the Full-Factorial Matrix

Test No.	Subject Gender	Deflect. Plate	Distance (mm)	Wheel Rotation	Inflator kPa	Bag Matl (denier)	Tether	Bag Fold	Abrasion Score
CA9137	M	No	225	90°	475	420	No	Acc	5
CA9138	M	No	225	90°	475	420	Yes	Acc	5
CA9139	M	No	225	90°	475	420	No	Rev	4
CA9140	M	No	225	90°	475	420	Yes	Rev	1
CA9141	M	No	225	90°	350	420	No	Acc	5
CA9142	M	No	225	90°	350	420	Yes	Acc	4
CA9143	M	No	225	90°	350	420	No	Rev	2
CA9144	M	No	225	90°	350	420	Yes	Rev	1

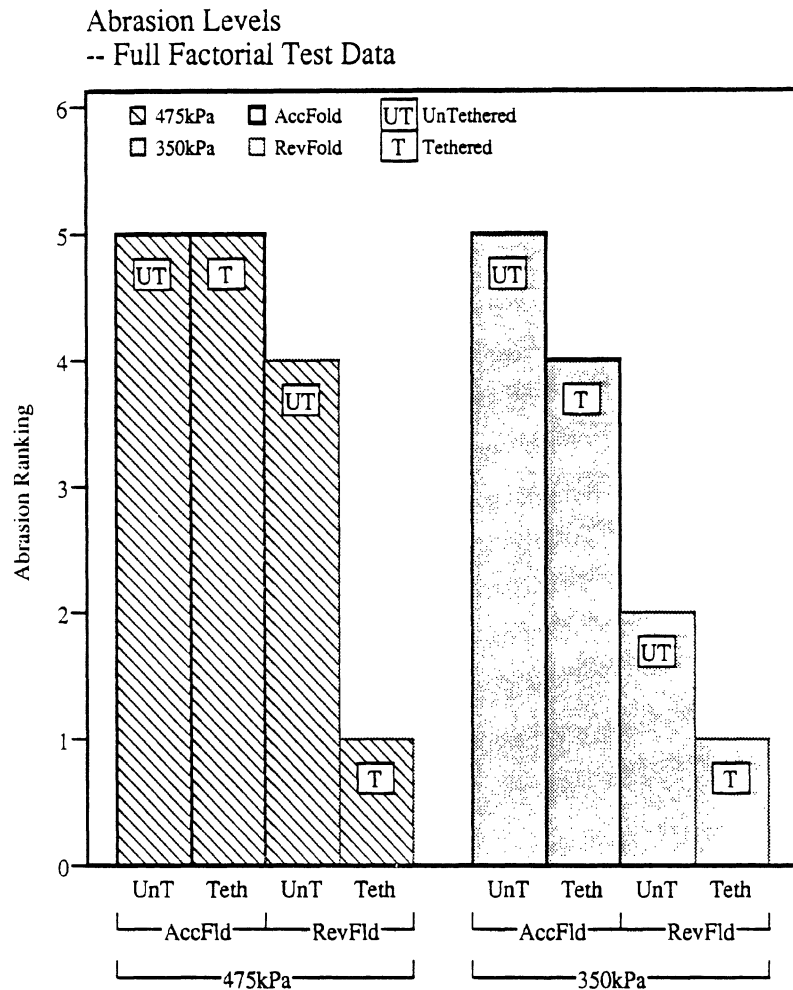


Figure 14. Bar graph of mean injury scores for different test conditions used in the full-factorial matrix.

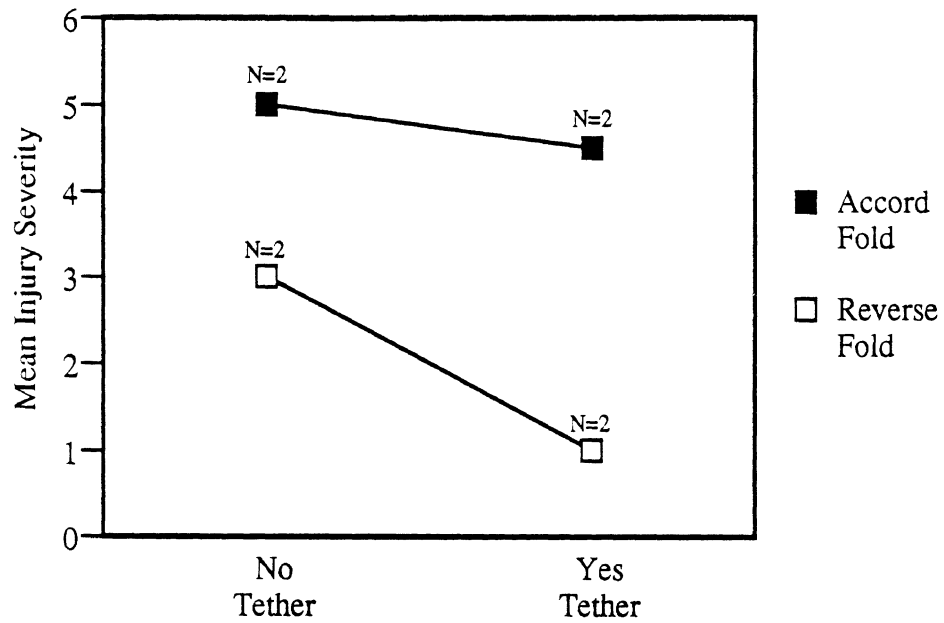


Figure 15. Plot of mean injury scores for different combinations of tether and fold in the full-factorial matrix.

Table 17  
Mean Injury Scores for Combinations of  
Tether and Airbag-Fold Conditions from Tests in the  
Full-Factorial Matrix

	Reverse-type fold	Accordion Fold	Row Means
No Tether	3	5	4
Tether	1	4.5	2.75
Column Means	2	4.75	3.375

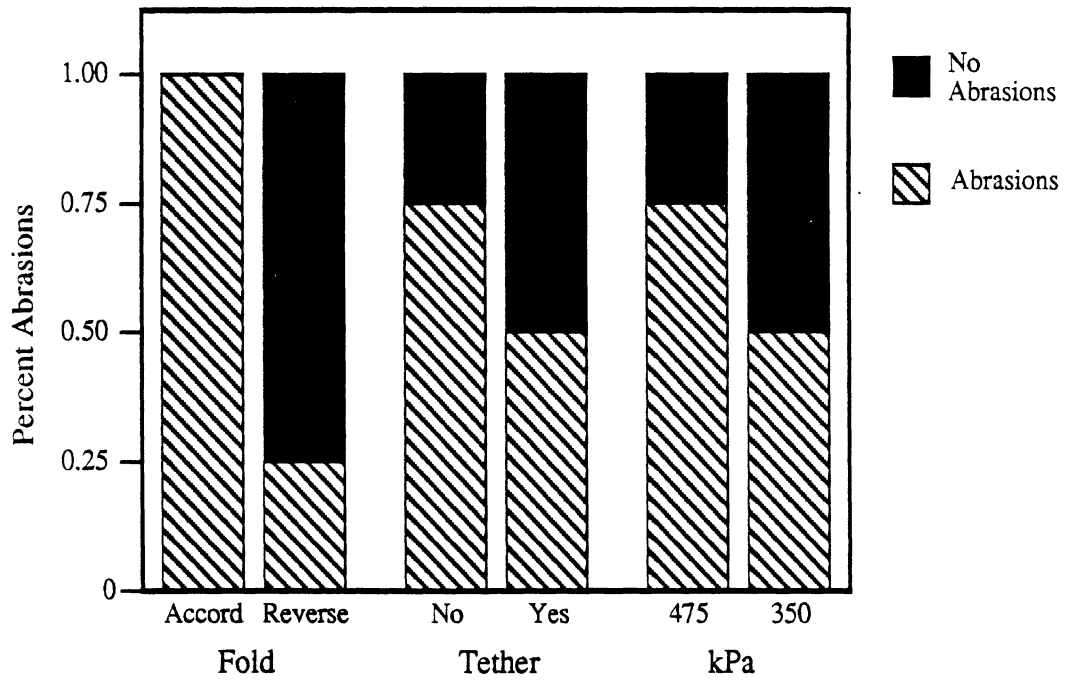


Figure 16. Plot of percentages of *abrasions* and *no abrasions* from contingency tables derived from the full-factorial matrix.

fold resulted in abrasion-level injuries, while only 25% of tests with the reverse-type fold resulted in abrasions. Without a tether, 75% of the tests resulted in abrasions, while with a tether, 50% of the tests produced abrasion injuries. For inflator pressure, the results are similar with 75% of tests with the 475-kPa inflator producing abrasion and 50% of the 350-kPa tests producing abrasion.

Table 18 summarizes the results of analysis of variance applied to the injury scores and test conditions of the full-factorial matrix. As indicated by the *F*-statistic values, these results confirm the observations previously made that airbag fold has the most dramatic effect on abrasion injuries, followed by a marginal effect of tethering, and a very weak effect of inflator pressure. No significant interaction effects between tether and pressure, pressure and fold, tether and fold, or pressure, tether, and fold are indicated by these results.

Table 18  
Results of Analysis of Variance on  
Abrasion Scores from the Full-Factorial Matrix

Condition	DF	SS	MS	F Statistic	p
Pressure -P	1	1.125	1.125	<2.00	
Tether-T	1	3.125	3.125	3.95	<0.25
P x T	1	.125	.125		
Fold-F	1	15.125	15.125	24.20	<0.05
P x F	1	.125	.125	8	
T x F	1	1.125	1.125		
P x T x F	1	1.125	1.125		

### 3.6 COMPILATION OF RESULTS FROM ALL TESTS

Figures 17a and 17b show the overall composition of the 38 tests for which abrasion injury scores were determined. Note that the preliminary tests are not included since abrasion injury scores were not assigned to these tests due to the fact that a physician was not on site to examine the skin at the time of the test. While taken together, the complete sample of tests does not equally represent all of the factors and their interactions, analyses of the combined data base can offer additional insight into the factors involved in abrasion injuries.

### Test Summary

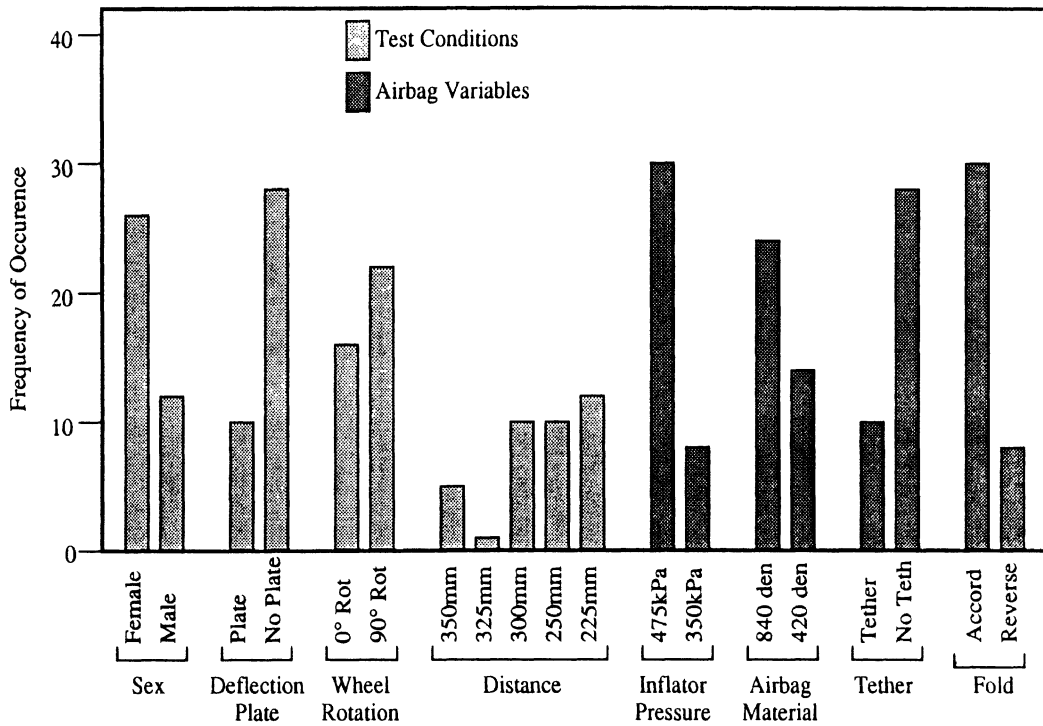


Figure 17a. Bar graph showing numbers of tests conducted with different airbag and deployment test conditions.

### Test Summary

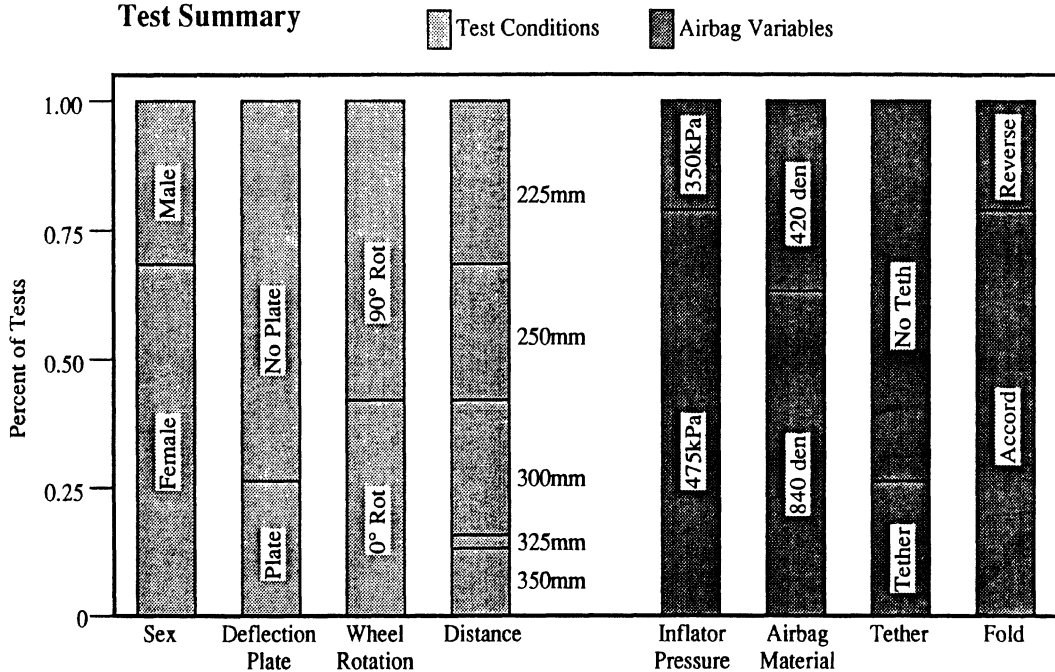


Figure 17b. Percentages of tests involving the different levels of deployment and airbag conditions.

### 3.6.1 Contingency-Table Analysis

An alternative analysis technique to ANOVA is contingency-table analysis, which is often called log-linear modeling. For this analysis of the injury data from the 38 tests, the injuries are divided into the two categories of *abrasion* or *no abrasion* as described previously. For each treatment (test condition) of interest, a contingency table is constructed with the counts of observations placed in the appropriate cells based on test conditions and injury results (*abrasion* versus *no abrasion*).

Tables 19a through 19c are the contingency tables for airbag fold, tether, and inflator pressure. Analysis of these data involves the following procedure. For each cell, a number is found that represents the number of observations that should be in that cell if a particular model is appropriate. In Table 19a, for example, these numbers would represent the number of observations expected in each cell assuming that the two variables, fold and abrasion, have no relationship. The actual numbers in the tables are then compared to the expected cell frequencies using the chi-square statistic. If the actual and expected cell frequencies are significantly different, the chi-square statistic will be large, indicating that the two variables are not independent and that a relationship exists.

As shown by the chi-square statistic at the top of each table, these results confirm the findings of the full-factorial tests that airbag fold technique has a significant effect on abrasion injuries, with reverse-type folding resulting in fewer abrasions than accordion-type folding. The results for airbag tether further substantiate and strengthen the previous observation that a tether reduces abrasions. The results for inflator pressure indicate that this variable has very little influence on abrasions for the levels tested and the other conditions of these tests.

These results are illustrated graphically in Figure 18 which shows the percentages of *abrasions* and *no abrasions* for the three factors. In looking at these percentages, it is important to note that the number of tests for each variable is not the same but rather is as indicated in Tables 19a through 19c.

The contingency-table technique can also be used to conduct more complex analyses and examine the interactions of different variables. From the full-factorial tests, for example, analysis of variance had shown that there was no interaction between tether

Table 19a  
 Contingency Tabulation and Chi-Square Statistic  
 for Effects of *AIRBAG FOLD TECHNIQUE* on Skin Abrasion  
 from Combined Data Base

<b>Chi-Square = 11.176 (p=0.0008)</b>			
EFFECT	REVERSE	ACCORDION	TOTALS
NO ABRASION	7	7	14
ABRASION	3	21	24
TOTALS	10	28	38

Table 19b  
 Contingency Tabulation and Chi-Square Statistic  
 for Effects of *TETHER* on Skin Abrasion  
 from Combined Data Base

<b>Chi-Square = 6.412 (p=0.0113)</b>			
EFFECT	TETHERED	UNTETHERED	TOTALS
NO ABRASION	7	7	14
ABRASION	1	23	24
TOTALS	8	30	38

Table 19c  
 Contingency Tabulation and Chi-Square Statistic  
 for Effects of *INFLATOR PRESSURE*  
 on Skin Abrasion from Combined Data Base

<b>Chi-Square = 0.754 (p=0.3852)</b>			
EFFECT	350 kPA	475 kPA	TOTALS
NO ABRASION	4	10	14
ABRASION	4	20	24
TOTALS	8	30	38

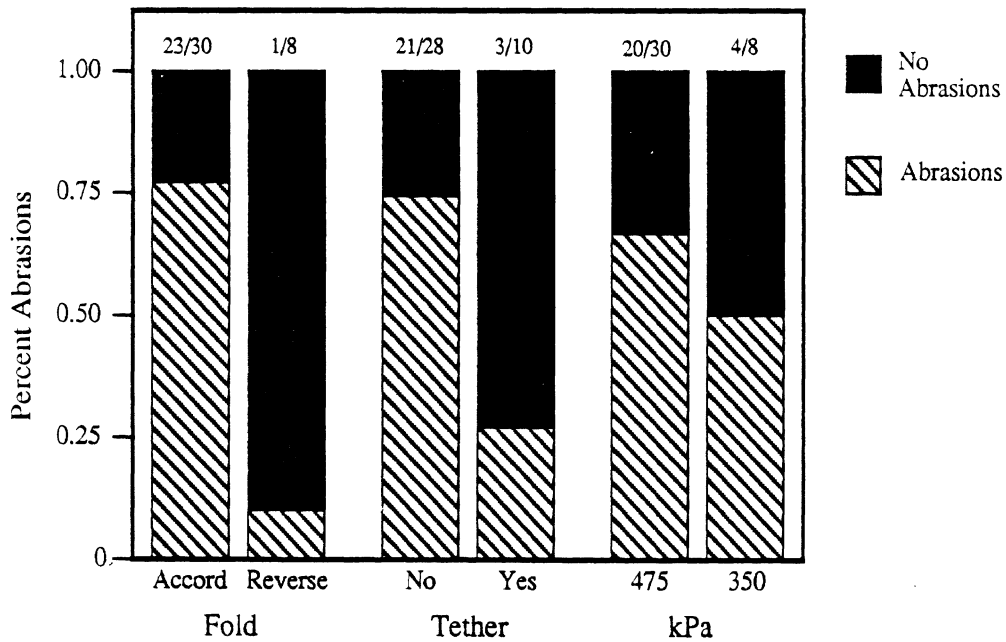


Figure 18. Plot of percentages of *abrasions* and *no abrasions* from contingency tables derived from the combined data base.

Table 20  
Three-Way Contingency Table for Fold, Tether, and Abrasion  
from the Combined Data Base

G-Square = 0.418 (p=0.5182)					
INJURY	NO TETHER		WITH TETHER		TOTALS
	Reverse	Accordion	Reverse	Accordion	
ABRASION	3 3.170	4 3.830	4 3.83	3 3.170	14
NO ABRASION	1 0.830	20 20.17	0 0.170	3 2.830	24
TOTALS	4	24	4	6	38

Note: In each cell, actual frequencies are listed above expected frequencies.



and fold. However, Figure 15 suggests that the tether might work better with reverse-type folding than with accordion-type folding. Table 20 shows a three-way contingency table for fold, tether, and abrasion and includes the expected values for each cell assuming no interaction between fold and tether in producing abrasion. Visual inspection of the table along with the G-square value of 0.418 ( $p=0.5182$ ) (same as chi-square but used in more complicated analyses) support the ANOVA results as being correct in that there is no evidence that the tether works differently for the different folds.

This observation is further substantiated by looking at the mean injury scores, rather than the frequencies of abrasions. These values are shown in Table 21 and plotted in Figure 19 for tether and airbag fold conditions for the combined data base. As with the three-way contingency table analysis, the results indicate similar effects of tether for both the reverse- and accordion-type folding. Again, however, the differences in the sample sizes for the four data points should be noted.

It is also interesting to note the relative effects of tether and airbag fold from the mean injury score data displayed in Table 21 and Figure 19. The mean injury score is seen to drop from 3.83 to 2.83 for accordion-type folding and from 2.25 to 1.0 for reverse-type folding with the addition of a tether. Going from accordion-type folding to reverse-type folding, the mean injury score is seen to drop from 3.83 to 2.24 for untethered airbags, and from 2.83 to 1.0 for the tethered airbags. While keeping in mind the nature of this combined data base and the differences in sample size for the different mean injury scores, these data further support the findings that airbag fold technique has a stronger *overall* effect on the severity of abrasions than does airbag tethering.

### 3.6.2 Effect of Distance on Abrasion Injuries

One of the goals of this study was to determine the distance or range of distances at which abrasion occurs during airbag deployment. In a previous study with anesthetized pigs, abrasions had resulted from tests conducted at 240 mm with both tethered and untethered airbags with 475-kPa inflators, but no abrasions were found at 260 mm. As described in Section 2.3, it was eventually concluded from the "Determination-of-Abrasion-Distance" test series that a distance of 225 mm was needed to *consistently* produce abrasions with a 475-kPa inflator and untethered airbag. This is in general agreement with the findings from tests with anesthetized pigs. However, in

Table 21  
 Mean Injury Scores for Combinations of  
 Tether and Airbag-Fold Conditions for  
 the Combined Data Base

	Reverse Fold		Accordion Fold	
	Mean	N	Mean	N
No Tether	2.25	4	3.83	24
Tether	1.00	4	2.83	6

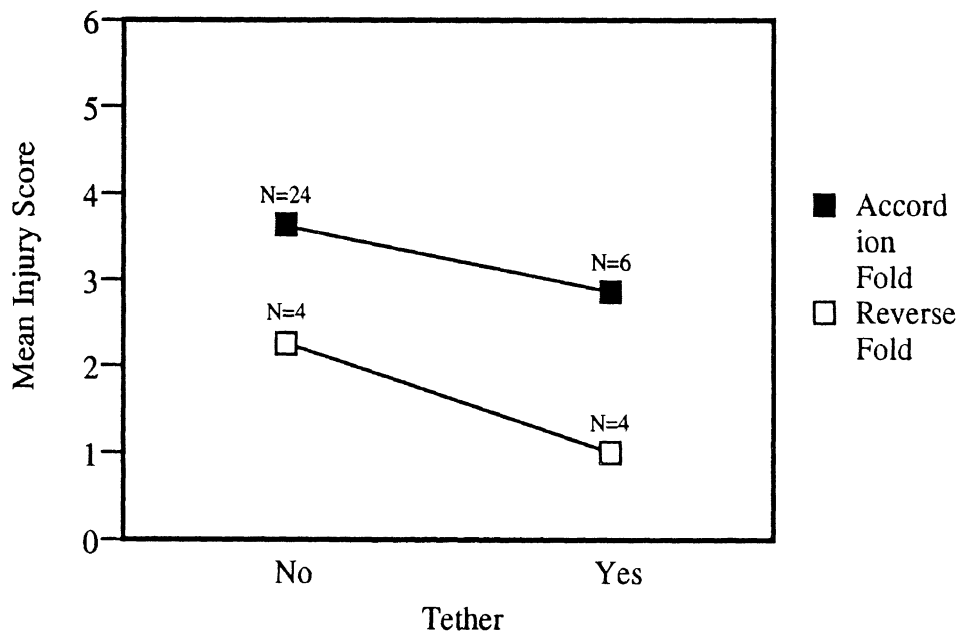


Figure 19. Plot of mean injury scores for different combinations of tether and fold from the combined data base.

preliminary tests with human volunteers, abrasions were obtained for tests conducted at distances ranging from 250 to 350 mm, and it was subsequently found that abrasions could result using distances ranging from 225 mm to 350 mm. Overall, however, there was a general impression that abrasions are more likely to occur with untethered airbags if the distance is between 300 and 350 mm than if the distance is between 250 and 300 mm.

In order to take a closer look at this issue, the contingency table for distance and abrasion shown in Table 22 was constructed. As indicated by the chi-square value, a relationship between the two variables exists. Figures 20a and 20b show this relationship graphically using the abrasion/no abrasion categorization and the mean injury score at the different distances. In both cases, a U-shaped effect of distance on abrasion is indicated where abrasions are more likely and/or more severe at both close (225 to 250 mm) and far (325 to 350 mm) distances. While this relationship seems real, the influence of the deflection plate on eight of the tests conducted at 250 and 300 mm may be a confounding factor and further investigation of this observation is warranted.

Table 22  
Contingency Tabulation and Chi-Square Statistic  
for Effects of *DISTANCE* on Skin Abrasion  
from Combined Data Base

<b>Chi-Square = 7.272 (p=0.0637)</b>						
EFFECT	DISTANCE (mm)					TOTALS
	225	250	300	325	350	
NO ABRASION	3	5	6	0	0	14
ABRASION	9	5	4	1	5	24
TOTALS	12	10	10	1	5	38

### 3.6.3 Effect of Tether by Distance

In the analysis of variance of the full-factorial test results, the effect of tether was found to be marginal, while in the contingency-table analysis, the effect was quite strong. An obvious candidate to explain this difference is the fact that all tests in the full-factorial design were conducted at 225 mm where the tether might be expected to have much less effect.

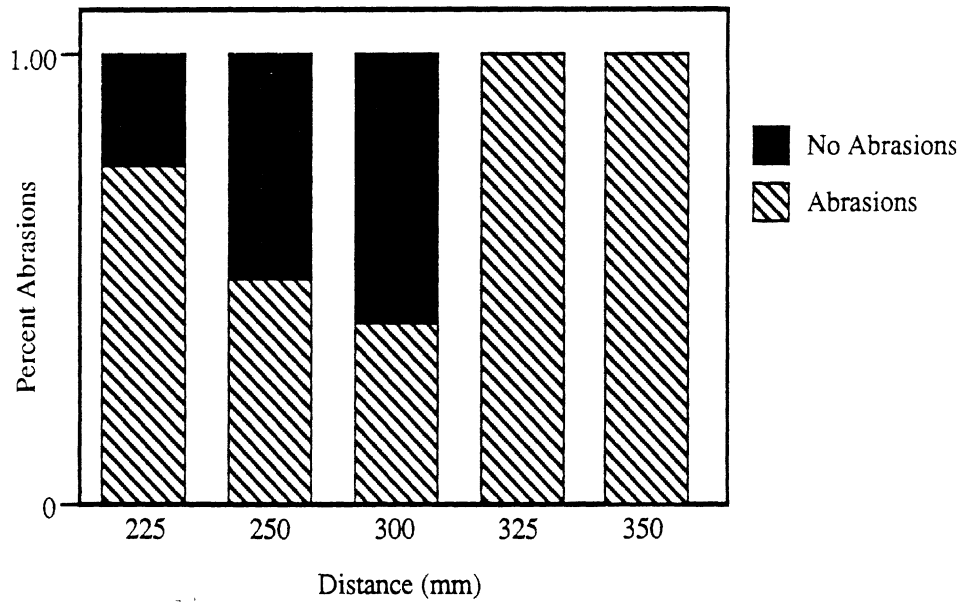


Figure 20a. Plot of percentage of tests producing *abrasions* and *no abrasions* at different distances for the combined data base.

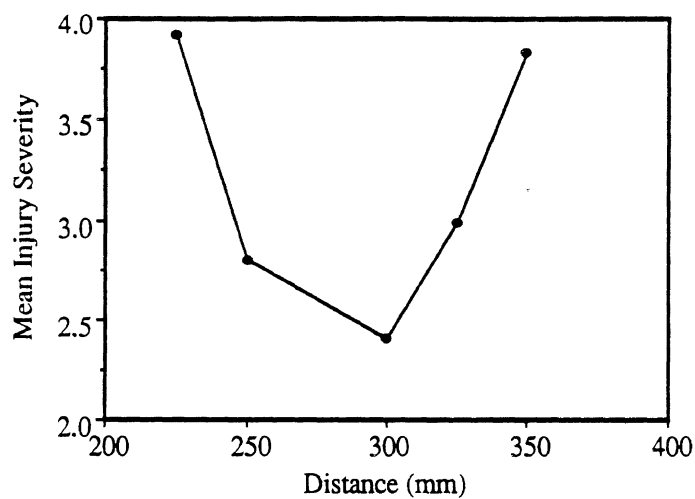


Figure 20b. Plot of mean injury scores at different distances for the combined data base.

While it was quite obvious from the test results that the tether has a dramatic effect in preventing abrasions for distances above 300 mm since no abrasions resulted from tests with tethered airbags for distances of 250 mm or greater, Table 23 and the bar graph of Figure 21 were constructed to take a closer look at this issue. The G-square value of 1.843 ( $p=0.379$ ) in the three-way contingency table indicates that there is not a significant interaction between distance and tether while the bar graph supports the hypothesis of tether/distance interaction, with the tether having a pronounced effect for distances of 250 mm and greater.

It is suspected that the discrepancy between statistical results and visual observations could be a result of the small numbers of observations in some columns of the contingency table. Whatever the reason, however, the effect of the tether in reducing abrasions at 225 mm, which is well short of the tethered distance, is worth noting. An explanation for this possible and unexpected benefit (which was not seen in the pig tests) is not immediately apparent, but may be due to the effect of the tether on airbag kinematics even before the restrictive effects of the tether are imposed as discussed below. Further testing with tethered and untethered airbags at distances of 225 mm is needed to confirm the potential benefits of a tether at these distances.

### 3.7 MECHANISMS OF ABRASIONS

In the course of conducting the airbag deployment tests into the legs of human volunteers, two primary types of airbag kinematics corresponding to the two types of airbag fold technique (accordion-type and reverse-type) were noted from the high-speed films. With accordion-type folding, the two primary flaps of the airbag deploy to the left and right (top and bottom with the steering wheel rotated 90 degrees). This type of kinematics is illustrated in Figure 22 which shows one frame of the high-speed film taken at 3000 fps from two of the deployments in the full-factorial test matrix. The tests shown are for an untethered and tethered airbag, respectively, each with accordion-type folding and 350-kPa inflator. It will be noted that, for the untethered airbag, the top flap with the steering wheel rotated 90 degrees, extends out further than the bottom flap and reaches the leg first. With the tethered airbag, the two flaps extend out together and reach the leg almost simultaneously.

Table 23  
 Three-Way Contingency Table for Tether, Distance, and Abrasion  
 from the Combined Data Base

<b>G-Square = 1.483 (p=0.379)</b>										
INJURY	225 mm		250 mm		300 mm		350 mm		TOTALS	
	Teth	No Teth	Teth	No Teth	Teth	No Teth	Teth	No Teth		
ABRASION	1 0.49	2 2.51	2 2.38	3 2.62	4 4.13	2 1.87	0 0.0	0 0.0	14	
NO ABRASION	6 6.51	3 2.49	5 4.62	0 0.38	4 3.87	0 0.13	5 5.0	0 0.0	24	
TOTALS	7	5	7	3	8	2	5	0	38	

Note: In each cell, actual frequencies are listed above expected frequencies.

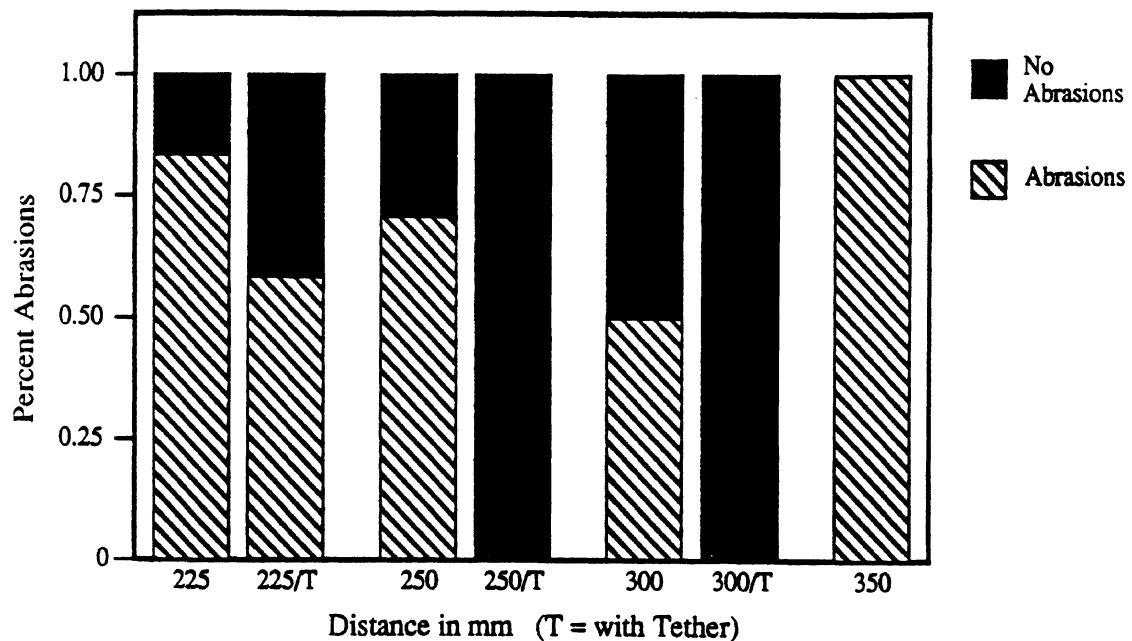


Figure 21. Effect of tether on abrasion frequency at different distances for the combined data base.

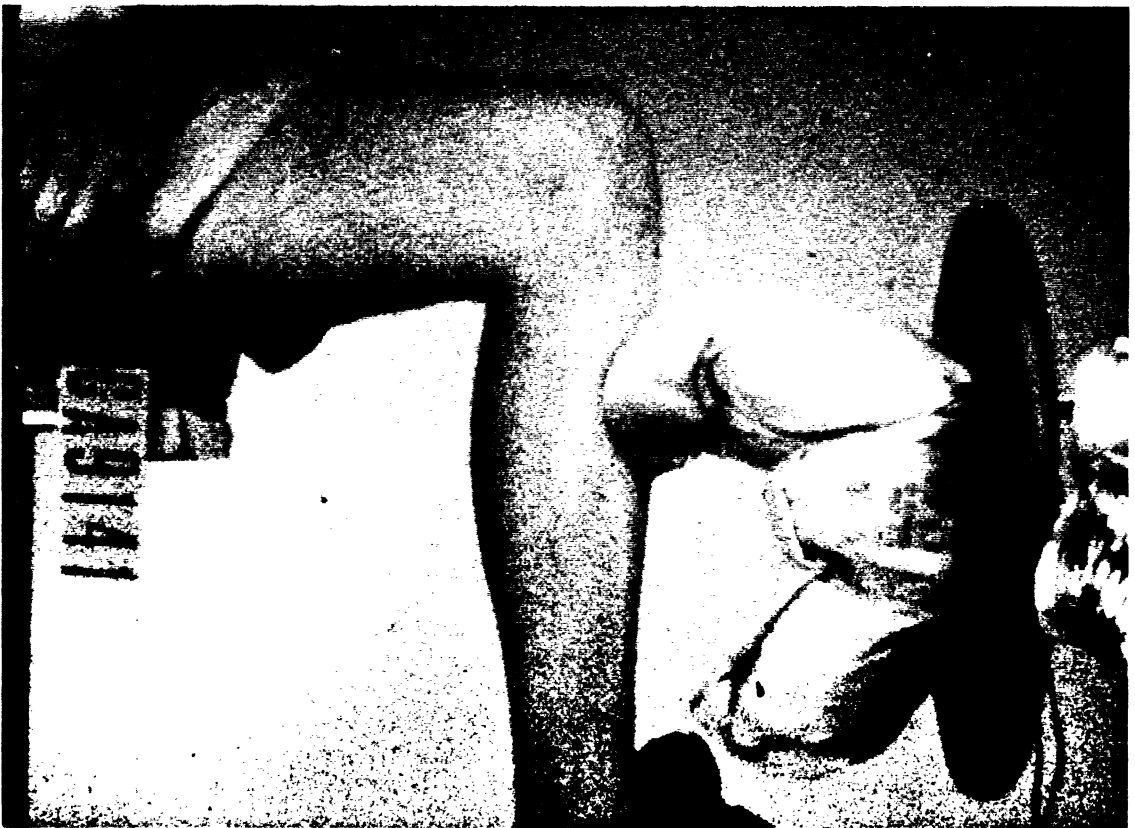
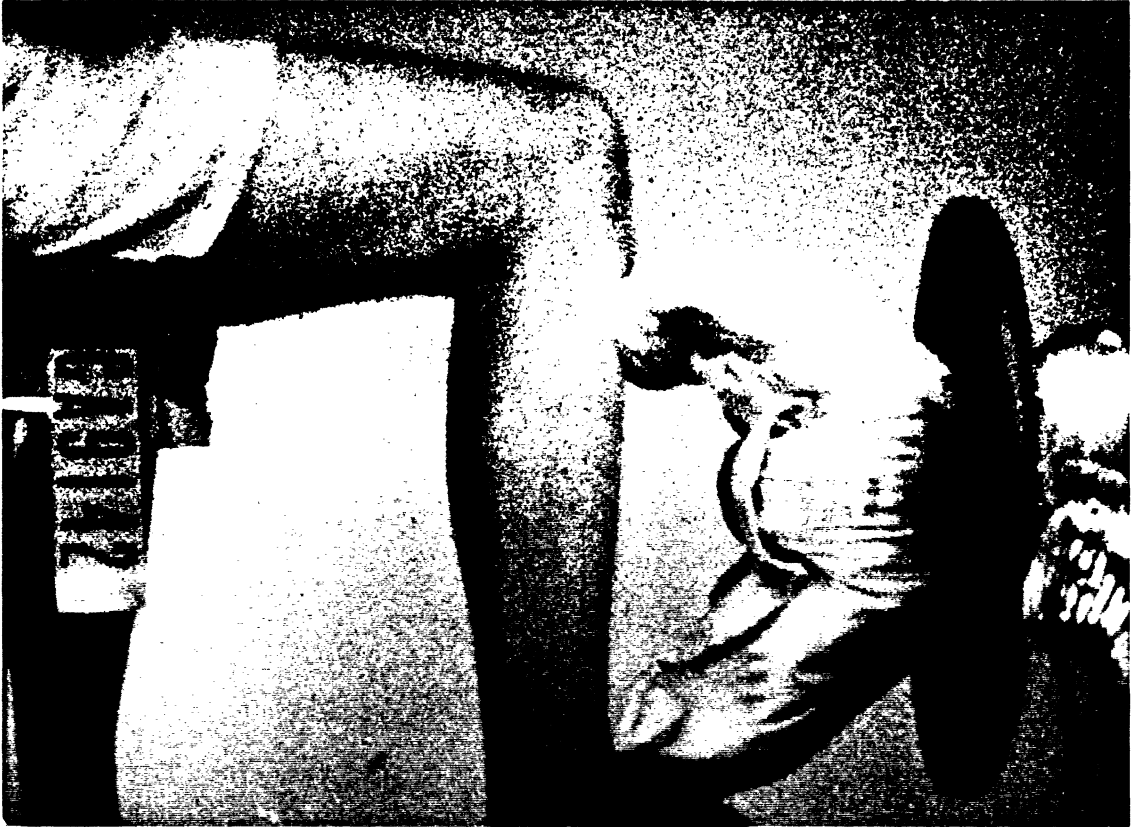


Figure 22. Side-view, stop-action photographs from high-speed films of untethered (top) and tethered (bottom) airbags with *accordion-type folding*. Steering wheel and module have been rotated 90 degrees from straight-ahead driving orientation.





The skin contact and injury regions corresponding to impact of the skin by these partially inflated folds of airbag material are clearly evident in the photos of Figure 23 and are above and below the center of the target area. In addition, Figure 24 shows the colored markings on the airbag surfaces picked up from the skin in two tests with untethered airbags. The streaked patterns demonstrate the wiping action of the airbag upward and downward along the front of the tibia. While the colored streaks extend mostly along the full length of the midline of the airbag surface, it is the markings near the top of the airbags near the seams that correspond to the markings on the skin closest to the site of primary hyperemia and abrasion.

With reverse-type folding, the airbag kinematics and interaction with the skin surface are quite different. Figure 25 shows single frames taken from 3000-fps high-speed films of two tests with airbags installed with reverse-type folding and 475-kPa inflators, one untethered and the other tethered. In both cases, the airbag deploys so that the leading edge is at the center of the airbag which contacts the skin surface near the center of the target area. As illustrated in Figure 26, abrasions resulted with the untethered airbag but only a small area of hyperemia resulted from the tethered airbag. In each case, the pattern of skin contact is significantly different from that found with accordion-type folding. In addition to being at the center of the target area instead of above and below the center, the contact is more of a stamping or imprinting type of contact than a wiping action. This is also evident from the photos of Figure 27 which show the imprints of the colored markings picked up by the airbag surface. The colors are picked up with amazingly little smearing and are located near the center of the airbag surface.

### 3.8 ESTIMATIONS OF AIRBAG VELOCITIES

For the eight tests in the full-factorial matrix, high-speed films were taken at 3000 fps and velocities of the leading edge of the airbag during deployment were roughly estimated by film analysis as described in Section 2.4. Table 24 shows the average velocities for the first half and second half of deployments, where the halfway point is the mid-distance between the undeployed module cover and the center of the surface of the targeted area on the tibia (i.e., half of 225 mm or about 112 mm).



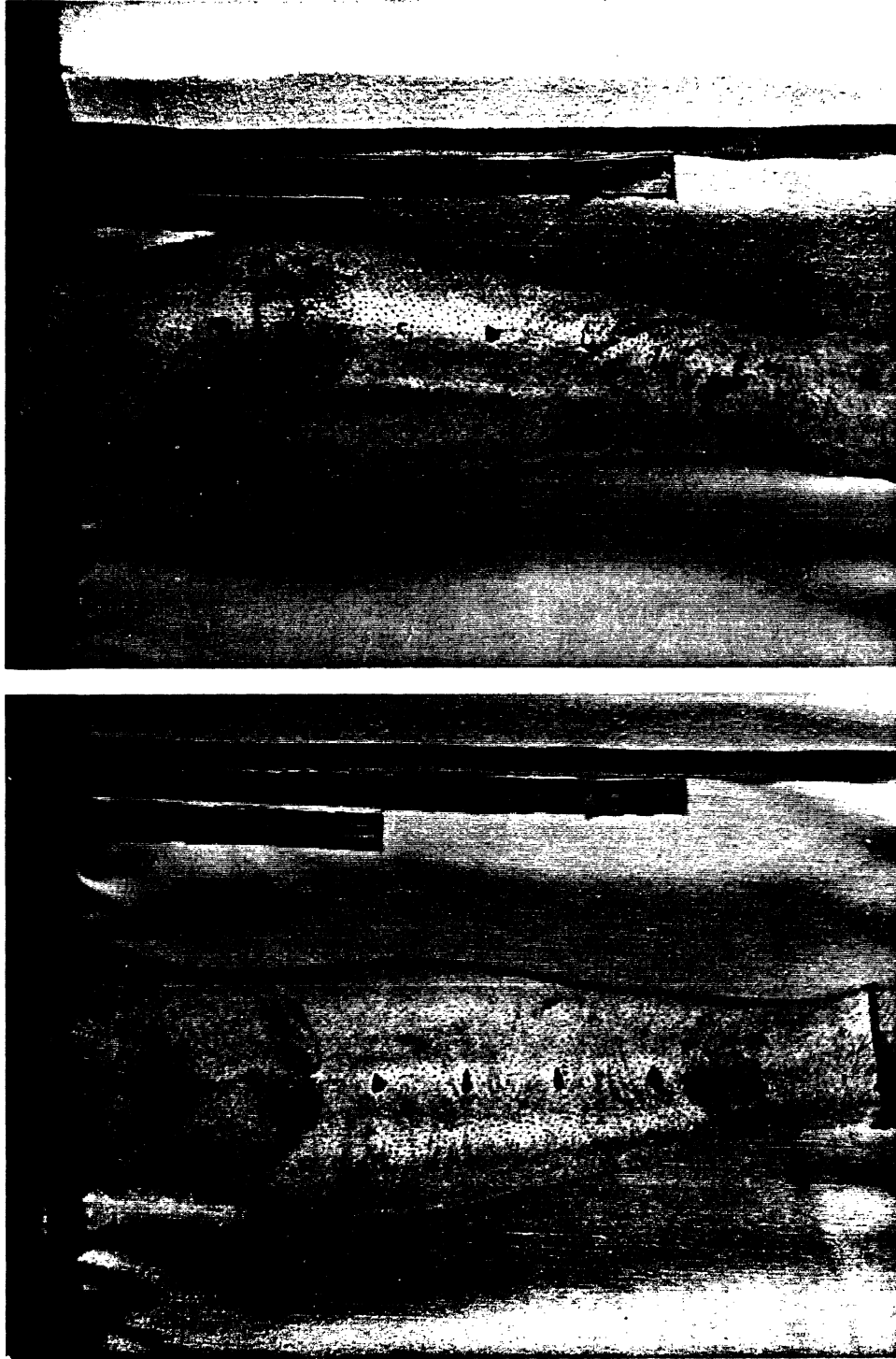


Figure 23. Abrasions and erythema resulting from deployments of airbags installed in module with *accordion-type fold*. Note areas of significant abrasion above and below the center of targeted area.





Figure 24. Surfaces of airbags with *accordion-type folding* showing smeared colors along the centerline of the bag that were picked up from the subject's leg.





Figure 25. Side-view, stop-action photograph from high-speed films of untethered (top) and tethered (bottom) airbags with *reverse-type folding*. Steering wheel and module have been rotated 90 degrees from the straight-ahead driving orientation.





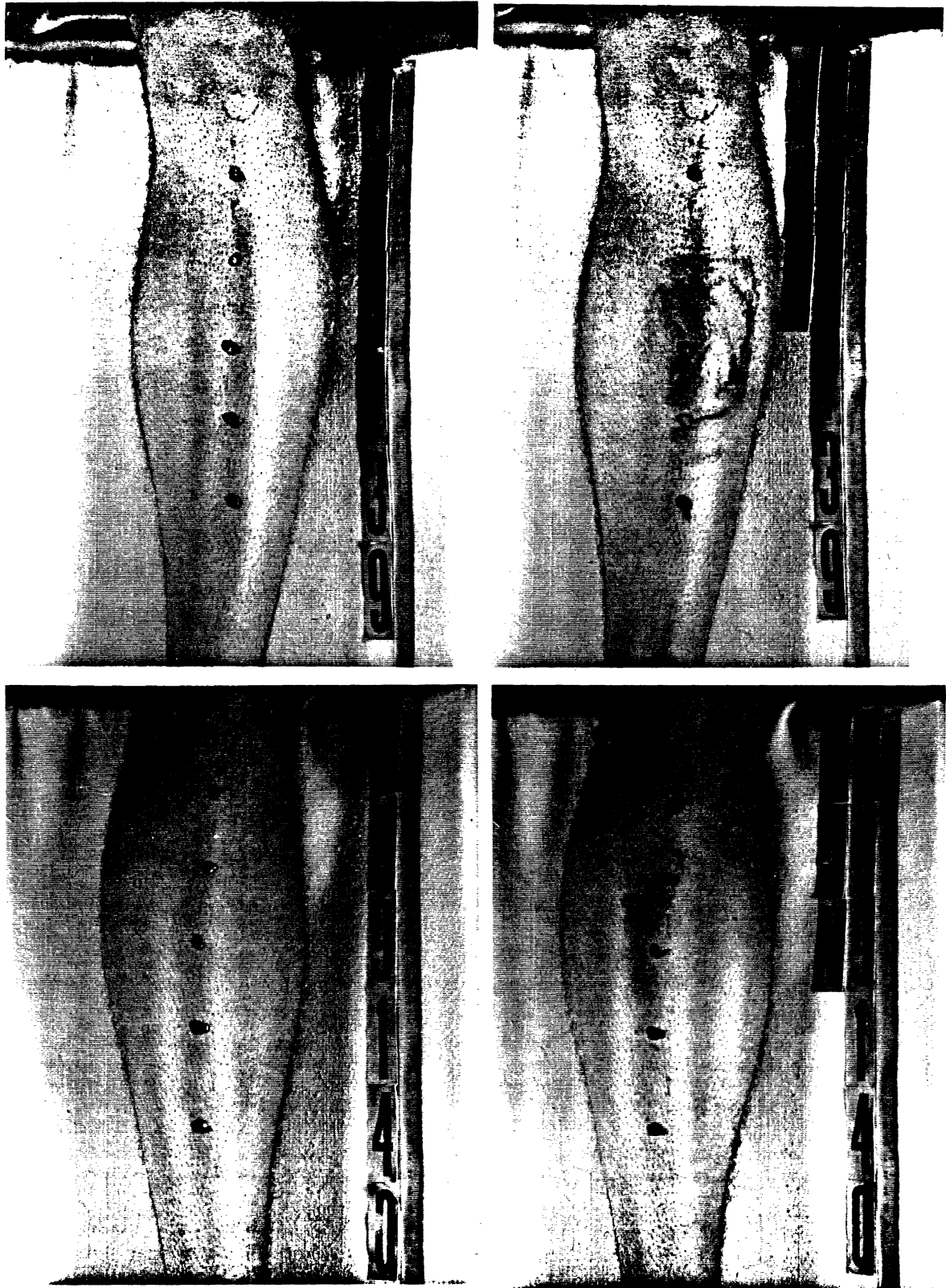


Figure 26. Pre- and post-test photographs of subjects' legs after tests using airbags with *reverse-type folding*. Post-test photos are taken five minutes after airbag deployment.



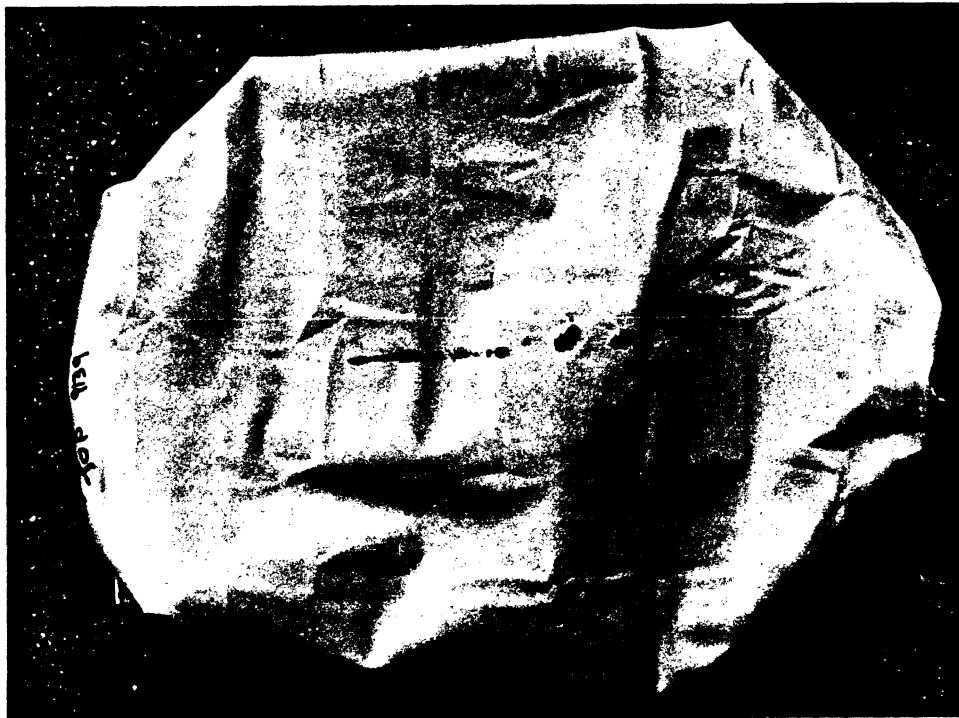


Figure 27. Surfaces of airbags with *reverse-type folding* showing colors picked up at the center of the bag without smearing.



Table 24  
Velocities Estimated from Tests in the Full-Factorial Matrix

Test Number	Inflator kPa	Bag Matl (denier)	Tether	Bag Fold	Velocity * 1st Half	Velocity 2nd Half
CA9137	475	420	No	Acc	77.9	127.1
CA9138	475	420	Yes	Acc	61.0	125.0
CA9139	475	420	No	Rev	61.5	156.1
CA9140	475	420	Yes	Rev	66.1	105.5
CA9141	350	420	No	Acc	65.6	155.3
CA9142	350	420	Yes	Acc	66.1	107.2
CA9143	350	420	No	Rev	64.1	105.0
CA9144	350	420	Yes	Rev	56.8	69.2

\* Note: Velocities given in mph.

With the exception of the last test, the velocities during the second half of the distance to the leg are seen to be nearly twice those during the first half. Also, it will be noted that, for both first- and second-half velocities and ignoring the second-half velocity for the last test, there is little difference between the velocities for the 475-kPa inflators and the 350-kPa inflators. In fact, the two highest velocities of 156 mph and 155 mph were found for 475- and 350-kPa inflators, respectively. There is also little difference in velocities for the different folds and the two tests with the highest velocities include one with accordion-type folding and one with reverse-type folding. With the exception of the first two tests, the tether has a significant effect on the second-half velocity but, as one might expect, has little effect on the first-half velocity. With the tether, the average second-half velocity is about 102 mph while, without the tether, it is about 136 mph.

The second-half velocity for the last test (CA9144) is significantly lower than the second-half velocities for any other test. A re-analysis of the films confirmed this result. As shown in Figure 28, the kinematics of this deployment are significantly different from those of the other airbags with reverse-type folding and are characterized by a large surface area of the airbag moving outward and reaching the leg surface almost simultaneously. As indicated by the photos in Figure 29, this deployment resulted in no abrasion injury and almost no hyperemia. Further testing is required to determine whether these deployment kinematics, which appear to be very desirable from an abrasion-injury perspective, are a repeatable result of the combination of reverse-type fold, 350-kPa inflator, and tethering. Since these airbags are currently folded by hand, it is possible that there is significant variability in the deployment kinematics and that the results are not repeatable.





Figure 28. Side-view, stop-action photograph from high-speed films of tethered airbag with *reverse-type folding* and *350 kPa inflator*. Steering wheel and module were rotated 90 degrees from the straight-ahead driving orientation.





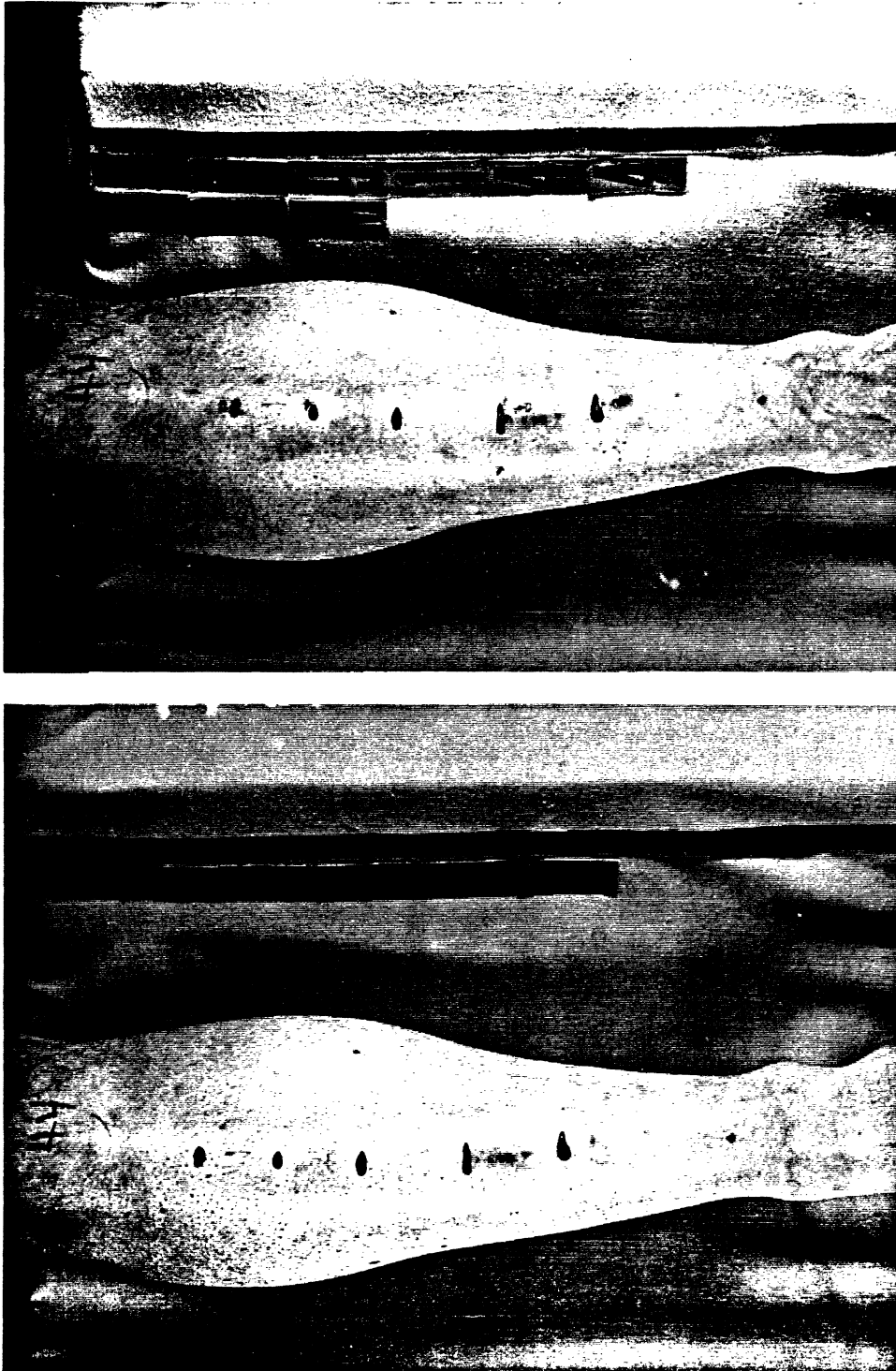


Figure 29. Pre- and post-test photographs of subject's leg for a test with *tethered* airbag with *reverse-type folding* and 350 kPa inflator at a distance of 225 mm (9 in).



#### IV. DISCUSSION, CONCLUSIONS, AND RECOMMENDATIONS FOR FUTURE WORK

In this study, deployments of airbags into human skin have been successfully used to determine the relative contributions of different airbag design parameters and deployment factors to the likelihood and severity of abrasions to the face and neck, and to improve the understanding of the mechanisms by which these abrasions occur. Factors studied have included distance, airbag folding technique, inflator pressure, airbag material, and airbag tethering.

With regard to the subject-to-module distance at which abrasions can occur, the results of this study confirm the preliminary findings of a previous study with anesthetized pigs in which skin abrasions were produced at a distance of 240 mm with both untethered and tethered airbags using 475-kPa inflators and accordion-type folding, but were not produced at a distance of 260 mm. A distance less than 250 mm (i.e., 225 mm) was necessary to *consistently* achieve abrasions to the skin over the front of the tibia with the same, untethered airbags as were used in the pig tests. In addition, for untethered airbags with 475-kPa inflators and accordion-type folding, abrasions were found to occur at distances up to 350 mm (14 in) and there was some evidence that abrasions were less likely and less severe for distances between 250 and 300 mm than for distances less than 250 mm or greater than 325 mm.

For tethered airbags, no abrasions resulted when the initial distance was 250 mm or greater, except for one test in the preliminary test series where an unrated abrasion was obtained at a distance of 250 mm. The tether thus appears to offer significant benefit to reducing abrasions in real-world crashes since, based on these results, no abrasions would be produced if the occupant is more than 250 mm (10 in) away from the airbag module at the time of contact from the deploying airbag. However, while tethering of the airbag was found to have a dramatic influence on reducing skin abrasions, especially at distances of 250 mm and greater, the use of reverse-type folding instead of accordion-type folding had an even greater effect on reducing skin abrasions at a distance of 225 mm as well as overall (i.e., considering all distances from 225 mm to 350 mm).

For distances greater than 225 mm (i.e., 250 mm and greater), at which one would expect the tether to have its greatest effect on reducing skin abrasions, the results of this study do not provide sufficient information to confirm whether reverse-type folding or tethering has the more significant effect on reducing abrasions, nor do they clarify if the combination of tethering and reverse-type folding offers any advantage over implementation of either condition by itself. In large part, this is due to the fact that relatively few tests were conducted at distances of 250 mm or more with airbags having the reverse-type folding or with a tether. Also, most of the tests that were conducted with tethered and reverse-type-fold airbags at distances other than 225 mm were in the Taguchi test matrix where the use of a chest deflection plate may have masked the effects of these factors.

If, for example, one looks only at results of tests conducted for distances greater than 225 mm in which abrasions were quantified (a sample size of 26 that does not include any of the full-factorial or preliminary test series), there are only four tests in which airbags had reverse-type folding and five tests with tethered airbags. All but one of these tests (i.e., one with a tethered airbag) are in the Taguchi test matrix for which the chest deflection plate was used, and two of the tests included both reverse-type folding and tethering.

With these limitations of the data set in mind, a compilation of the abrasion results shows that there were no abrasions for airbags with reverse-type folding (zero out of four) and no abrasions for airbags with tethers (zero out of five) at distances greater than 225 mm. While these findings suggest that the effects of using airbags with reverse-type folding or tethers are essentially equivalent and that either condition will eliminate all abrasions for distances of 250 mm and greater, the data set is considered too limited to have confidence in this conclusion. Also, considering that the results for tests in the full-factorial matrix showed that reverse-type folding has a greater effect than tethering in reducing skin abrasions at distances of 225 mm, the results of this study suggest that use of reverse-type folding has a more significant *overall* effect (i.e., at all distances) in reducing skin abrasions than does the use of tethers.

The fact that abrasions were obtained at a distance of 225 mm with tethered airbags suggests that using tethered airbags will not, by itself, prevent all abrasions in the real-world. This conclusion is based on information about driver positioning with

respect to the steering wheel such as shown in Figure 30 which plots chin-to-wheel-center distances versus stature for 100 subjects tested in a seating buck configured to sport, sedan, and minivan interior package geometries as shown in Figure 31. As indicated, even before an impact occurs, many shorter drivers sit so that their chin is less than 250 mm from the center of the steering wheel. Given that forward motion of the occupant can occur prior to complete deployment of the airbag, one would expect even closer distances in some crash situations.

Corresponding to the differences in severities and frequencies of skin abrasions resulting from airbags with different types of folding, high-speed films of the deploying airbags demonstrate distinctly different kinematics for the accordion-type fold and the reverse-type fold which appear to be closely linked to the mechanisms of skin abrasion. With accordion-type folding, two unfilled flaps or wings deploy at high velocity and strike the skin with a wiping-type of motion which produces abrasions at distances up to 350 mm for untethered airbags. For reverse-type folding, the center of the airbag deploys and fills first with little or no shearing action when impact with the skin is made. While abrasions can be produced by this stamping-like contact, the likelihood and severity appear to be significantly less than for accordion-type folding.

It should also be noted, however, that the flaps of an airbag installed with the accordion-type fold deploy to the left and right of a steering wheel positioned in the straight-ahead position and may miss a driver's face and neck if he/she is centered on the steering wheel. On the other hand, the airbag installed with reverse-type folding, deploys at the center and will make contact with the centered driver. The importance of this positioning factor on the likelihood of abrasion is difficult to assess and has not been factored into the above conclusions regarding the effects of airbag fold on skin abrasion.

The results of this study have, somewhat surprisingly, shown that there is little difference in abrasion potential for the two different inflator pressures used. In fact, the results of the tests in the Taguchi matrix suggest that the 350-kPa inflator is more likely to produce abrasions than the 475-kPa inflator. While this finding is not considered statistically significant due to the minimal abrasions obtained in these tests, due, in part, to the use of a "chest" deflection plate, there is little evidence in the study to suggest that the 475-kPa inflator is more likely to produce abrasions than is the 350-kPa inflator. This conclusion is supported by the finding that the peak velocities of the airbag material from the tests with 475-kPa inflators are not significantly different from the velocities for

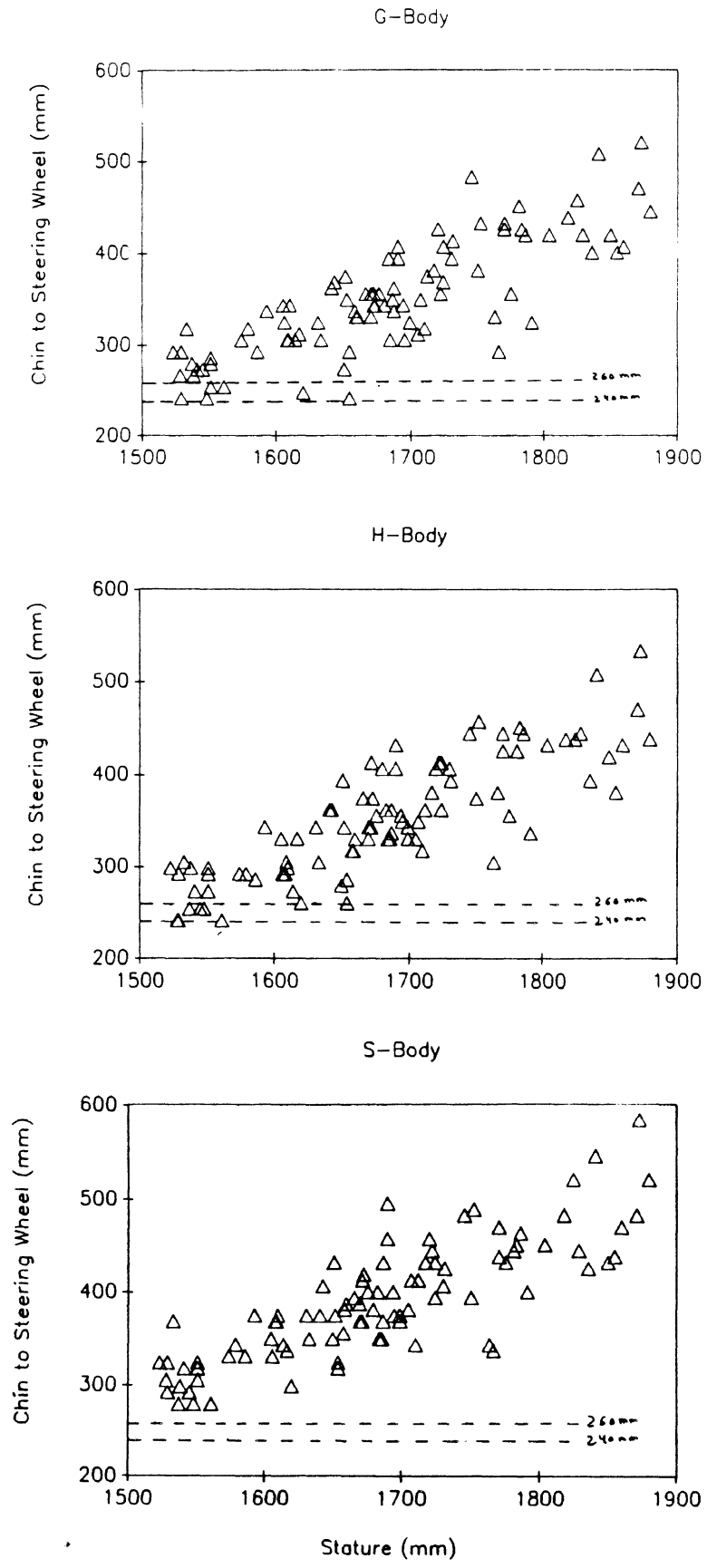


Figure 30. Chin-to-steering-wheel distance for 100 subjects seated in test buck configured to sport (G-body), sedan (H-body), and minivan (S-body) seating packages.



Figure 31. Photos of subjects seated in sedan- and sport-type vehicle package configurations with close chin-to-steering-wheel distances.

tests with the 350-kPa inflators, in spite of the fact that the noise of the deployment is substantially louder and subjects generally reported a sensation of greater "blast" exposure for tests in which the 475-kPa inflator was used. It should be noted, however, that these velocities were measured for tests conducted at distances of 225 mm and it may be that the higher velocity inflators will produce higher velocities and have more abrasion-producing potential for distances greater than 300 mm with untethered airbags.

The conclusions and observations of this study are based on a relatively small sample of tests considering the number of different airbag and test conditions which have been incorporated into the study. The initial position of the subject relative to the module is clearly an important factor which can influence the effect and importance of other factors and needs further study. Also, there was little opportunity in this study to examine the issue of variability in susceptibility to abrasion between subjects with different skin characteristics. Additional testing of several subjects for the same airbag deployment and test conditions would provide useful information on this important factor which has not been considered in the results of this study.

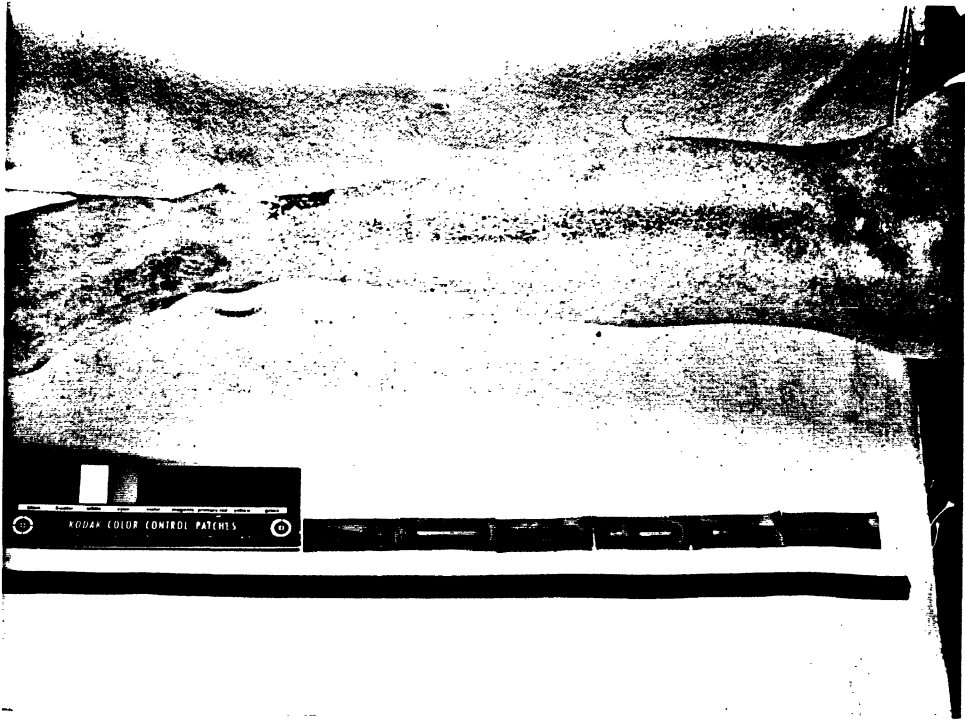
Finally, it should be noted that the effect of body region and skin support structures have not been addressed in this study. All but one test were performed on the skin overlying the front of the tibia which is relatively tight and supported by bone. Only one test was conducted on the skin overlying the relaxed calf muscle and this resulted in more serious abrasions than an identical test at the tibia. The skin over the jaw, which is a common region for abrasions in the field, is supported differently than either of these since the skin is relatively loose but the jaw is quite rigid. It is possible that, for the velocities of airbag impacts which produce abrasions, the looseness of the skin and the underlying support structure make little difference in abrasion results, but further study of this issue is needed.



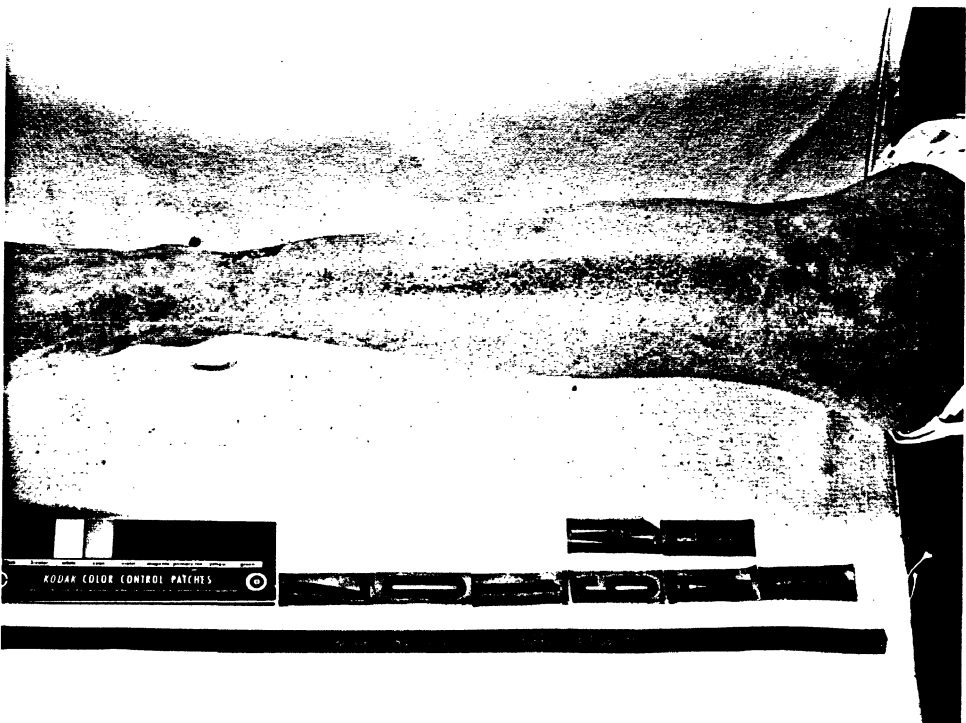
APPENDIX A

PHOTOGRAPHS OF SUBJECTS' LEGS TAKEN BEFORE  
AND FIVE MINUTES AFTER AIRBAG DEPLOYMENTS  
IN THE TAGUCHI TEST MATRIX





PRE-TEST PHOTO

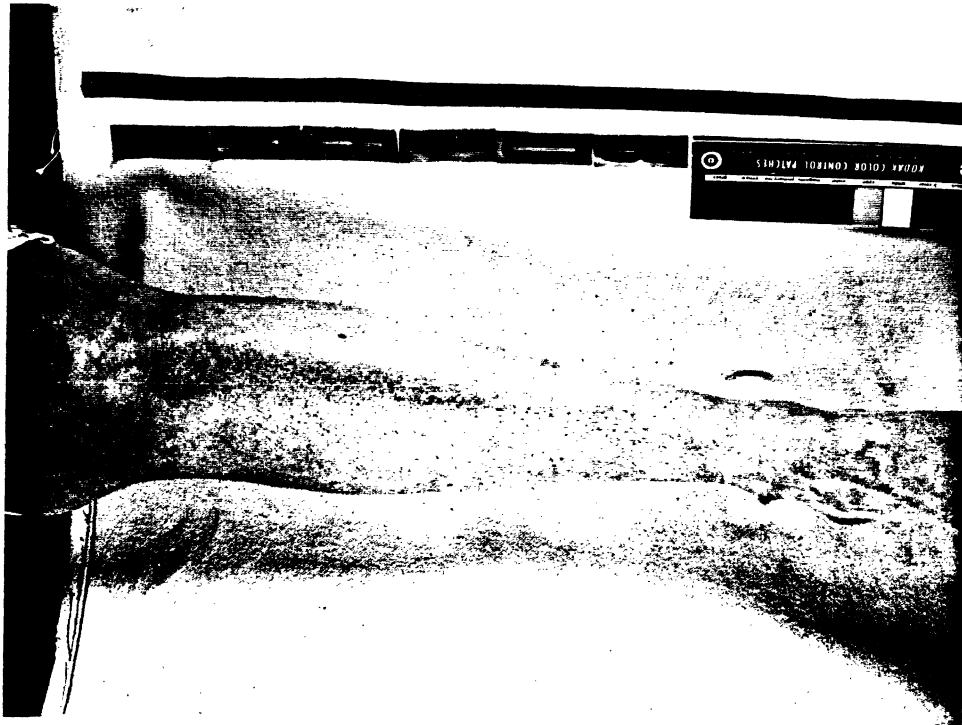


5 MINUTE POST-TEST PHOTO

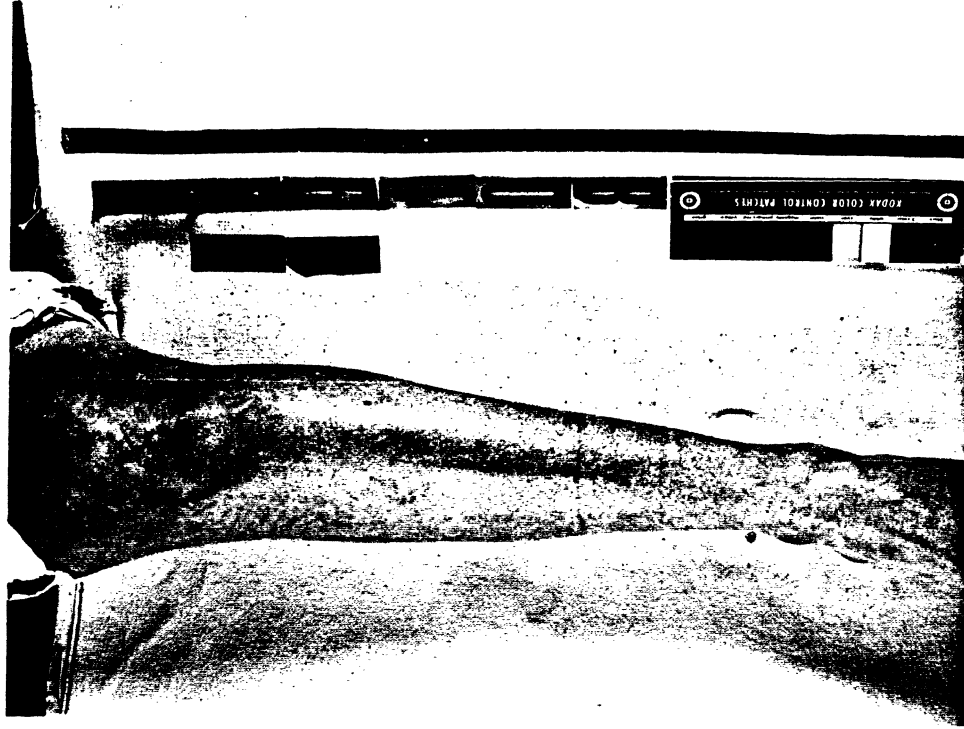
**TEST NO. CA9107: ABRASION SCORE = 1**

Female, WITH deflection plate, 300 mm, NO wheel rotation,  
420 denier, TETHER, REVERSE Fold, 350 kPa inflator.





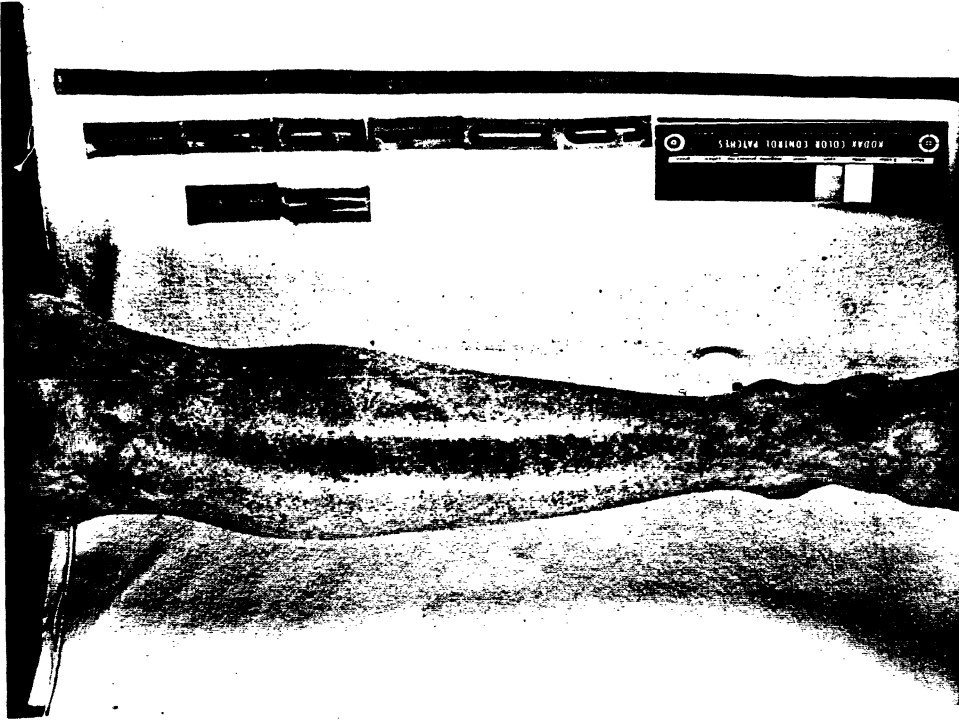
PRE-TEST PHOTO



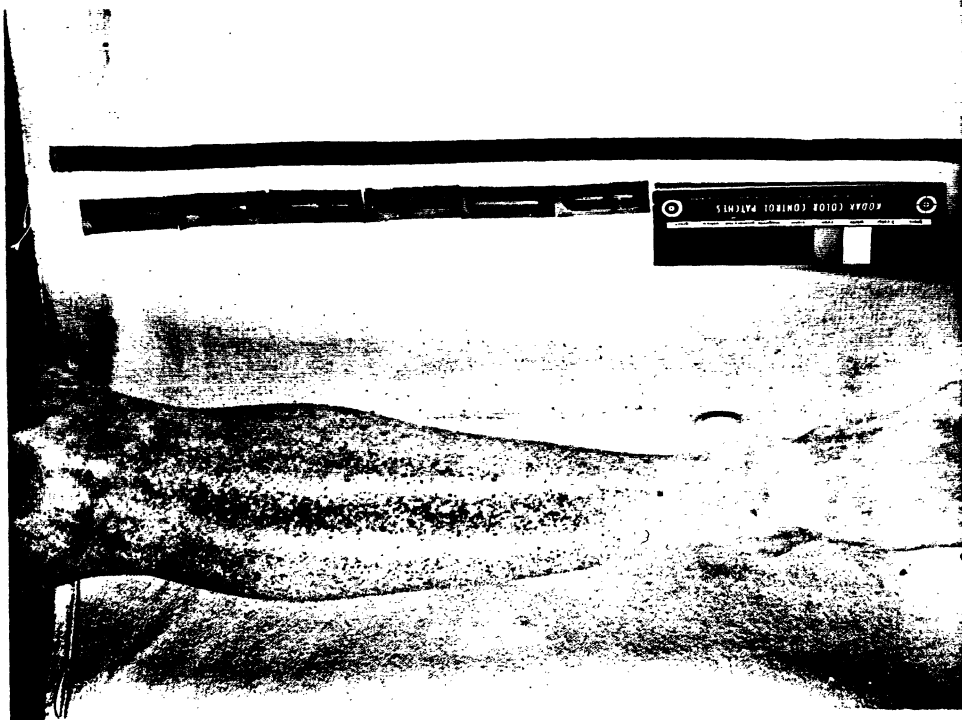
5 MINUTE POST-TEST PHOTO

**TEST NO. CA9108: ABRASION SCORE = 1**  
Female, WITH deflection plate, 300 mm, NO wheel rotation,  
420 denier, NO TETHER, REVERSE Fold, 475 kPa inflator.





5 MINUTE POST-TEST PHOTO

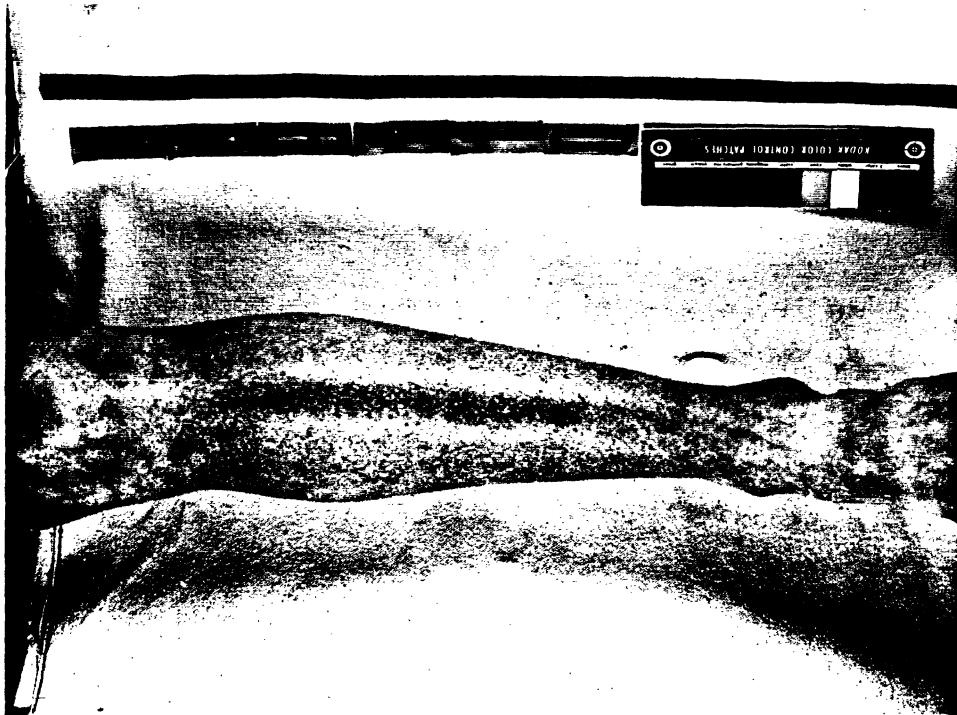


PRE-TEST PHOTO

TEST NO. CA9109: ABRASION SCORE = 1  
Female, WITH deflection plate, 250 mm, NO wheel rotation,  
420 denier, TETHER, ACCORDIAN Fold, 475 kPa inflator.







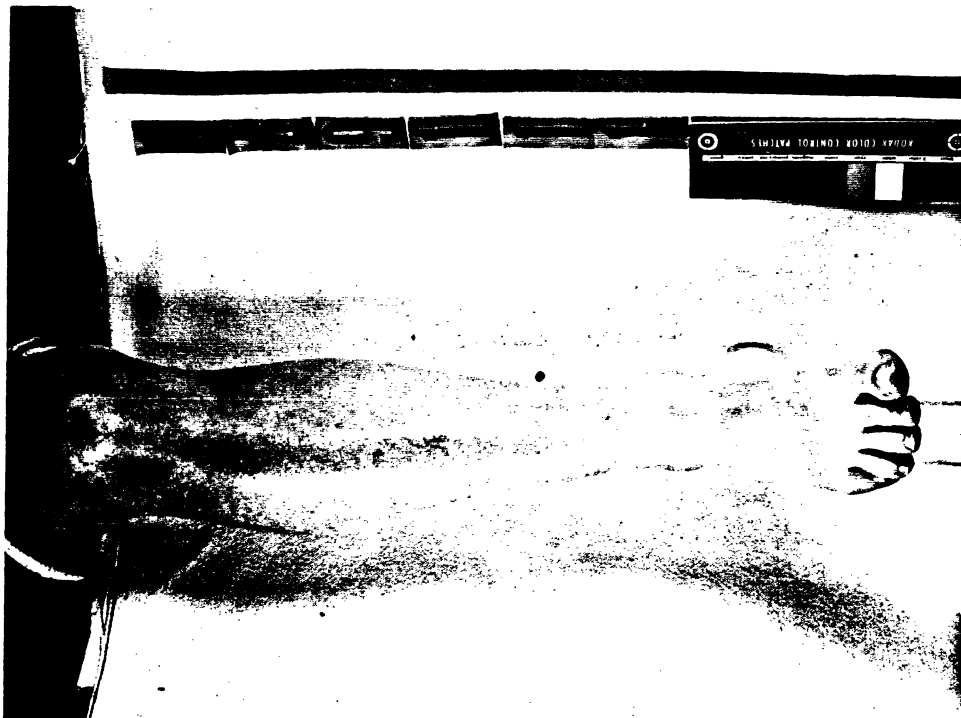
PRE-TEST PHOTO



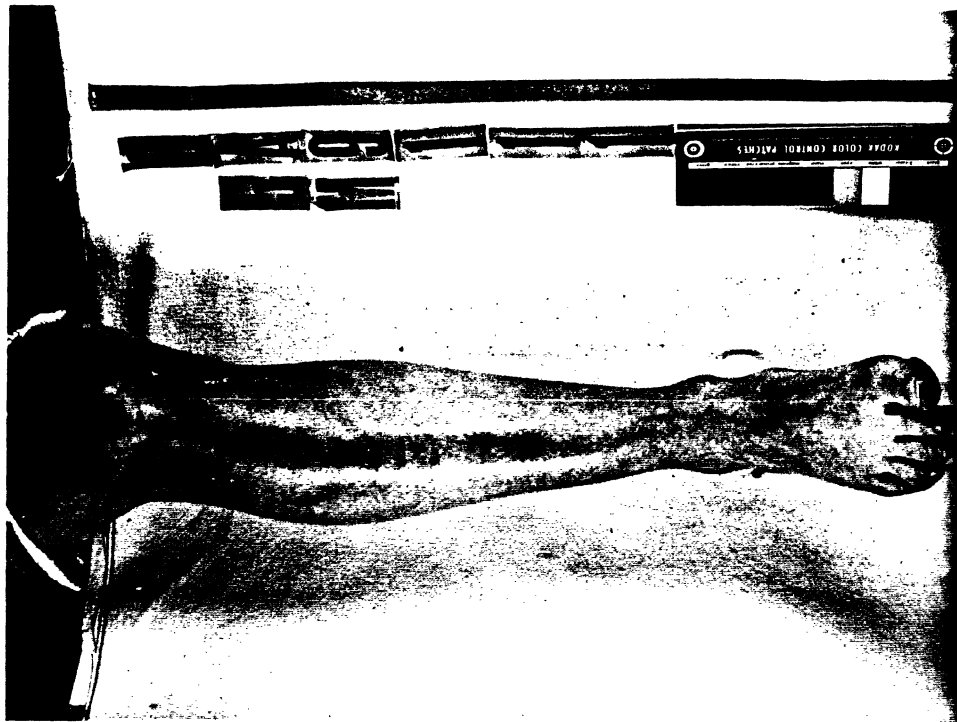
5 MINUTE POST-TEST PHOTO

**TEST NO. CA9110: ABRASION SCORE = 3**  
Female, WITH deflection plate, 250 mm, NO wheel rotation,  
420 denier, NO TETHER, ACCORDIAN Fold, 350 kPa inflator.





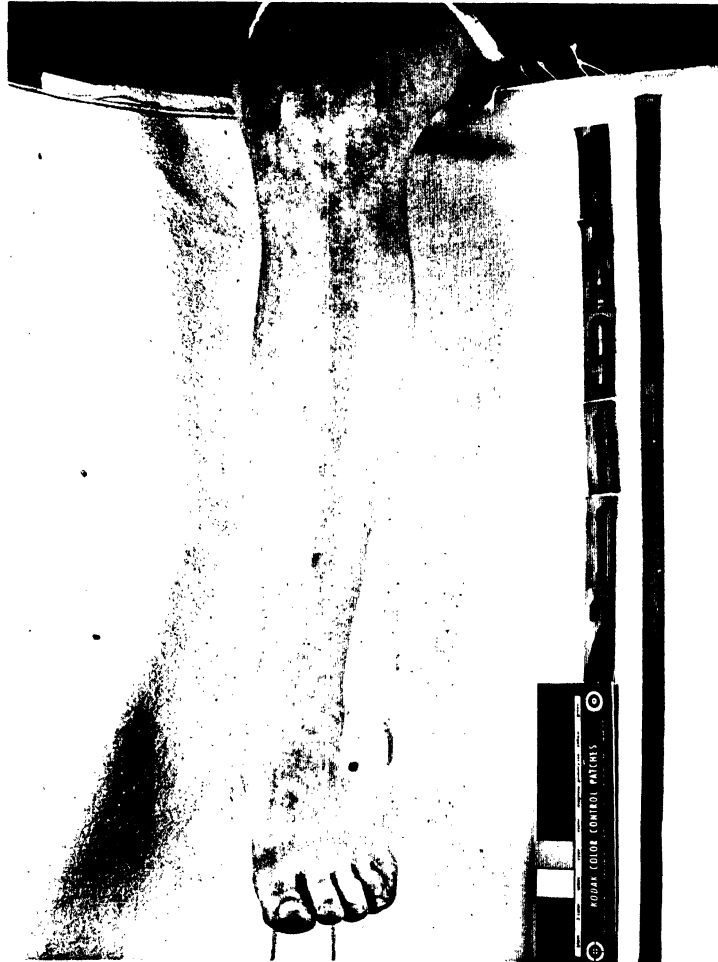
PRE-TEST PHOTO



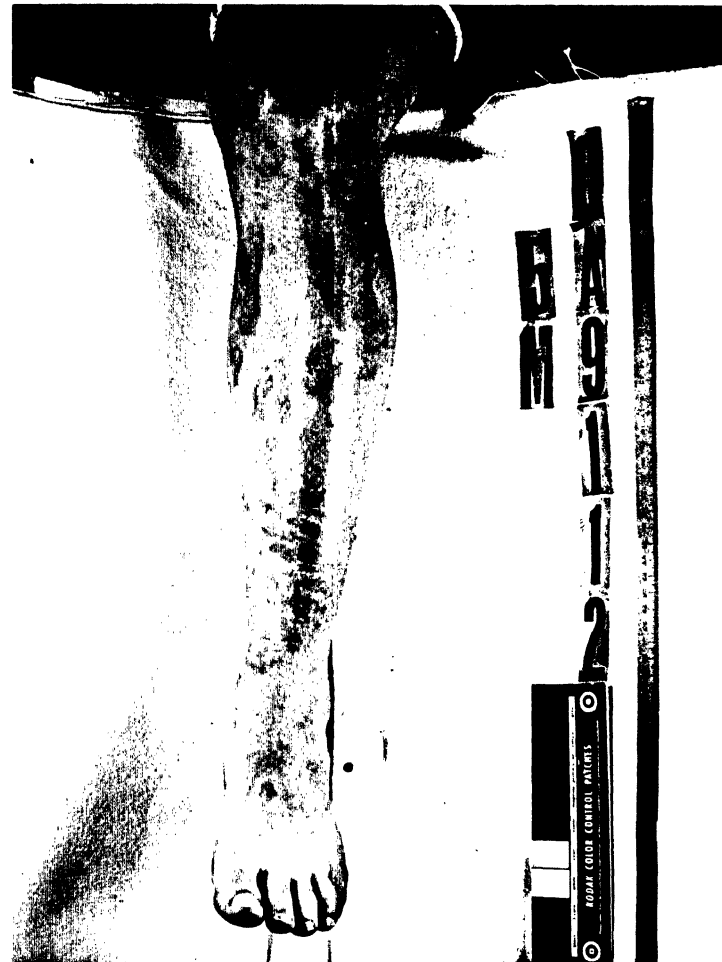
5 MINUTE POST-TEST PHOTO

**TEST NO. CA9111: ABRASION SCORE = 1**  
Female, WITH deflection plate, 300 mm, NO wheel rotation,  
840 denier, TETHER, ACCORDIAN Fold, 475 kPa inflator.





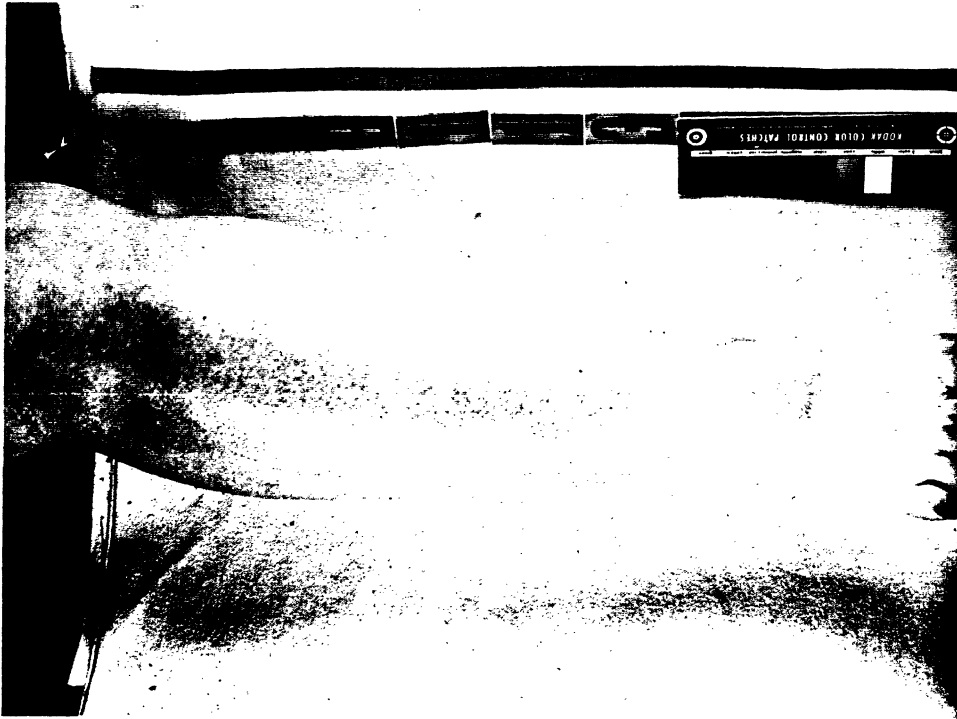
PRE-TEST PHOTO



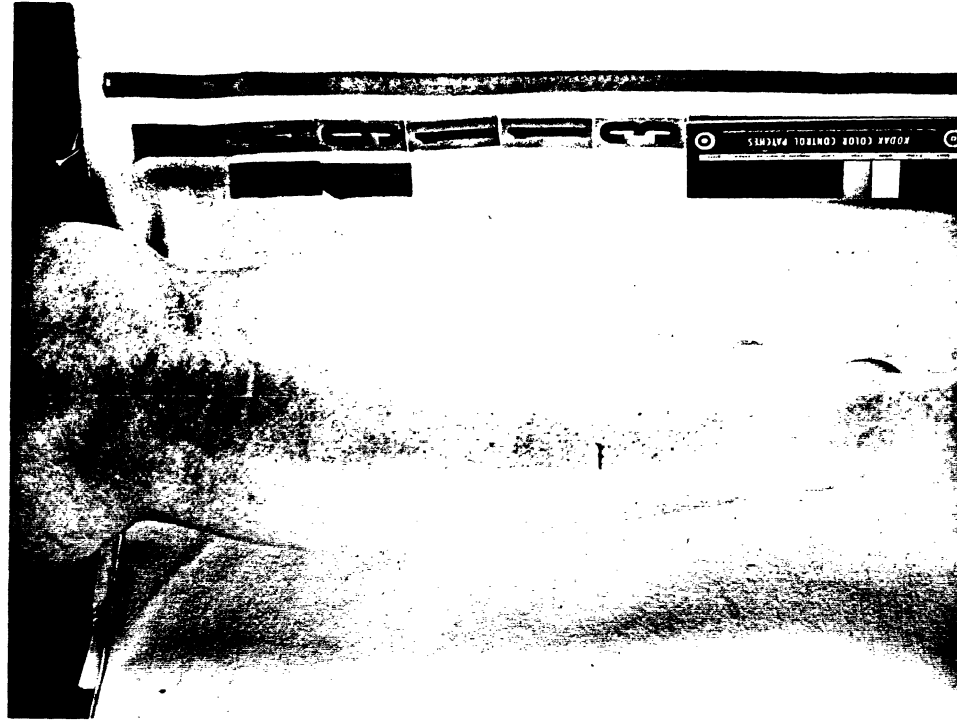
5 MINUTE POST-TEST PHOTO

**TEST NO. CA9112: ABRASION SCORE = 4**  
Female, WITH deflection plate, 300 mm, NO wheel rotation,  
840 denier, NO TETHER, ACCORDIAN Fold, 350 kPa inflator.





PRE-TEST PHOTO

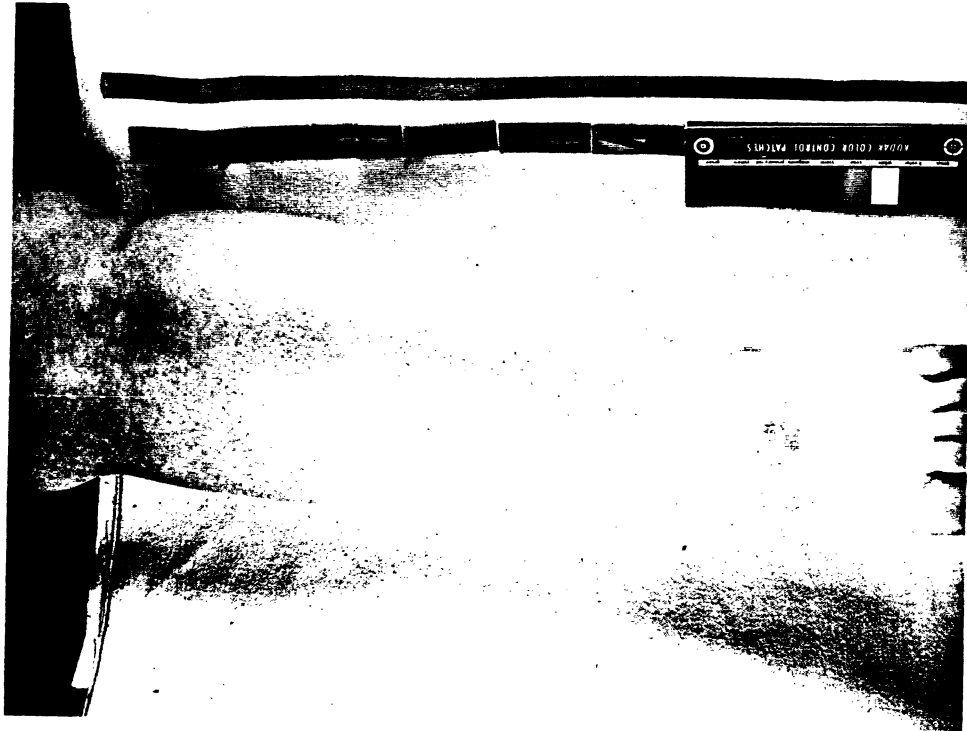


5 MINUTE POST-TEST PHOTO

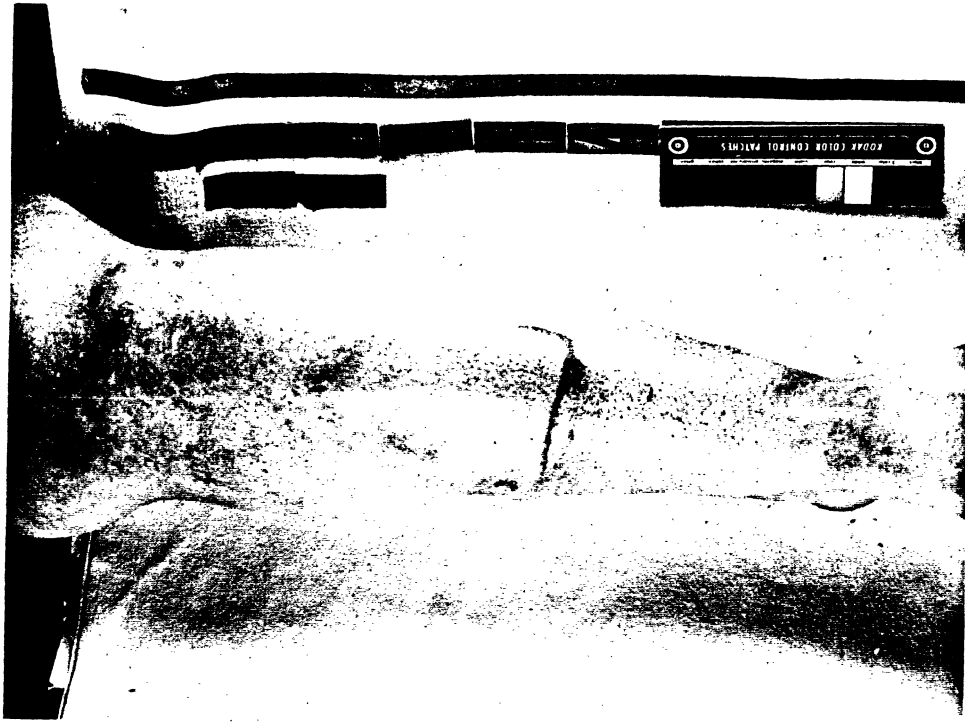
**TEST NO. CA9113: ABRASION SCORE = 1**  
Female, WITH deflection plate, 250 mm, NO wheel rotation,  
840 denier, TETHER, REVERSE Fold, 350 kPa inflator.







PRE-TEST PHOTO



5 MINUTE POST-TEST PHOTO

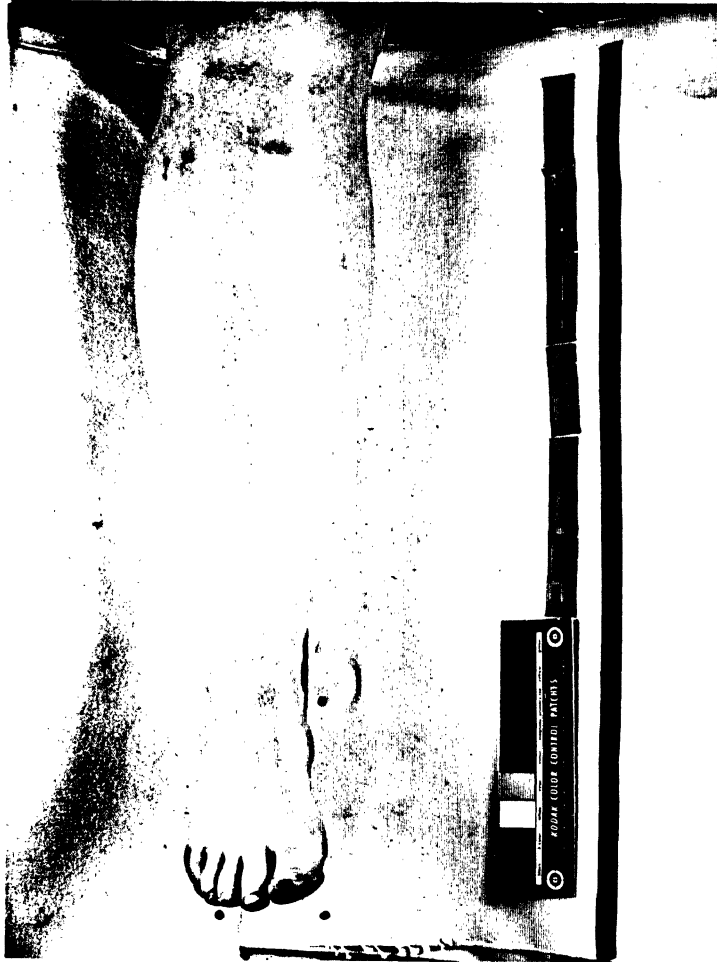
**TEST NO. CA9114: ABRASION SCORE = 2**  
Female, WITH deflection plate, 250 mm, NO wheel rotation,  
840 denier, NO TETHER, REVERSE Fold, 475 kPa inflator.



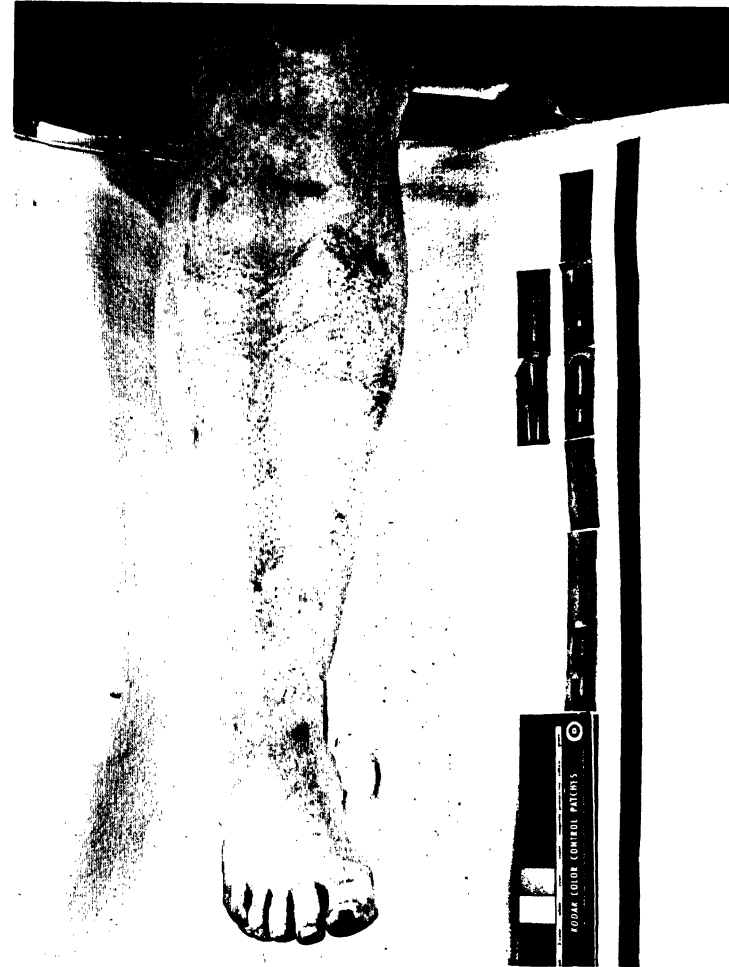
APPENDIX B

PHOTOGRAPHS OF SUBJECTS' LEGS TAKEN BEFORE  
AND FIVE MINUTES AFTER AIRBAG DEPLOYMENTS  
IN THE DEFLECTION-PLATE-EFFECTS AND  
DETERMINATION-OF-ABRASION-DISTANCES TEST MATRICES





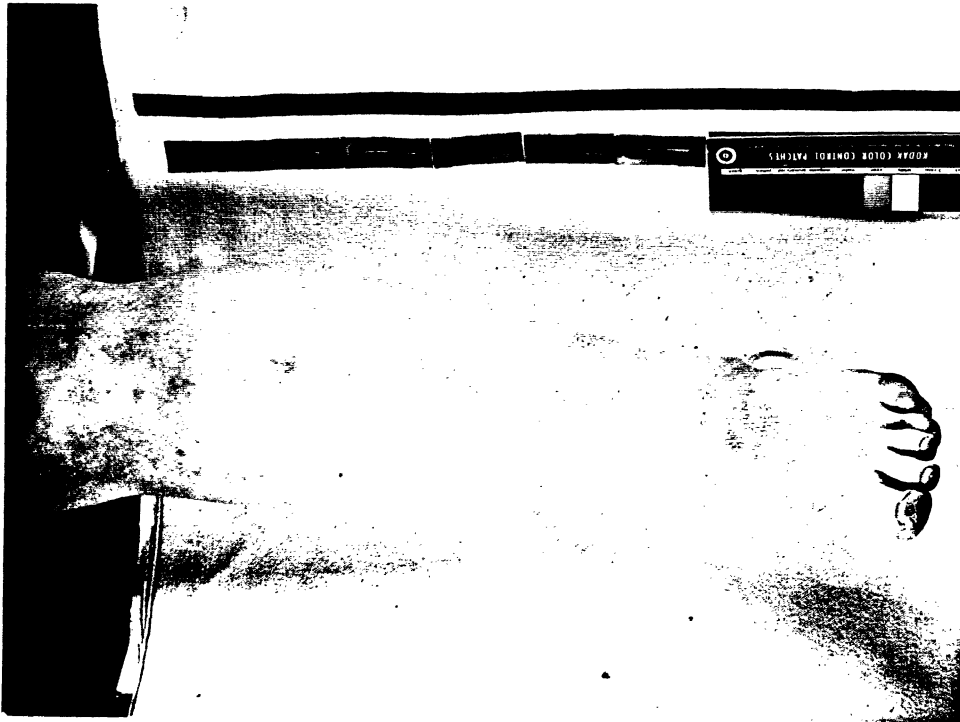
PRE-TEST PHOTO



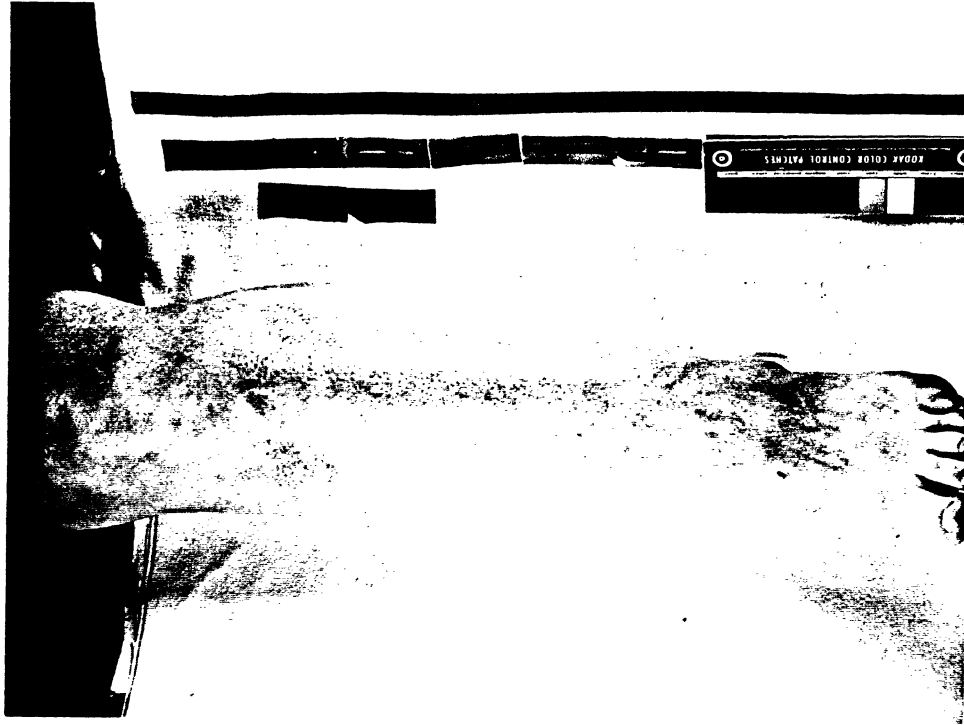
5 MINUTE POST-TEST PHOTO

**TEST NO. CA9115: ABRASION SCORE = 3**  
Female, WITH deflection plate, 300 mm, NO wheel rotation,  
840 denier, NO TETHER, ACCORDIAN Fold, 475 kPa inflator.





PRE-TEST PHOTO



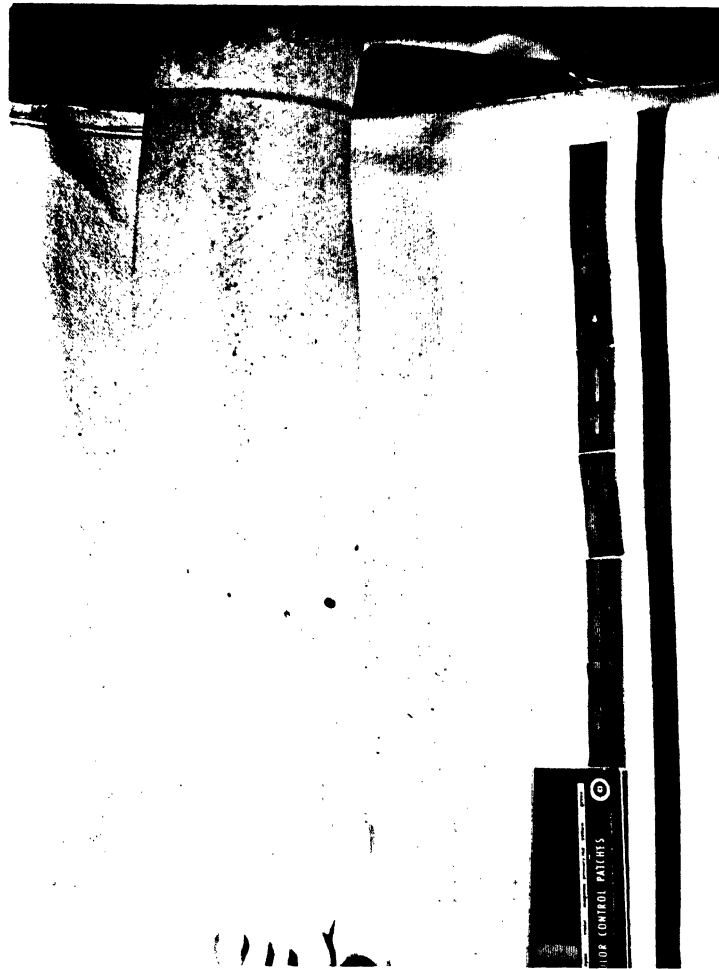
5 MINUTE POST-TEST PHOTO

TEST NO. CA9116: ABRASION SCORE = 4

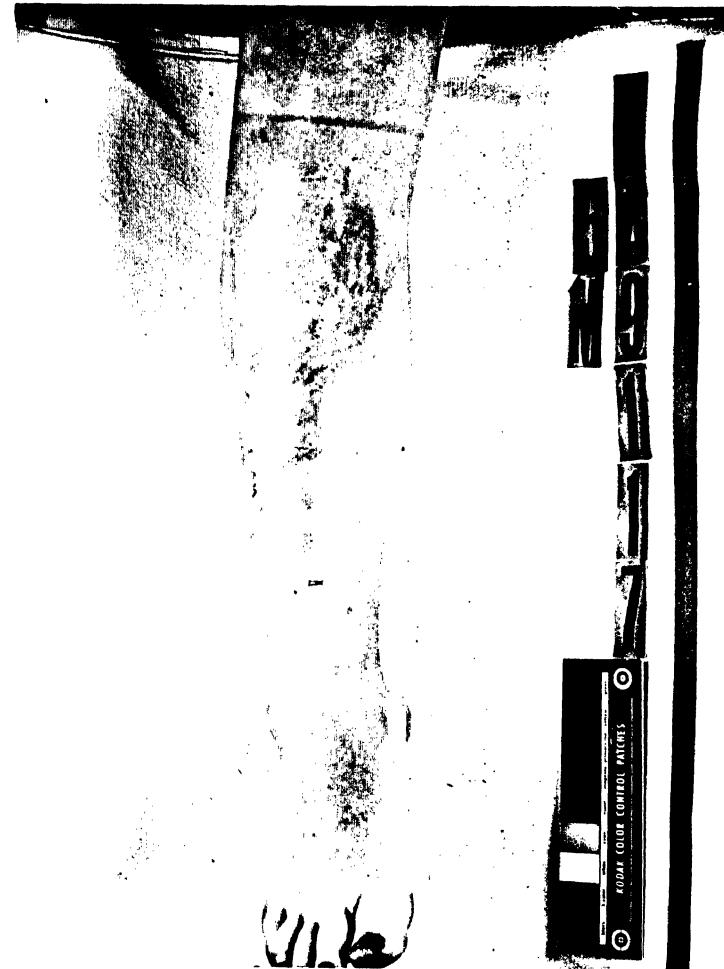
Female, NO deflection plate, 300 mm, NO wheel rotation,  
840 denier, NO TETHER, ACCORDIAN Fold, 475 kPa inflator.







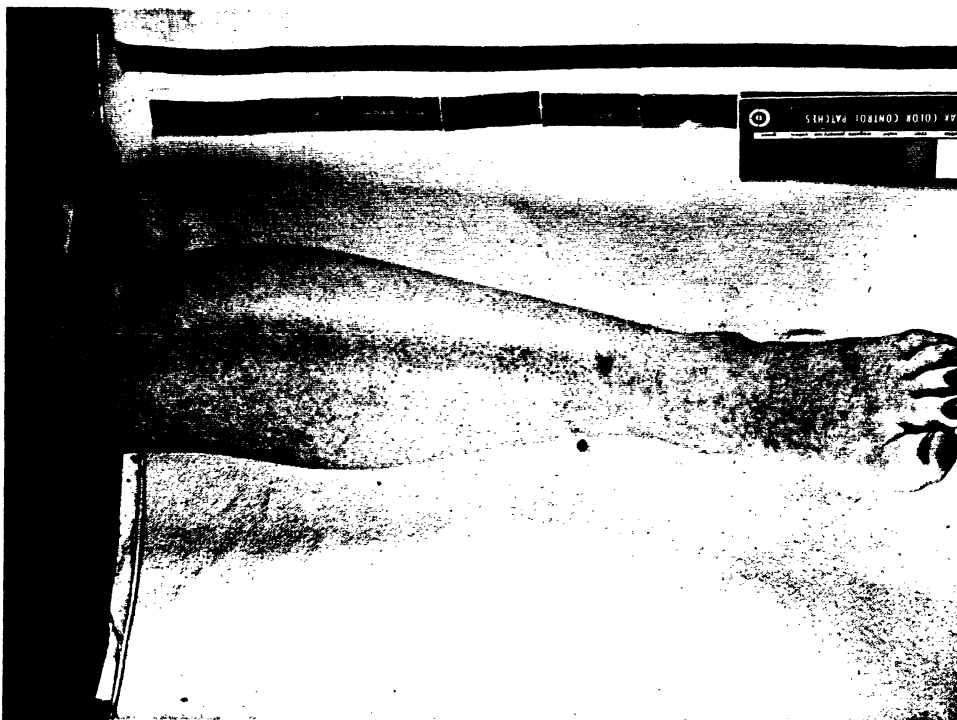
PRE-TEST PHOTO



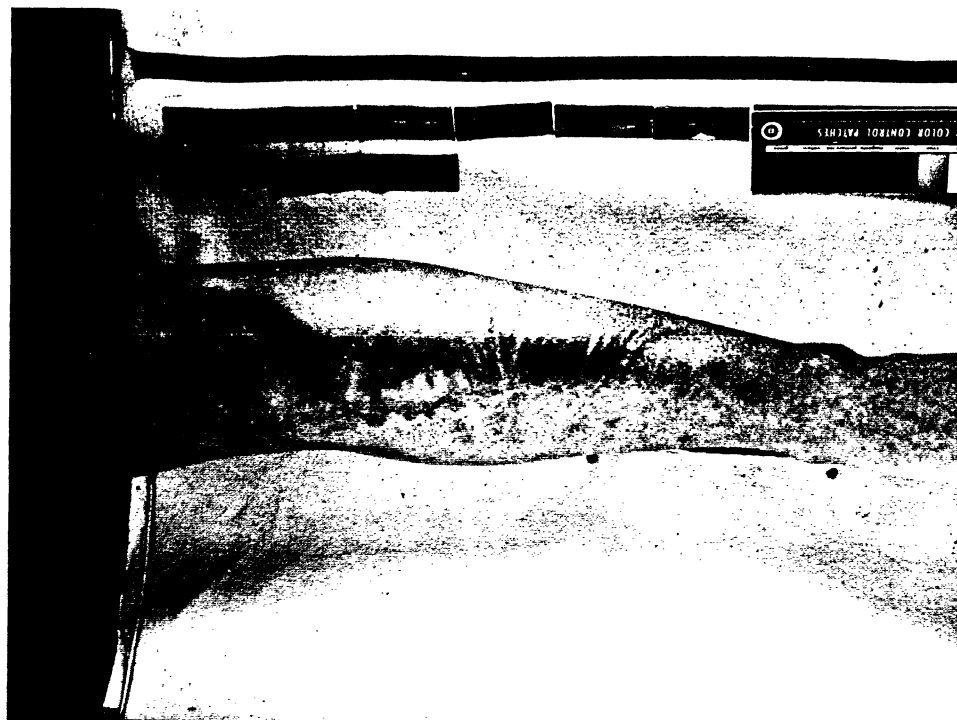
5 MINUTE POST-TEST PHOTO

**TEST NO. CA9117: ABRASION SCORE = 1**  
Female, WITH deflection plate, 350 mm, NO wheel rotation,  
840 denier, NO TETHER, ACCORDIAN Fold, 475 kPa inflator.





PRE-TEST PHOTO

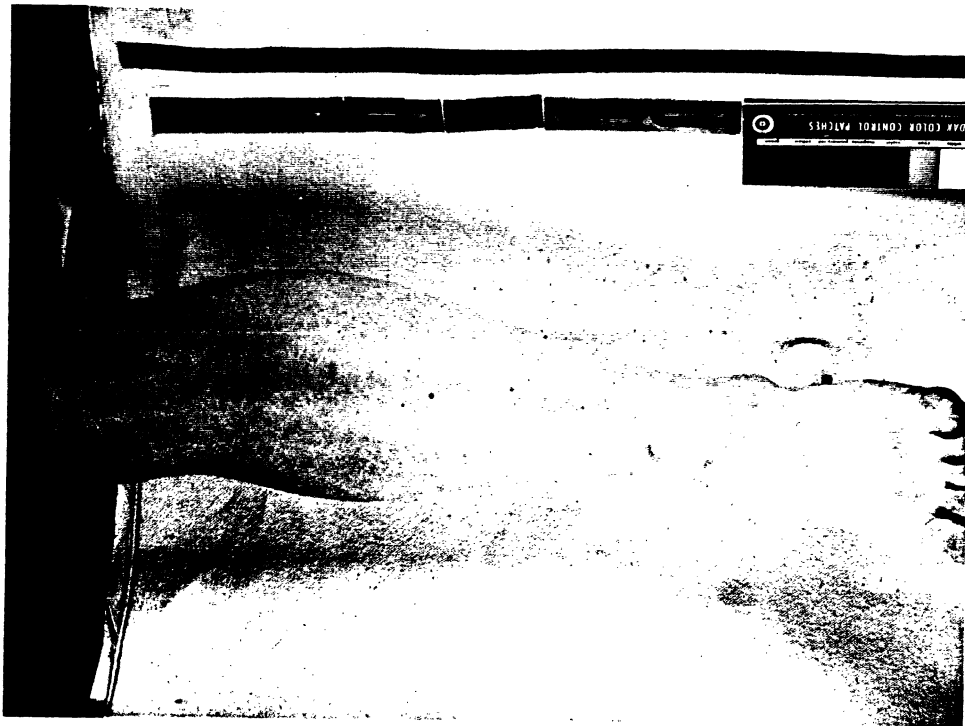


5 MINUTE POST-TEST PHOTO

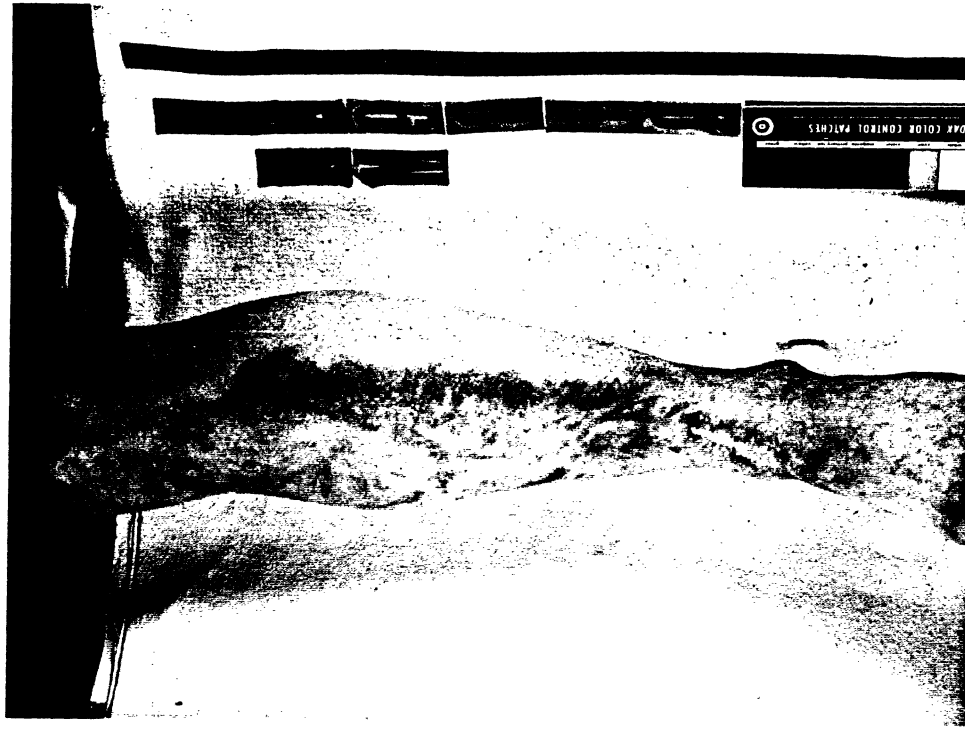
TEST NO. CA9118: ABRASION SCORE = 4

Female, NO deflection plate, 350 mm, NO wheel rotation,  
840 denier, NO TETHER, ACCORDIAN Fold, 475 kPa inflator.





PRE-TEST PHOTO

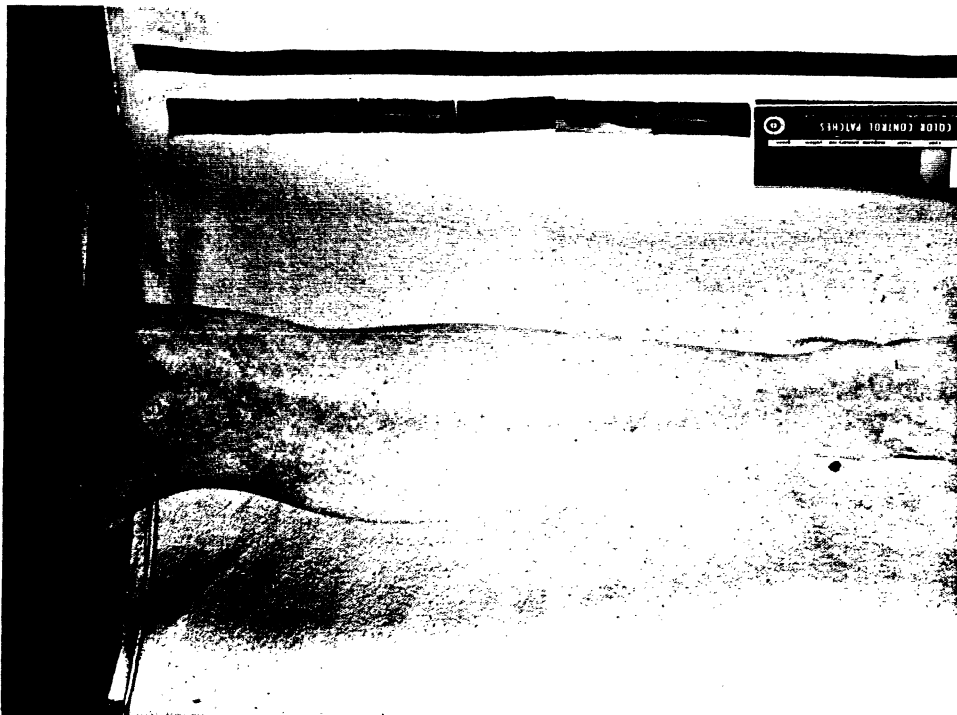


5 MINUTE POST-TEST PHOTO

**TEST NO. CA9119: ABRASION SCORE = 3**

Female, NO deflection plate, 350 mm, NO wheel rotation,  
840 denier, NO TETHER, ACCORDIAN Fold, 475 kPa inflator.





PRE-TEST PHOTO



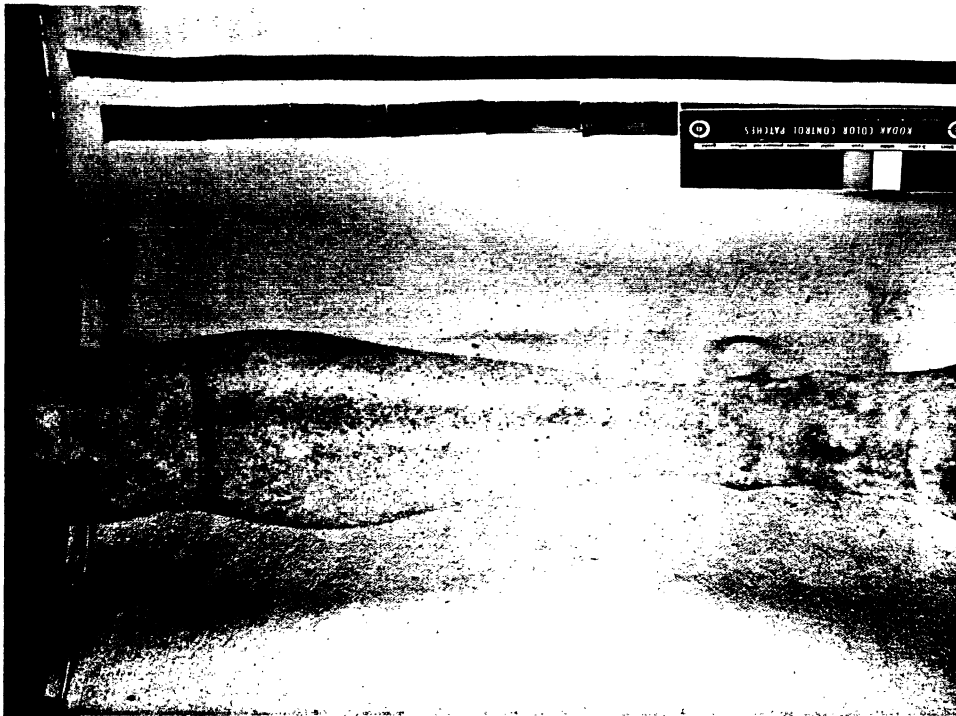
5 MINUTE POST-TEST PHOTO

TEST NO. CA9120: ABRASION SCORE = 4

Female, NO deflection plate, 300 mm, NO wheel rotation,  
840 denier, NO TETHER, ACCORDIAN Fold, 475 kPa inflator.







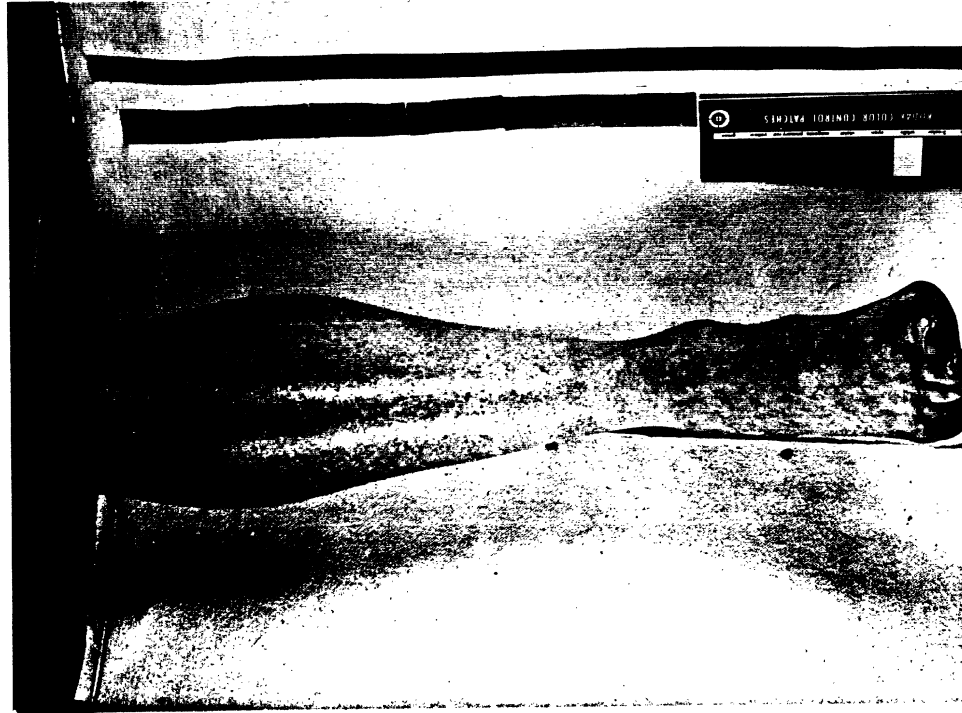
PRE-TEST PHOTO



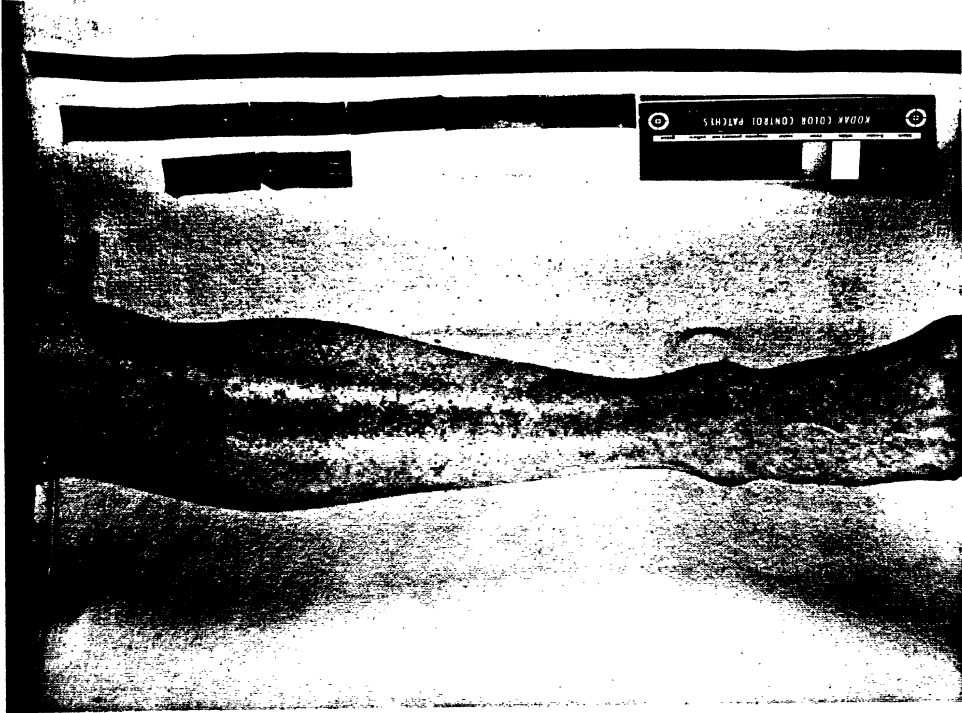
5 MINUTE POST-TEST PHOTO

**TEST NO. CA9121: ABRASION SCORE = 1**  
Female, NO deflection plate, 300 mm, NO wheel rotation,  
840 denier, NO TETHER, ACCORDIAN Fold, 475 kPa inflator.





PRE-TEST PHOTO



5 MINUTE POST-TEST PHOTO

TEST NO. CA9122: ABRASION SCORE = 4

Female, NO deflection plate, 250 mm, NO wheel rotation,  
840 denier, NO TETHER, ACCORDIAN Fold, 475 kPa inflator.





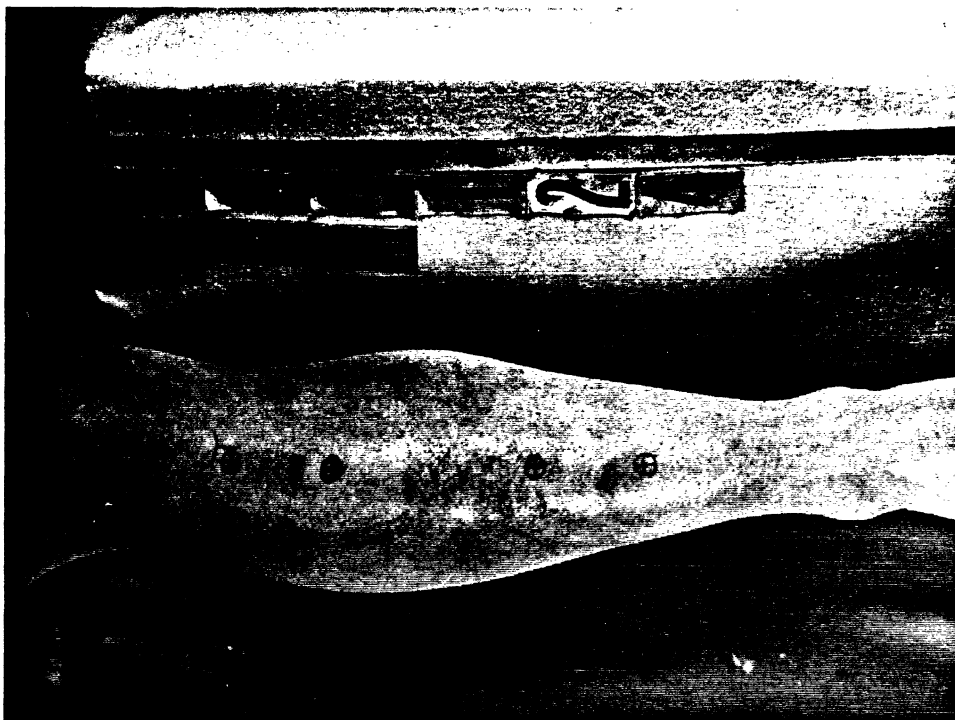
PRE-TEST PHOTO



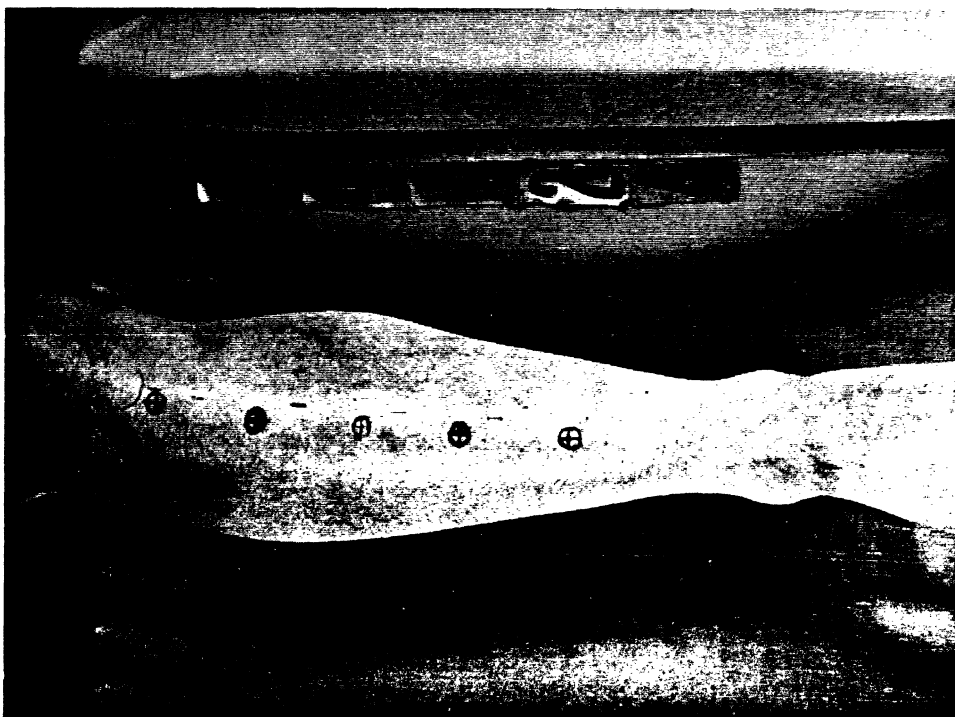
5 MINUTE POST-TEST PHOTO

**TEST NO. CA9123: ABRASION SCORE = 1**  
Female, NO deflection plate, 300 mm, 90° wheel rotation,  
840 denier, NO TETHER, ACCORDIAN Fold, 475 kPa inflator.





5 MINUTE POST-TEST PHOTO

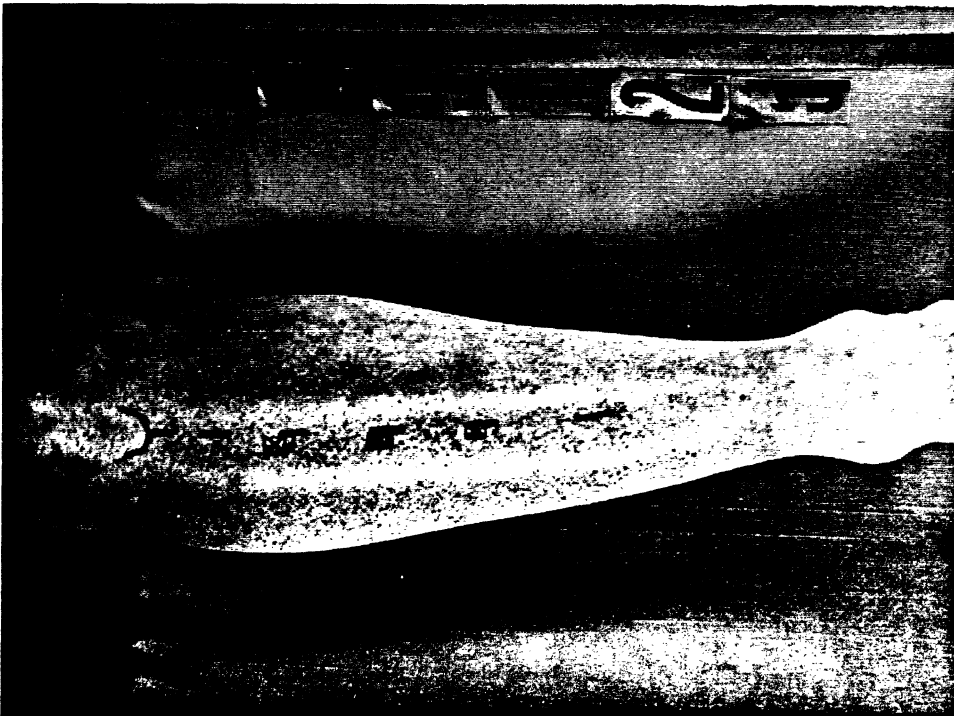


PRE-TEST PHOTO

TEST NO. CA9124: ABRASION SCORE = 5  
Female, NO deflection plate, 250 mm, 90° wheel rotation,  
840 denier, NO TETHER, ACCORDIAN Fold, 475 kPa inflator.



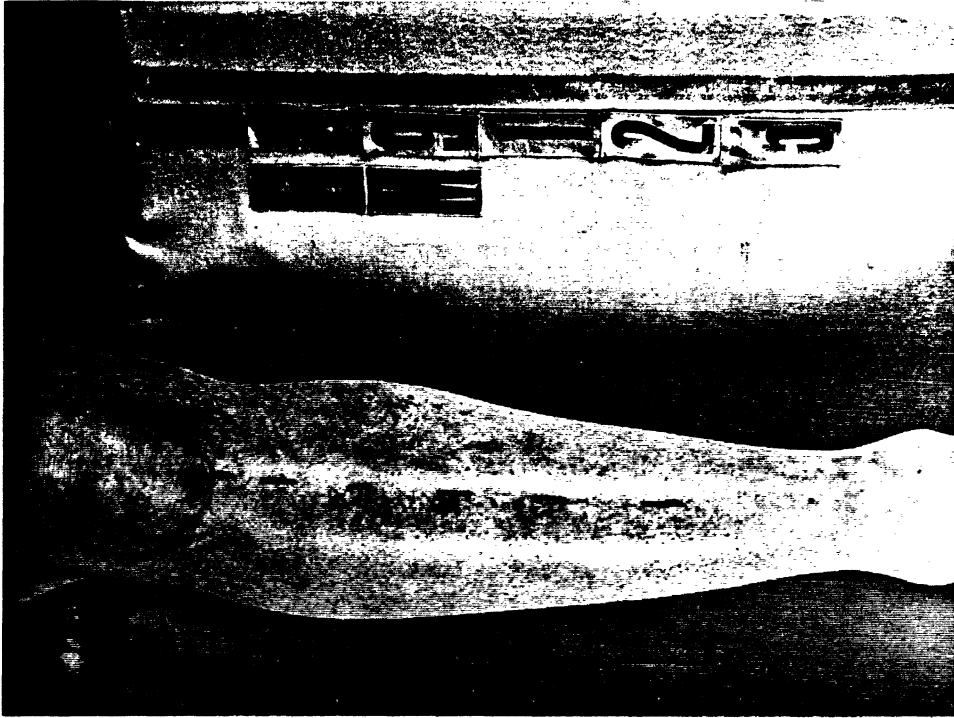




PRE-TEST PHOTO

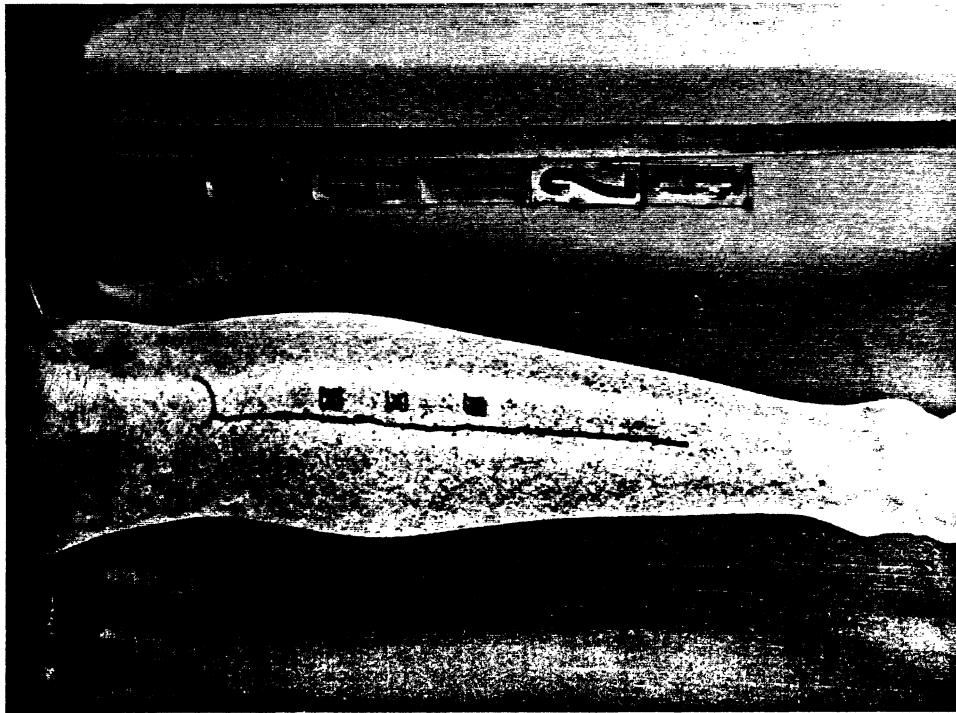
TEST NO. CA9125: ABRASION SCORE = 1

Female, NO deflection plate, 250 mm, 90° wheel rotation,  
840 denier, NO TETHER, ACCORDIAN Fold, 475 kPa inflator.

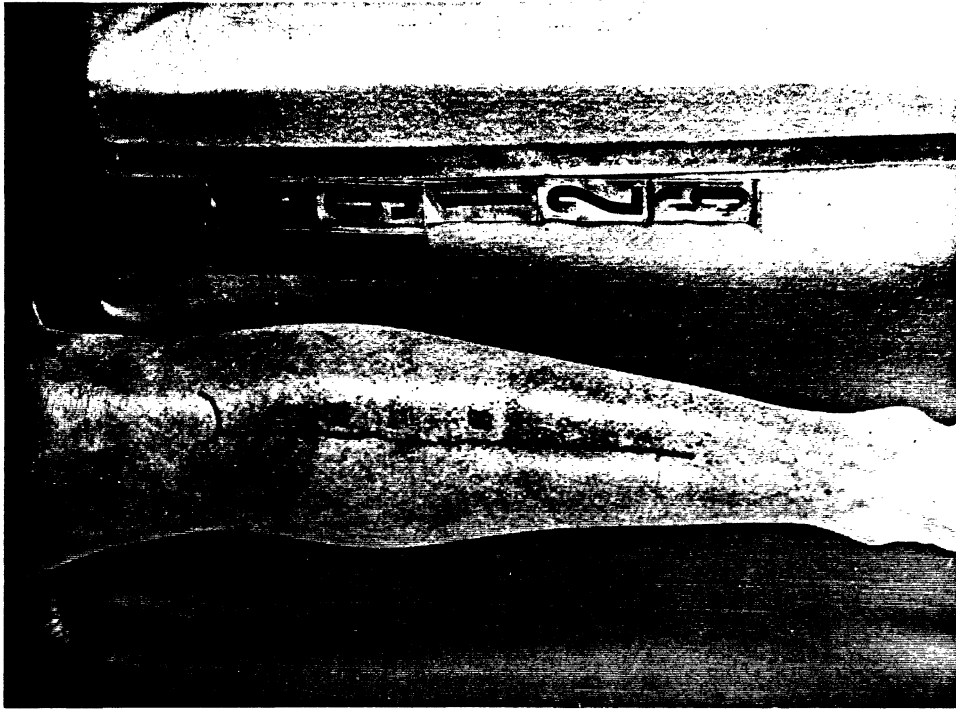


5 MINUTE POST-TEST PHOTO





PRE-TEST PHOTO

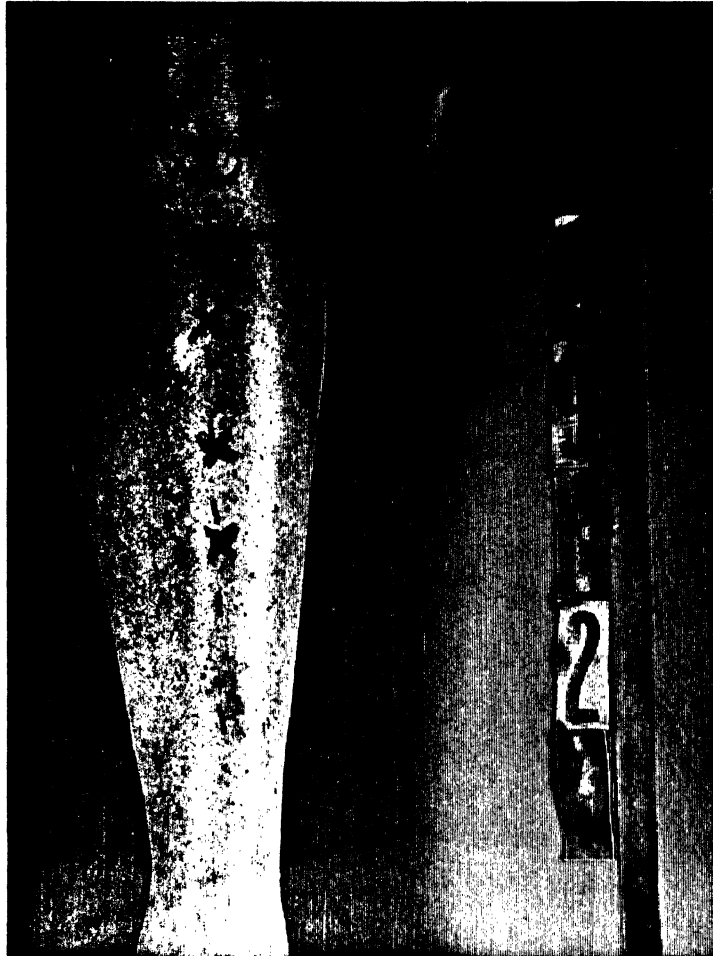


5 MINUTE POST-TEST PHOTO

TEST NO. CA9126: ABRASION SCORE = 5

Female, NO deflection plate, 225 mm, 90° wheel rotation,  
840 denier, NO TETHER, ACCORDIAN Fold, 475 kPa inflator.





PRE-TEST PHOTO



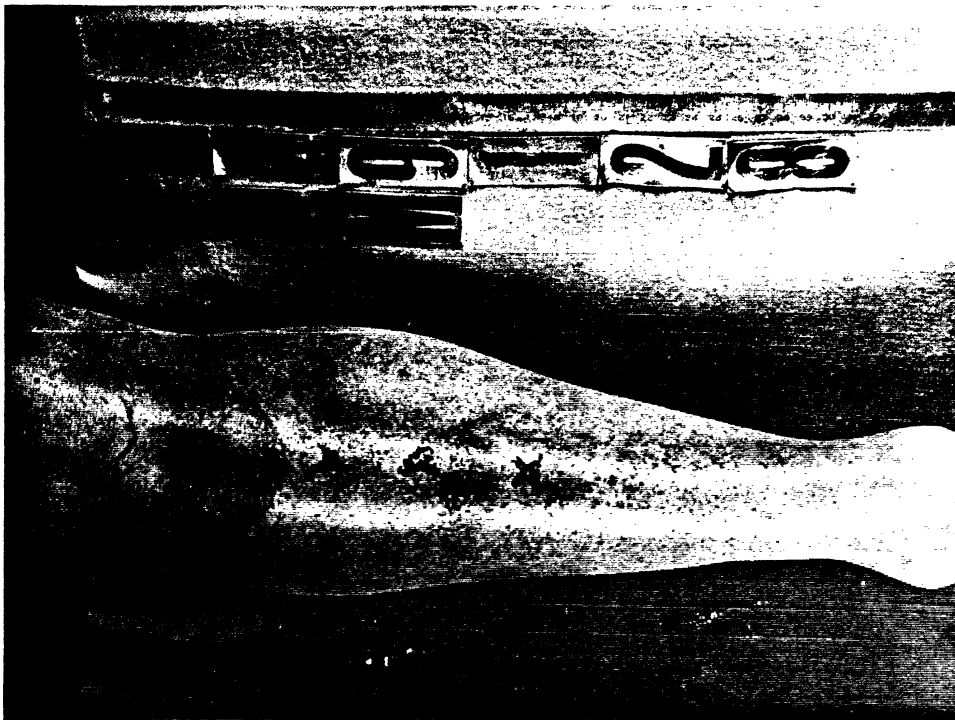
5 MINUTE POST-TEST PHOTO

**TEST NO. CA9127: ABRASION SCORE = 5**  
Female, NO deflection plate, 250 mm, 90° wheel rotation,  
840 denier, NO TETHER, ACCORDIAN Fold, 475 kPa inflator.





PRE-TEST PHOTO



5 MINUTE POST-TEST PHOTO

TEST NO. CA9128: ABRASION SCORE = 5  
Female, NO deflection plate, 225 mm, 90° wheel rotation,  
840 denier, NO TETHER, ACCORDIAN Fold, 475 kPa inflator.







PRE-TEST PHOTO



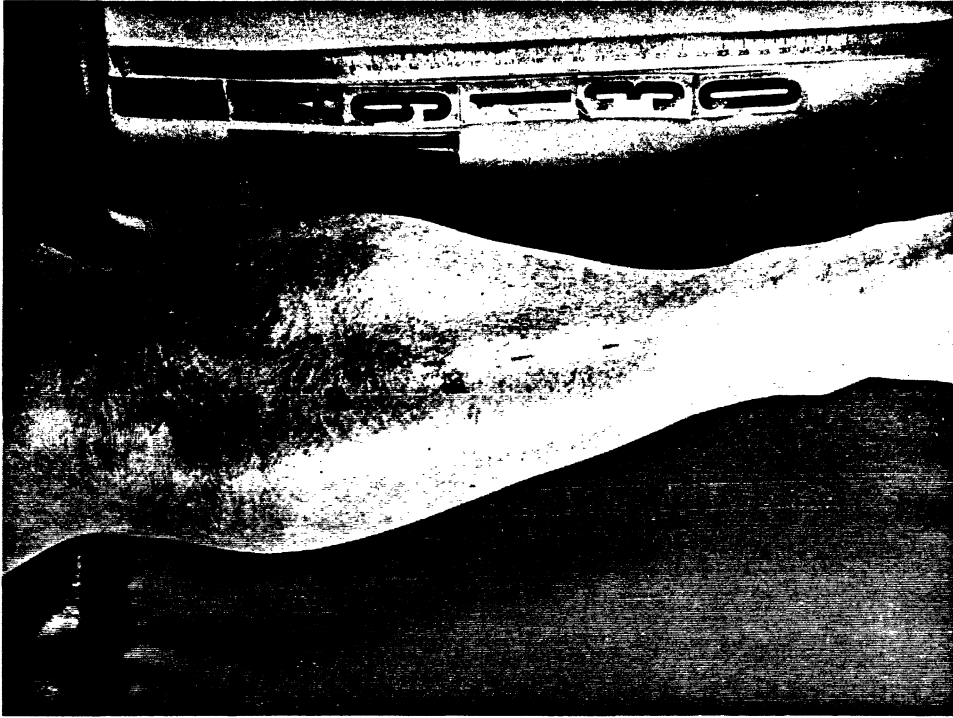
5 MINUTE POST-TEST PHOTO

**TEST NO. CA9129: ABRASION SCORE = 4**  
Female, NO deflection plate, 350 mm, 90° wheel rotation,  
840 denier, NO TETHER, ACCORDIAN Fold, 475 kPa inflator.





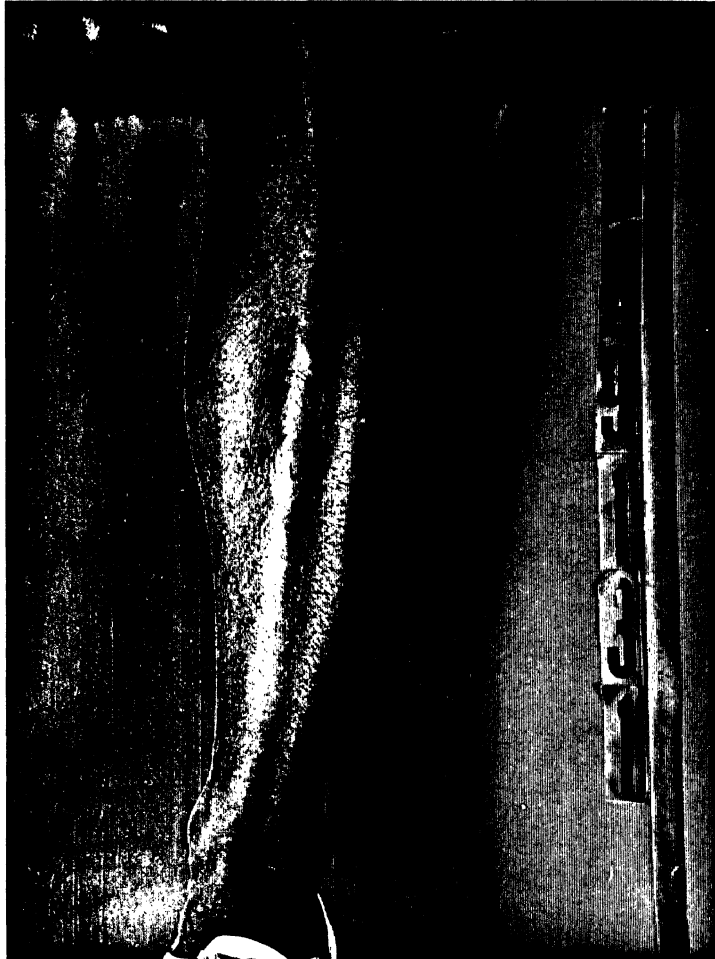
PRE-TEST PHOTO



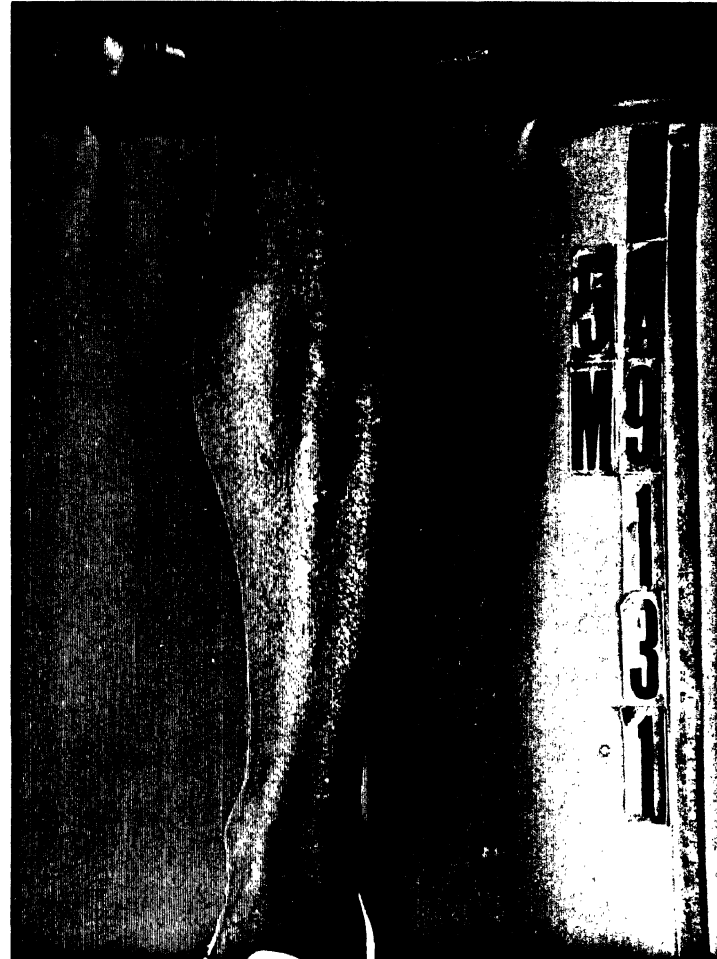
5 MINUTE POST-TEST PHOTO

TEST NO. CA9130: ABRASION SCORE = 3  
Female, NO deflection plate, 325 mm, 90° wheel rotation,  
840 denier, NO TETHER, ACCORDIAN Fold, 475 kPa inflator.





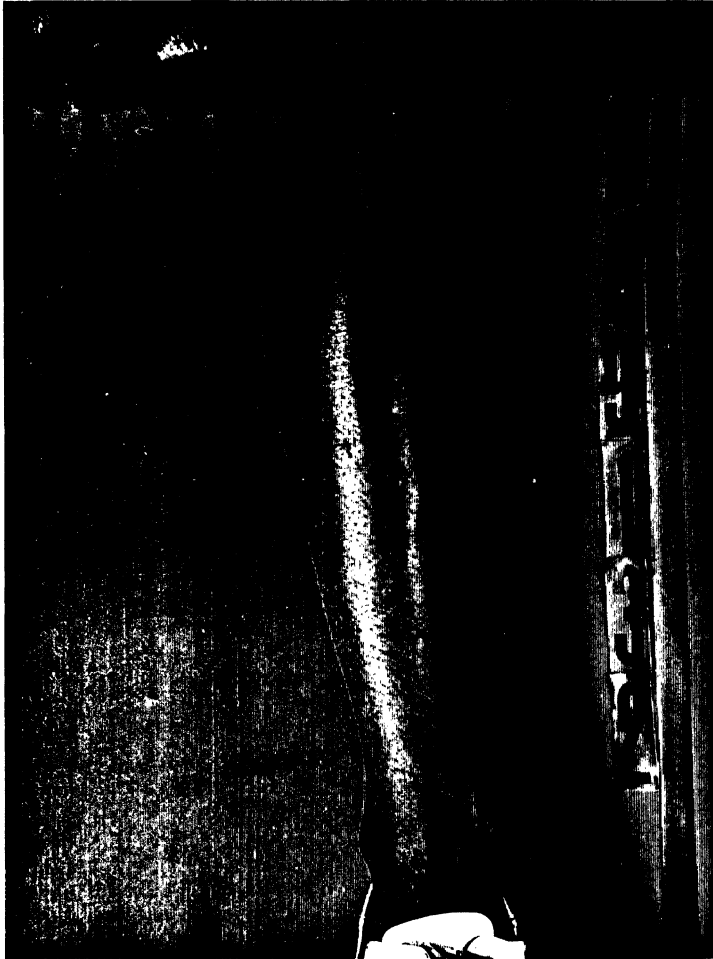
PRE-TEST PHOTO



5 MINUTE POST-TEST PHOTO

**TEST NO. CA9131: ABRASION SCORE = 1**  
Female, NO deflection plate, 250 mm, 90° wheel rotation,  
420 denier, TETHER, ACCORDIAN Fold, 475 kPa inflator.





PRE-TEST PHOTO

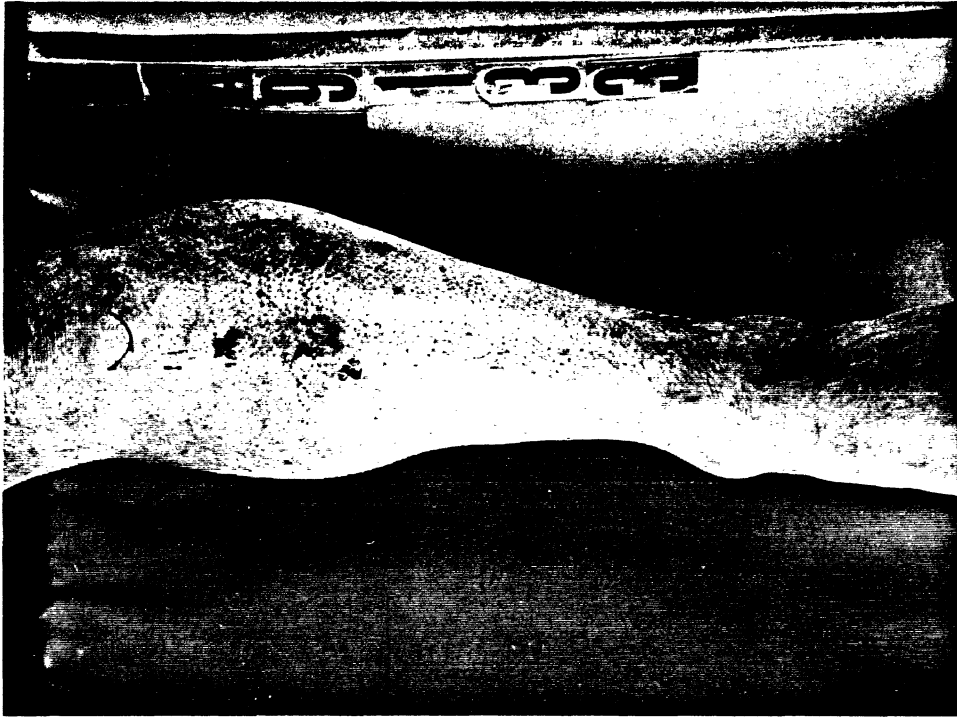


5 MINUTE POST-TEST PHOTO

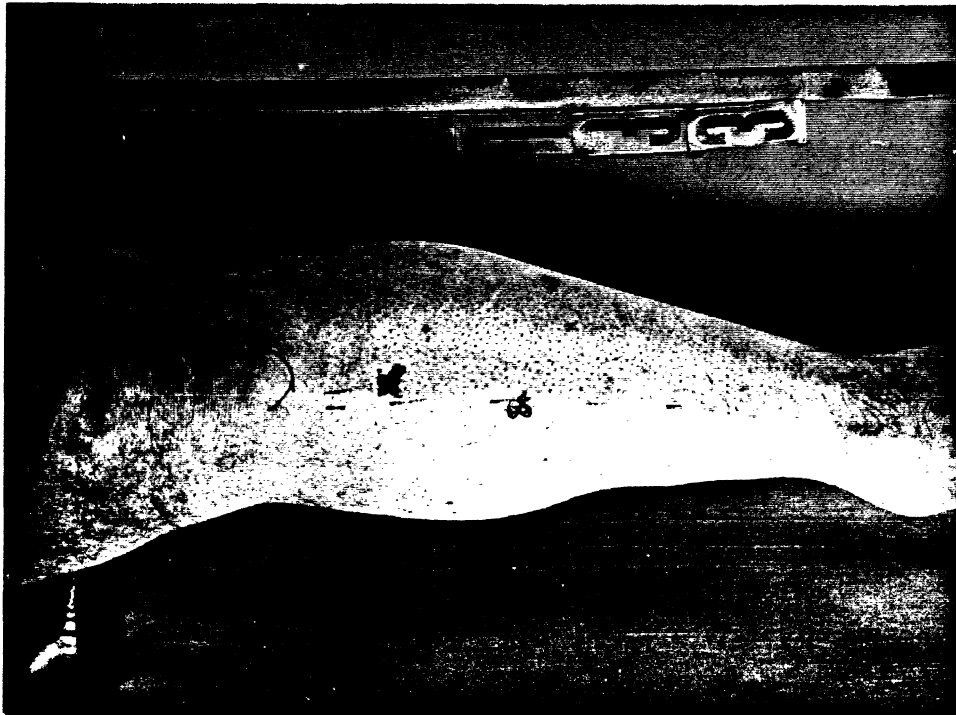
**TEST NO. CA9132: ABRASION SCORE = 5**  
Female, NO deflection plate, 225 mm, 90° wheel rotation,  
420 denier, TETHER, ACCORDIAN Fold, 475 kPa inflator.







5 MINUTE POST-TEST PHOTO



PRE-TEST PHOTO

TEST NO. CA9133: ABRASION SCORE = 5  
Male, NO deflection plate, 350 mm, 90° wheel rotation,  
840 denier, NO TETHER, ACCORDIAN Fold, 475 kPa inflator.





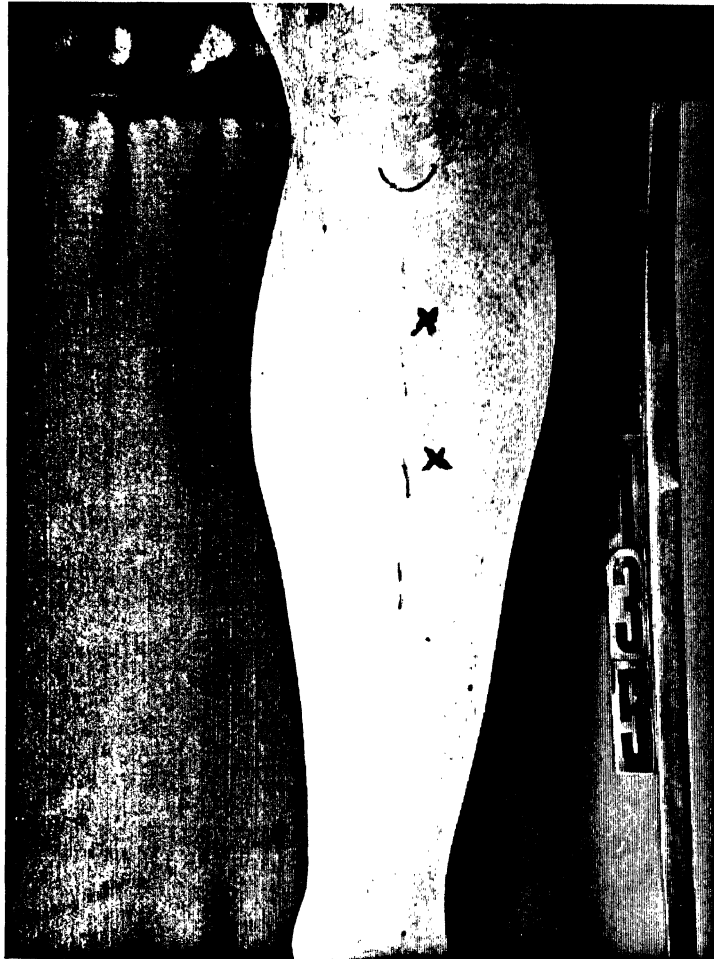
PRE-TEST PHOTO



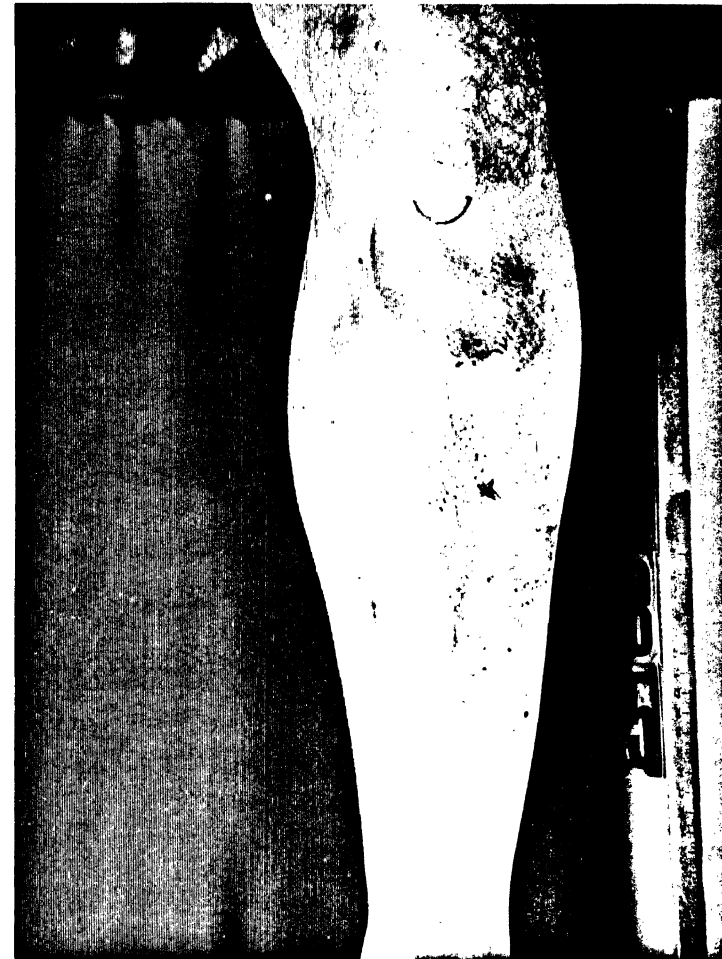
5 MINUTE POST-TEST PHOTO

**TEST NO. CA9134: ABRASION SCORE = 5**  
Male, NO deflection plate, 300 mm, 90° wheel rotation,  
840 denier, NO TETHER, ACCORDIAN Fold, 475 kPa inflator.





PRE-TEST PHOTO



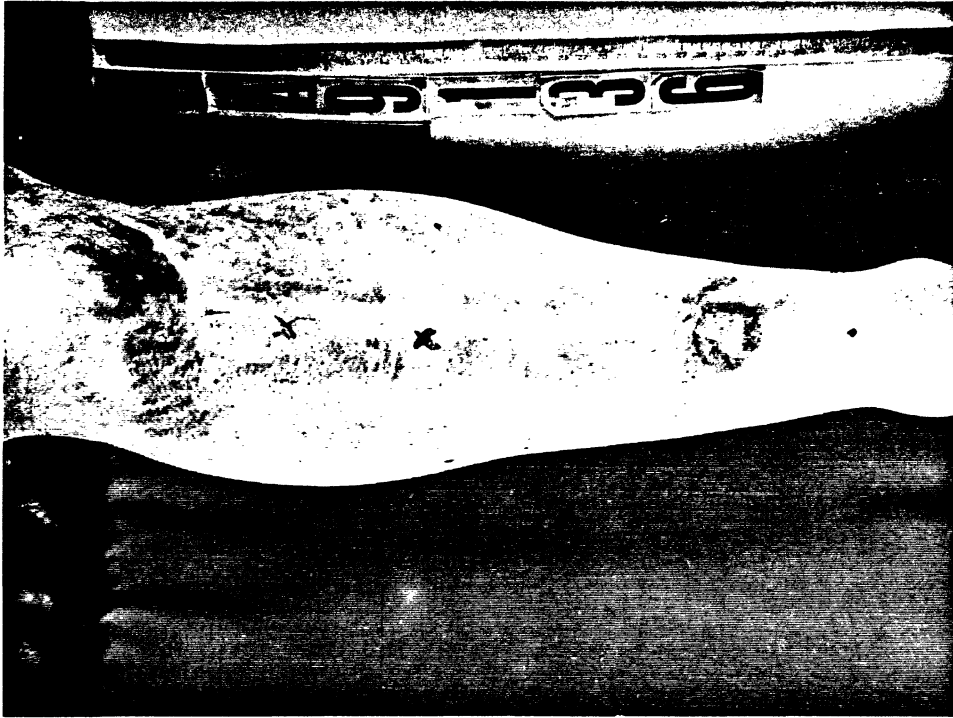
5 MINUTE POST-TEST PHOTO

**TEST NO. CA9135: ABRASION SCORE = 5**  
Male, NO deflection plate, 250 mm, 90° wheel rotation,  
840 denier, NO TETHER, ACCORDIAN Fold, 475 kPa inflator.





PRE-TEST PHOTO



5 MINUTE POST-TEST PHOTO

**TEST NO. CA9136: ABRASION SCORE = 5**  
Male, NO deflection plate, 225 mm, 90° wheel rotation,  
840 denier, NO TETHER, ACCORDIAN Fold, 475 kPa inflator.





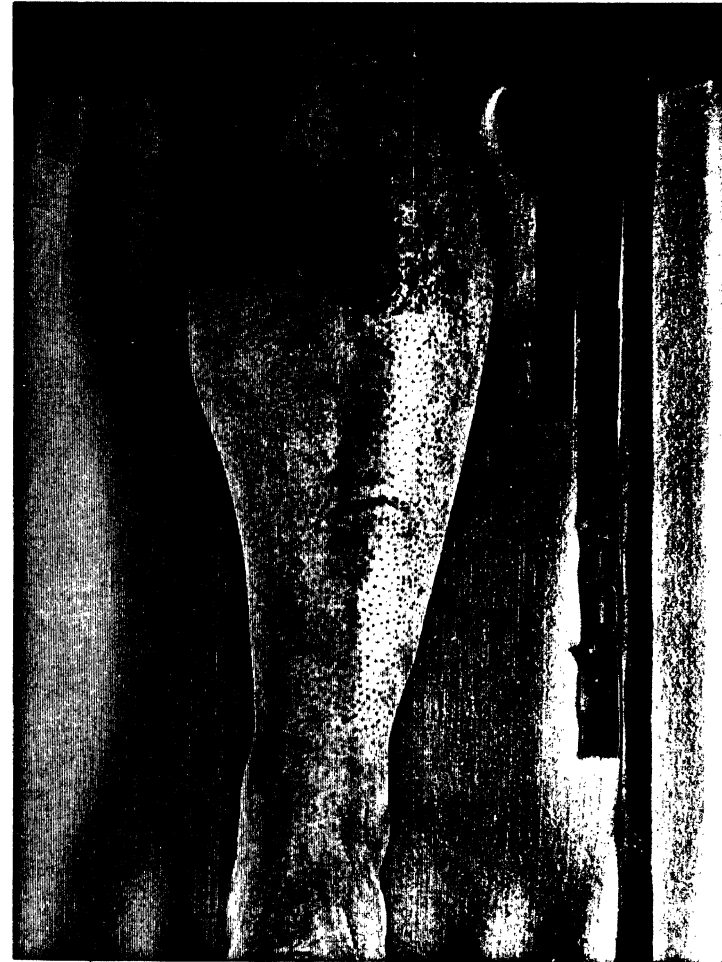
APPENDIX C

PHOTOGRAPHS OF SUBJECTS' LEGS TAKEN BEFORE  
AND FIVE MINUTES AFTER AIRBAG DEPLOYMENTS  
IN THE FULL-FACTORIAL TEST MATRIX





PRE-TEST PHOTO



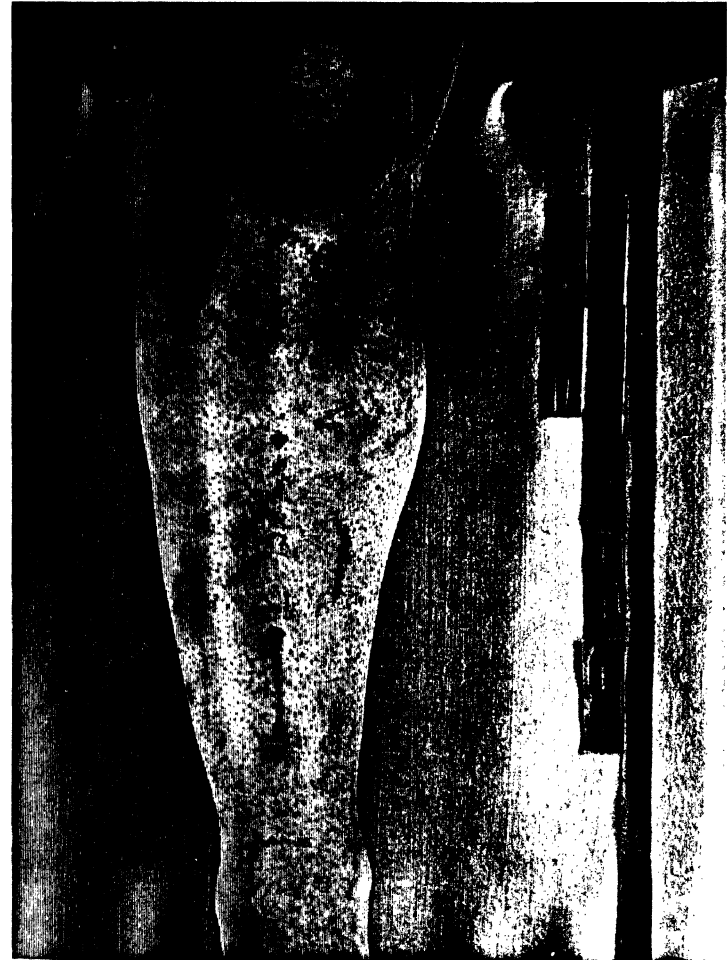
5 MINUTE POST-TEST PHOTO

**TEST NO. CA9137: ABRASION SCORE = 5**  
Male, NO deflection plate, 225 mm, 90° wheel rotation,  
420 denier, NO TETHER, ACCORDIAN Fold, 475 kPa inflator.





PRE-TEST PHOTO



5 MINUTE POST-TEST PHOTO

**TEST NO. CA9138: ABRASION SCORE = 5**  
Male, NO deflection plate, 225 mm, 90° wheel rotation,  
420 denier, TETHER, ACCORDIAN Fold, 475 kPa inflator.





PRE-TEST PHOTO

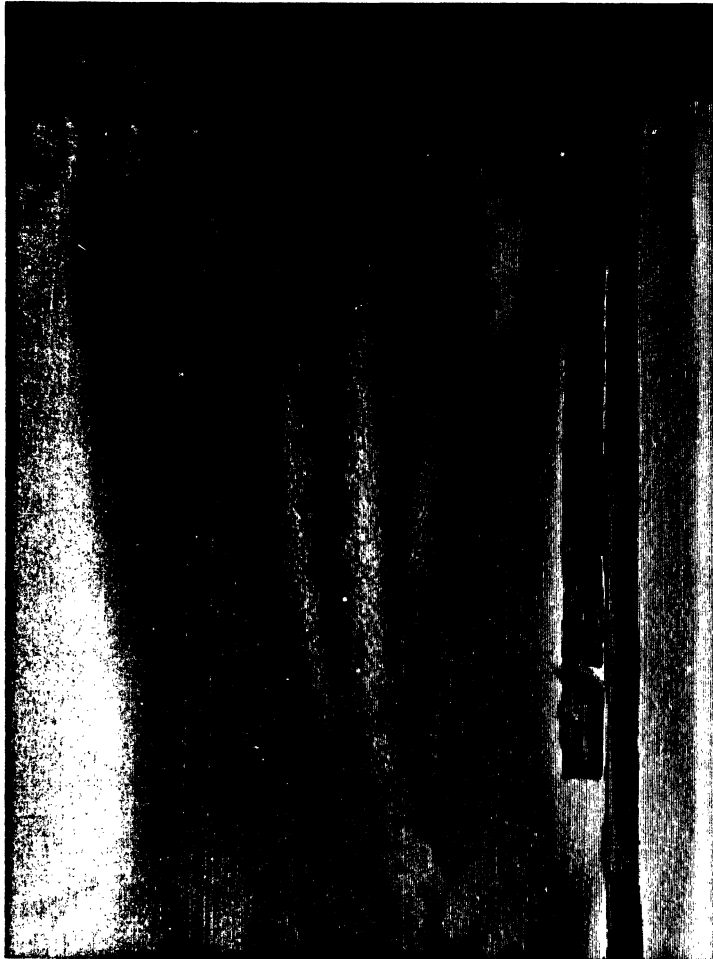


5 MINUTE POST-TEST PHOTO

TEST NO. CA9139: ABRASION SCORE = 4  
Male, NO deflection plate, 225 mm, 90° wheel rotation,  
420 denier, NO TETHER, REVERSE Fold, 420 kPa inflator.







PRE-TEST PHOTO



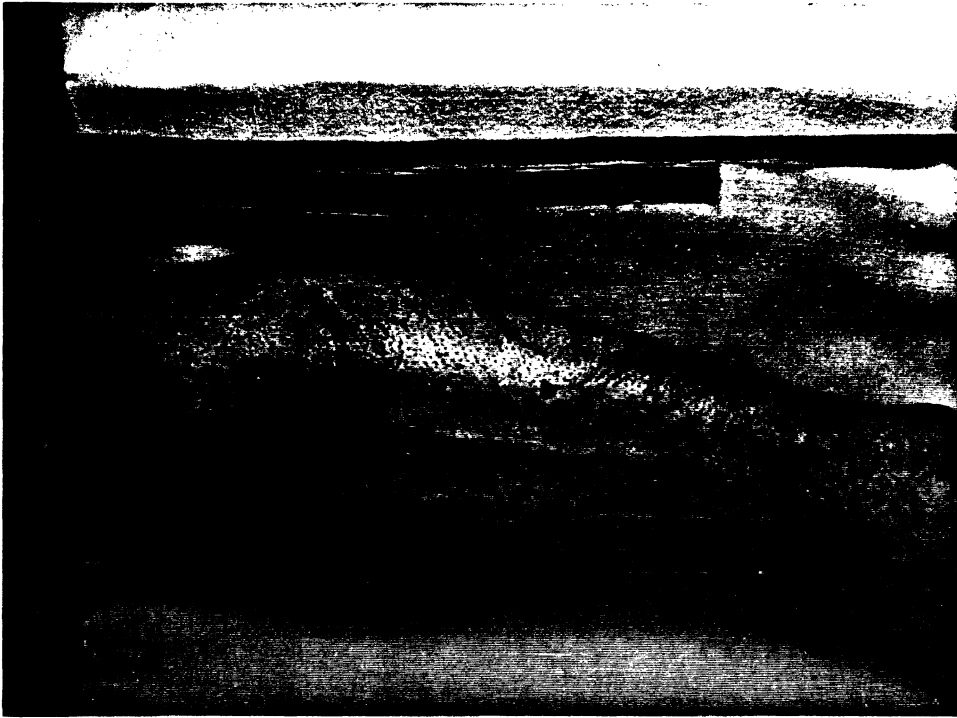
5 MINUTE POST-TEST PHOTO

**TEST NO. CA9140: ABRASION SCORE = 1**  
Male, NO deflection plate, 225 mm, 90° wheel rotation,  
420 denier, TETHER, REVERSE Fold, 475 kPa inflator.





PRE-TEST PHOTO



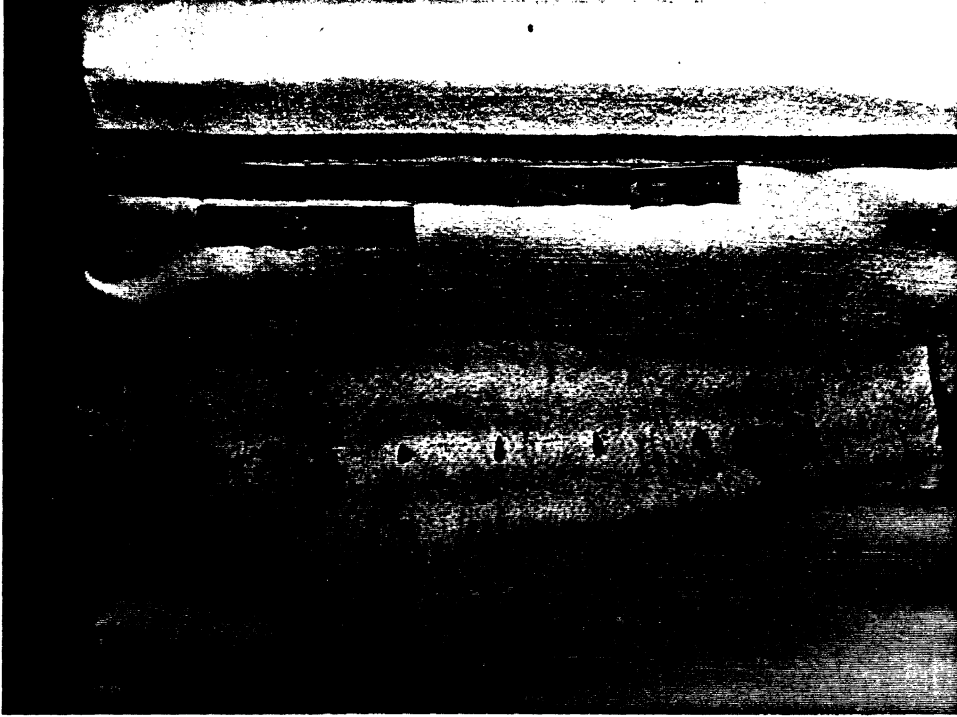
5 MINUTE POST-TEST PHOTO

**TEST NO. CA9141: ABRASION SCORE = 5**  
Male, NO deflection plate, 225 mm, 90° wheel rotation,  
420 denier, NO TETHER, ACCORDIAN Fold, 350 kPa inflator.





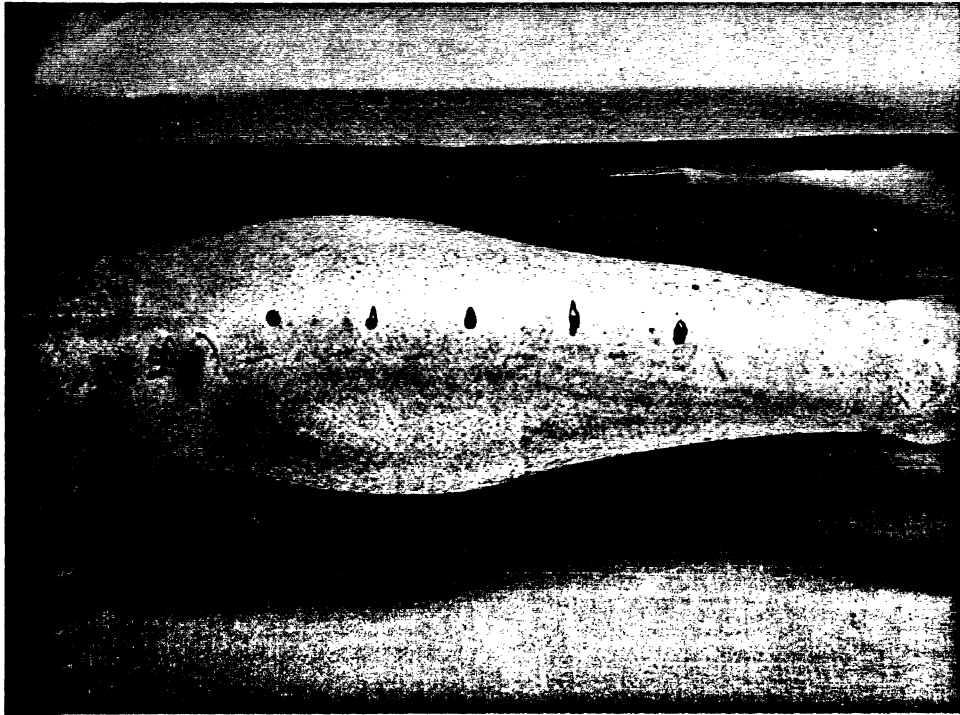
PRE-TEST PHOTO



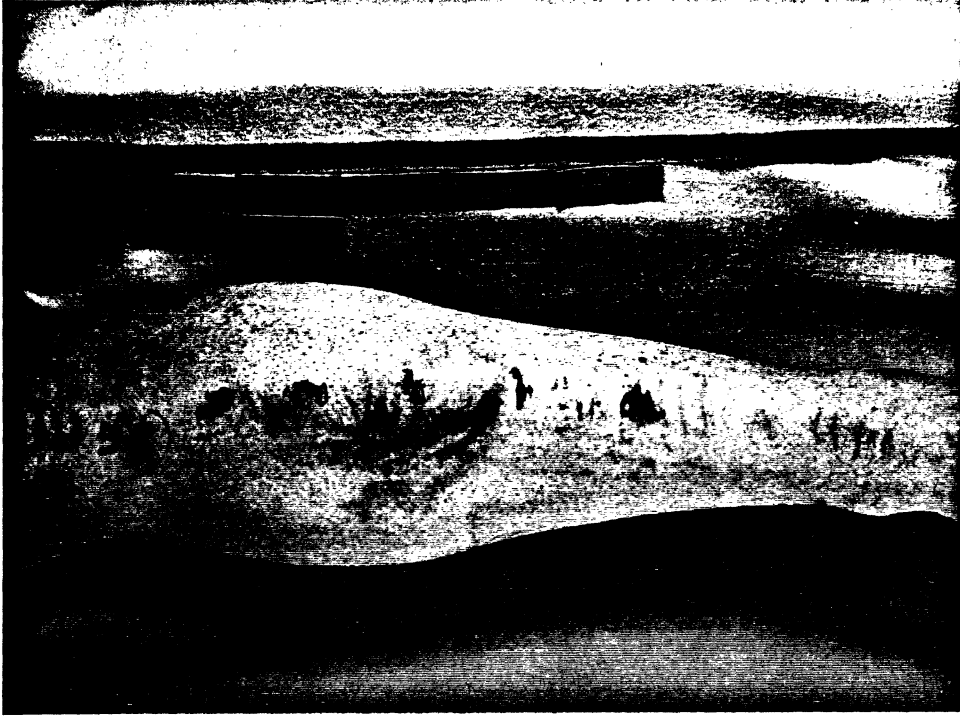
5 MINUTE POST-TEST PHOTO

**TEST NO. CA9142: ABRASION SCORE = 4**  
Male, NO deflection plate, 225 mm, 90° wheel rotation,  
420 denier, TETHER, ACCORDIAN Fold, 350 kPa inflator.





PRE-TEST PHOTO



5 MINUTE POST-TEST PHOTO

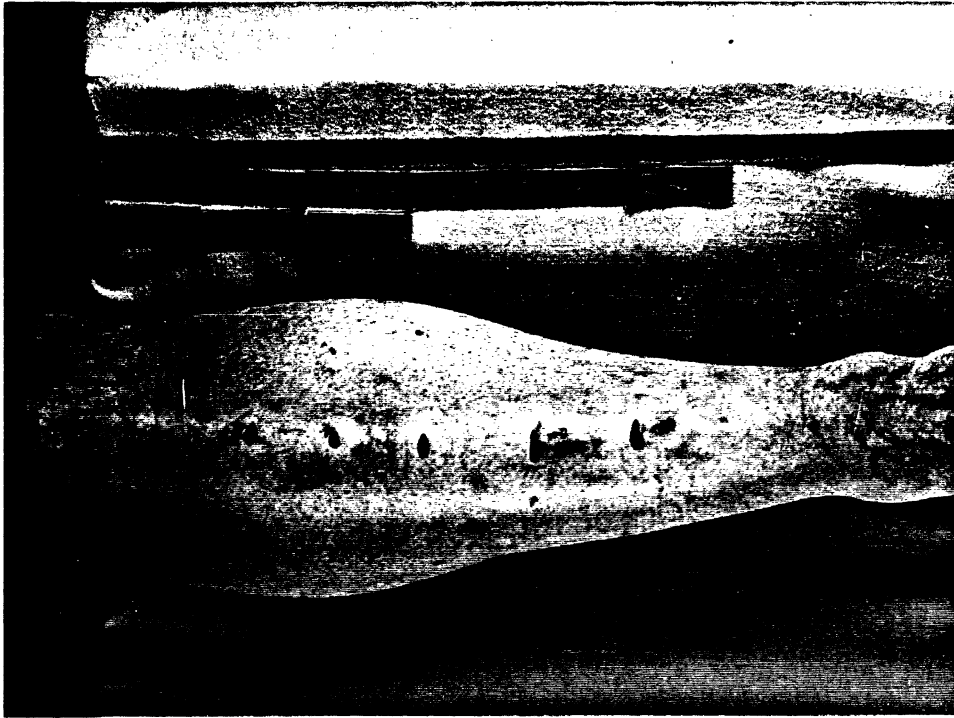
TEST NO. CA9143: ABRASION SCORE = 2  
Male, NO deflection plate, 225 mm, 90° wheel rotation,  
420 denier, NO TETHER, REVERSE Fold, 350 kPa inflator.







PRE-TEST PHOTO



5 MINUTE POST-TEST PHOTO

TEST NO. CA9144: ABRASION SCORE = 1  
Male, NO deflection plate, 225 mm, 90° wheel rotation,  
420 denier, TETHER, REVERSE Fold, 350 kPa inflator.

